



**FAST ANALYTICAL METHODOLOGIES BASED ON MOLECULAR  
SPECTROPHOTOMETRIC TECHNIQUES AND MULTIVARIATE DATA  
ANALYSIS**

**Vanessa del Rio Sánchez**

**ISBN: 978-84-693-9439-7  
Dipòsit Legal: T.64-2011**

**ADVERTIMENT.** La consulta d'aquesta tesi queda condicionada a l'acceptació de les següents condicions d'ús: La difusió d'aquesta tesi per mitjà del servei TDX ([www.tesisenxarxa.net](http://www.tesisenxarxa.net)) ha estat autoritzada pels titulars dels drets de propietat intel·lectual únicament per a usos privats emmarcats en activitats d'investigació i docència. No s'autoritza la seva reproducció amb finalitats de lucre ni la seva difusió i posada a disposició des d'un lloc aliè al servei TDX. No s'autoritza la presentació del seu contingut en una finestra o marc aliè a TDX (framing). Aquesta reserva de drets afecta tant al resum de presentació de la tesi com als seus continguts. En la utilització o cita de parts de la tesi és obligat indicar el nom de la persona autora.

**ADVERTENCIA.** La consulta de esta tesis queda condicionada a la aceptación de las siguientes condiciones de uso: La difusión de esta tesis por medio del servicio TDR ([www.tesisenred.net](http://www.tesisenred.net)) ha sido autorizada por los titulares de los derechos de propiedad intelectual únicamente para usos privados enmarcados en actividades de investigación y docencia. No se autoriza su reproducción con finalidades de lucro ni su difusión y puesta a disposición desde un sitio ajeno al servicio TDR. No se autoriza la presentación de su contenido en una ventana o marco ajeno a TDR (framing). Esta reserva de derechos afecta tanto al resumen de presentación de la tesis como a sus contenidos. En la utilización o cita de partes de la tesis es obligado indicar el nombre de la persona autora.

**WARNING.** On having consulted this thesis you're accepting the following use conditions: Spreading this thesis by the TDX ([www.tesisenxarxa.net](http://www.tesisenxarxa.net)) service has been authorized by the titular of the intellectual property rights only for private uses placed in investigation and teaching activities. Reproduction with lucrative aims is not authorized neither its spreading and availability from a site foreign to the TDX service. Introducing its content in a window or frame foreign to the TDX service is not authorized (framing). This rights affect to the presentation summary of the thesis as well as to its contents. In the using or citation of parts of the thesis it's obliged to indicate the name of the author.

**Fast analytical methodologies based on  
molecular spectrophotometric techniques  
and multivariate data analysis**

Doctoral Thesis

UNIVERSITAT ROVIRA I VIRGILI



UNIVERSITAT ROVIRA I VIRGLI  
FAST ANALYTICAL METHODOLOGIES BASED ON MOLECULAR SPECTROPHOTOMETRIC TECHNIQUES  
AND MULTIVARIATE DATA ANALYSIS  
Vanessa del Rio Sánchez  
ISBN:978-84-693-9439-7/ DL:T.64-2011

UNIVERSITAT ROVIRA I VIRGILI

Department of Analytical Chemistry and Organic Chemistry

Fast analytical methodologies based on  
molecular spectrophotometric techniques  
and multivariate data analysis

**VANESSA DEL RÍO SÁNCHEZ**

Doctoral Thesis

Supervisors

Dr. María Pilar Callao Lasmariás

Prof. María Soledad Larrechi García

Tarragona, 2010

UNIVERSITAT ROVIRA I VIRGLI  
FAST ANALYTICAL METHODOLOGIES BASED ON MOLECULAR SPECTROPHOTOMETRIC TECHNIQUES  
AND MULTIVARIATE DATA ANALYSIS  
Vanessa del Rio Sánchez  
ISBN:978-84-693-9439-7/ DL:T.64-2011



## UNIVERSITAT ROVIRA I VIRGILI

DEPARTAMENT DE QUÍMICA ANALÍTICA  
I QUÍMICA ORGÀNICA

Campus Sescelades  
C/ Marcel·lí Domingo, s/n  
43007 Tarragona  
Tel. 34 977 55 97 69  
Fax 34 977 55 84 46  
e-mail: secqaqo@quimica.urv.es

Dr. MARÍA SOLEDAD LARRECHI GARCÍA, Professor, and Dr. MARÍA PILAR CALLAO LASMARÍAS, Associate professor, both of the Department of Analytical Chemistry and Organic Chemistry at the Universitat Rovira i Virgili,

CERTIFY:

The Doctoral Thesis entitled: **“Fast analytical methodologies based on molecular spectrophotometric techniques and multivariate data analysis”**, presented by VANESSA DEL RÍO SÁNCHEZ to receive the degree of Doctor of the Universitat Rovira i Virgili, has been carried out under our supervision, in the Department of Analytical Chemistry and Organic Chemistry at the Universitat Rovira i Virgili, and all the results reported in this thesis were obtained from experiments conducted by the above mentioned student.

Tarragona, October 2010

Dr. María Pilar Callao Lasmarías

Prof. María Soledad Larrechi García

UNIVERSITAT ROVIRA I VIRGLI  
FAST ANALYTICAL METHODOLOGIES BASED ON MOLECULAR SPECTROPHOTOMETRIC TECHNIQUES  
AND MULTIVARIATE DATA ANALYSIS  
Vanessa del Rio Sánchez  
ISBN:978-84-693-9439-7/ DL:T.64-2011

*Ahora es el momento de tener un recuerdo agradecido a quienes a lo largo de estos años han dejado su huella en mí, compartiendo momentos de crisis y debilidad y momentos de felicidad, compartiendo sensaciones y experiencias. Experiencias sobre las que puedo recordar nombres. Nombres que me han ayudado a crecer, cambiar y madurar. A todos vosotros, GRACIAS.*

*En primer lugar, quisiera agradecer a mis directoras de tesis, la Profesora M. Soledad Larrechi y la Dra. M. Pilar Callao, la oportunidad de participar en este proyecto y de formar parte del grupo de Quimiometría, Cualimetría y Nanosensores, donde gracias a su ayuda, constante guía y soporte he podido formarme como investigadora.*

*Personalmente, a Marisol y Pili. GRACIAS por vuestros consejos, por vuestra constancia y dedicación, por reñirme cuando era necesario, por apoyarme en los malos momentos, por vuestras charlas de experiencia y por vuestra perdurable confianza.*

*Del mismo modo, también quisiera expresar mis agradecimientos al Dr. Joan Carles Ronda y a la Profesora Virginia Cádiz del grupo de Polímeros de la Universidad Rovira i Virgili, por vuestra valiosa ayuda orgánica, por vuestras aportaciones científicas y por ampliar mis conocimientos poliméricos. De manera especial, al Dr. Lucas Montero de Espinosa. Gracias por tu paciencia, por tu sencillez y por los momentos compartidos, tanto en el campo científico como en el personal.*

*Gracias también a todos los miembros del grupo de Quimiometría, Cualimetría y Nanosensores, a los que han pasado y a los que están actualmente. A F. Xavier Rius, por tu enorme sabiduría y por todo el afecto que me has brindado durante estos años. A Itziar, por compartir conmigo tus conocimientos. A Jordi, por las risas compartidas durante las prácticas. A Joan, por los buenos y divertidos momentos vividos durante los congresos. A Ricard, por la complicidad. A Alicia, por tu inocencia y las conversaciones sobre bomberos. A Alberto y Vero, que estabais aquí cuando llegué y me*



*enseñasteis a dar los primeros pasos quimiométricos. Ya todos aquellos con los que he compartido congresos, cafés, cenas, paellas, calçotadas, cumpleaños, castañadas... Gracias a Enrique, Paquita, Zayda, Jaume, Surya, Raquel, Gustavo, Alí, Ayse, Carolina, Xavi Jr. y Pascal.*

*A Joe. La canción que te compusimos es un buen resumen de todo lo que me has aportado durante estos años. "Un corazón que late, gritando JoeVilla, llevándolo en la mente por siempre jamás".*

*A Cris B, Rafa y Laura. Por vuestros primeros consejos, por nuestras reuniones a media tarde en el pasillo y por vuestras palabras de ánimo y apoyo.*

*Un agradecimiento especial al Dr. Santiago Macho. Gracias por estar siempre dispuesto a ayudarme con una sonrisa, por la paciencia que has tenido para solucionar todos mis problemillas técnicos, por dedicarme cada día parte de tu valioso tiempo, por todo lo que me has enseñado (Santi el Sabio), por los bocadillos y cafés, por los cotilleos, por las charlas sobre pádel y series y programas de televisión, por tu gran calidad humana, por tu sencillez, por tu humildad, por tu generosidad y por tu amistad. GRACIAS Santi.*

*A Idoia, Porque muchas de estas páginas estarían vacías si no hubiera sido por tu constante ayuda. MOLTES GRÀCIES. Gracias por dedicarme tiempo, tiempo para demostrar tu preocupación por mi, tiempo para escuchar mis problemas y ayudarme a buscarles solución, y sobre todo tiempo para sonreír y mostrarme tu afecto. He podido contar contigo cuando necesitaba en quién confiar y pedir consejo. Hemos demostrado que una verdadera amistad no conlleva necesariamente años, sino que se forma de momentos y experiencias especiales, como las que tú y yo hemos compartido en poco tiempo. Siempre tienes el consejo, la chispa y el ingenio para hacer sentir bien a cualquiera, te admiro por tu capacidad de hacer amigos, por tu carácter alegre, por tu*

*franqueza y por tu sinceridad. Por eso quiero darte las gracias, sólo por estar y haberte conocido. Y recuerda, como tú me has enseñado: Canta y sé feliz (LIBRE...).*

*Gracias también al Dr. Sergio Castellón y a la Dra. Aurora Ruiz. Por pararme en el pasillo durante estos últimos años para mostrarme siempre vuestro afecto e interés.*

*Esta facultad no sería lo mismo sin los cuatro pilares que sostienen el piso verde, porque ellas son las alegrías de la casa. Gracias a Tere, por ayudarnos durante las prácticas y facilitarnos los pedidos. Gracias a Avelina y a Olga, porque siempre con una sonrisa sois capaces de solucionar todos los trámites y papeleos necesarios. Gracias a Eulàlia, por tu nobleza, dulzura y sencillez.*

*A mis compañeros y amigos de licenciatura. A Laura, por darme tantos momentos memorables, divertidos y entrañables (llenaría páginas y páginas describiendo todo lo que me has hecho reír y disfrutar a tu lado, Gracias). A Antonio, porque entre reunión y reunión siempre has tenido un rato para cotillear conmigo. A Xavi, porque los dos estamos orgullosos de ser de Tarragona, lo que nos ha permitido ser cómplices y amigos. A Anna, por tener siempre las ideas tan claras y querer compartirlas conmigo. A Miquel, por estar siempre tan ocupado pero sin olvidarte nunca de mí, compartiendo partidos de fútbol, apuntes y largas conversaciones. A Tessa, por tus ganas increíbles de viajar y contar conmigo para ello. A Núria, por las fiestas de los primeros años de licenciatura y las reuniones posteriores.*

*Y a Pep (¡¡in Free!!) y a Helena. Por todas las horas pasadas en la biblioteca, por todos los trabajos que hemos hecho juntos, por ayudarme a estudiar, por compartir conmigo los momentos de tensión antes de un examen y los momentos de relajación de después. GRACIAS por vuestro apoyo y amistad.*

*Al Foix, ¡¡campeón!! Porque después de la E.S.O., el Bachillerato, la carrera y el doctorado creo que nuestros caminos ya se separan, porque durante todos estos años hay recuerdos que nunca olvidaré, por nuestro amigo Jacks y por las aventuras que juntos hemos vivido. A Kike, por la forma que tienes de ver y vivir la vida y por el aprecio que me has demostrado. A Isidro, el amigo de los alumnos, por tu bondad y generosidad.*

*A mis compañeros Cromatográficos, Poliméricos y Azucareros en general. Y a Miriam en particular. Porque no necesitamos decirnos una palabra cuando algo sucede, porque nuestro silencio nos delata y estallamos en risas y felicidad. Porque en poco tiempo son muchos los momentos que recordar, por los cotilleos, por las fiestas, por los viajes a Sevilla, por las risas, por los lloros y por los abrazos amigos.*

*A Xavi, el chico con más motes de la faz de la tierra, por tu paciencia, por las risas y las bromas, por contar conmigo y por tu confianza. Y también al resto de compañeros cuánticos: Sonia, Laia, Mireia, Alberto, Jessica, Pablo, Àlex, Eva y John.*

*Gracias a todos y cada uno de los integrantes del RECREATIVO DE JUERGA. Porque conseguimos formar un gran equipo de fútbol pero sobretodo un gran equipo de compañeros, compañeras, amigos y amigas. A Albert, por tener una gran paciencia como entrenador y un gran corazón como amigo. A Lidia, por tu incondicional apoyo como afición en el terreno de juego y en el terrero personal. A Laura, el muro del equipo. A Esther, la mejor capitana y una gran compañera y amiga. A Helena, por tu arte, tu salero y tu amistad (y también por tu mala leche). A Anabel, la mejor jugadora del torneo, por tu alegría y espontaneidad. A la Rojas, por correr y correr como si no existiera un mañana. A Idoia, por dejarse la piel (literalmente) como portera. A Miriam, la primera goleadora y la primera lesionada. A Irene, por la felicidad que*

*desprendes, por las clases de inglés y por las prácticas. A David, por tu timidez y por tu risa y simpatía. Y a Laura Ferreres, Ligia, Sabina, Isabel, Lidia y Víctor.*

*A aquellos que han compartido parte de su tiempo conmigo. A Ferran, Anna Pallarès y Lillian, por las risas en clase, entre clase y clase y fuera de clase. A Álvaro, de la ciudad costera por antonomasia, por las cervezas (¡¡que han sido muchas!!), por los jueves emblemáticos y por tu simpatía y cariño. A Aitor, también por los jueves emblemáticos y por tus graciosas canciones. A Martha, por tu lealtad y sencillez. A Pere, por introducirme en el mundo bioquímico. Al Francesc, por tu calma y compañía. A Laura y Benji, por los agradables y divertidos ratos compartidos, por las conversaciones, por los viajes en tren y por lo que vosotros ya sabéis.*

*A los amigos de congresos y compañeros de grandes viajes y grandes aventuras, tanto científicas como personales. A José Manuel Amigo, por tus piropos, tus consejos, tu ayuda y sobre todo tu encantadora e interesante compañía y amistad. A Juanillo, por las sidrerías, por los potes, por las charlas, por tu simpatía y por tu inconstante aprecio y amistad. A Silvia, porque un congreso fue suficiente para “ponerme la pierna encima”. A José Manuel Prats-Montalbán, un amigo “de diseño y calidad”. A Merche, por tu alegría y arte sevillano. Y a todos aquellos con los que he pasado un rato divertido y agradable: sois la ...i..*

*A mis compañeros y amigos de instituto que me han mostrado su apoyo durante todos estos años. A Adri, Ury, Lluís, Iñaki, Siscu, Coke, Víctor y Juanpere. Gracias por vuestras bromas, por las cenas y por las salidas nocturnas.*

*A mis amigos y amigas de LA TRIBU. Porque a pesar de todo lo que hemos pasado, siempre nos hemos apoyado en los malos momentos. A Kaus, Dani, Aitor, Estef, Vallver, Figa y Miki. Gracias a cada uno de vosotros por todas los momentos y experiencias compartidas.*

*Y gracias al Sergi, mi amigo y compañero de aventuras desde la E.S.O. hasta ahora. Por tus despistes, por tu risa, por tu felicidad, por tus malabares y equilibrios, por tu violín, por tu música y por tu locura.*

*MUCHAS GRACIAS a mis tres grandes y mejores amigas: Ana, Marina y Gisela. Gracias por todos los momentos que hemos compartido, momentos llenos de sentimientos y pensamientos, sueños y anhelos, secretos, risas y lágrimas y, sobre todo, AMISTAD. Gracias por hacerme feliz, por vuestra compañía y por vuestra confianza. Porque a pesar del tiempo, de la distancia, de las cosas que nos dijimos y de lo que no hemos compartido, siempre habéis estado cuando os he necesitado. Gracias por los Capafonts, por los Carnavales, por la Sala Zero, por las orquestas, por la Plaça de la Font, por las Santa Teclas, por los Amparitos Roca bailados, por los cafés, por las cervezas, por las borracheras y por todos los agradables momentos que hemos pasado juntas. De todo corazón, Gracias por seguir a mi lado.*

*A Edu, con el que he compartido el final del trayecto. Gracias por quererme y gracias por estar siempre a mi lado, compartiendo las caricias, los te quiero, los abrazos. Me has demostrado tu cariño siempre que podías. Me has enseñado a quererte de manera sin igual y a conocerte cada día más. Gracias por ser lo que eres, una persona maravillosa. Porque el decirte gracias y que te quiero no alcanzan a expresar mis verdaderos sentimientos y, sin embargo, sólo te puedo decir GRACIAS.*

*A mi familia, GRACIAS. A mis tíos, tías, primos y primas: Mari, Conchi, Chuchi, Paula, Merche, Tomás, Gema, Ignacio y Francis. Y especialmente a mi prima Raquel, que siempre me ha apoyado desde la distancia. Por los calimochos, por los quintitos, por las borracheras y por Loren. Y a mis YAYOS y a mis ABUELOS, por intentar comprenderme y compartir conmigo las diferentes etapas de mi vida.*

*A mi hermana Olga. Por tu inteligencia, por tu paciencia, por nuestras peleas y por nuestras risas, por ayudarme y por enseñarme, por nuestra complicidad, por nuestros secretos y por nuestra amistad. GRACIAS tata.*

*Y por supuesto, mi más profundo y sincero agradecimiento es para mis padres, que siempre me han apoyado y han confiado en mí, creyendo en mis posibilidades y dándome ánimos para seguir adelante. Me habéis regañado y castigado, pero siempre habéis sabido perdonar mis equivocaciones. Mama y Papa, gracias por la maravillosa formación y educación que me habéis regalado, por vuestra sabiduría, por vuestros valores, por vuestra protección, por vuestro sacrificio, por vuestra comprensión, por vuestro afecto, por vuestro cariño y por vuestro amor incondicional. Todo lo que soy os lo debo a vosotros. GRACIAS.*

UNIVERSITAT ROVIRA I VIRGLI  
FAST ANALYTICAL METHODOLOGIES BASED ON MOLECULAR SPECTROPHOTOMETRIC TECHNIQUES  
AND MULTIVARIATE DATA ANALYSIS  
Vanessa del Rio Sánchez  
ISBN:978-84-693-9439-7/ DL:T.64-2011

*Pelea por lo que quieres y no desesperes  
si algo no anda bien.  
Hoy puede ser un gran día  
y mañana también.  
Joan Manuel Serrat*



UNIVERSITAT ROVIRA I VIRGLI  
FAST ANALYTICAL METHODOLOGIES BASED ON MOLECULAR SPECTROPHOTOMETRIC TECHNIQUES  
AND MULTIVARIATE DATA ANALYSIS  
Vanessa del Rio Sánchez  
ISBN:978-84-693-9439-7/ DL:T.64-2011

## TABLE OF CONTENTS

<b>Chapter 1. Introduction</b>	21
1.1. Background	23
1.2. Objectives of the thesis	25
1.3. Structure of the thesis	27
1.4. References	30
<b>Chapter 2. Multivariate data analysis methods</b>	31
2.1. Introduction	33
2.2. Multidimensional spectroscopic analysis	34
2.3. Multivariate resolution methods	38
2.4. References	53
<b>Chapter 3. Analytical methods based on infrared spectroscopy and second-order data treatment for the quantitative monitoring of model polymer reactions from vegetable oils.</b>	57
3.1. Introduction	59
3.2. Results	67

3.2.1. A derivative epoxidized oil, the epoxidized methyl oleate from high oleic sunflower oil, as pre-polymer in the curing of epoxy resins.	67
3.2.1.1. Paper. <i>Spectroscopic and quantitative chemometric analysis of the epoxidised oil/amine system</i> . Journal of Near Infrared Spectroscopy, 18 (2010) 281-290.	69
3.2.1.2. Paper. <i>Effect of the temperature on the kinetic rate constants of a model curing reaction of epoxy resins from vegetable oils applying hybrid soft- and hard- approach to FTIR spectra data</i> . Submitted.	97
3.2.2. A new enone-containing triglyceride derivative, the enone-containing methyl oleate from high oleic sunflower oil, as pre-polymer in the curing aza-Michael reaction.	120
3.2.2.1. Paper. <i>Chemometric resolution of NIR spectra data of a model aza-Michael reaction with a combination of local rank exploratory analysis and multivariate curve resolution-alternating least squares (MCR-ALS) method</i> . Analytica Chimica Acta, 642 (2009) 148-154.	123
3.5. References	149
<b>Chapter 4.</b> Analytical methods based on sequential injection analysis and second-order data treatment for determining parameters of interest in the characterization of biodiesel.	153
4.1. Introduction	155

4.2. Paper. <i>Sequential injection titration method using second order signals. Determination of acidity in plant oils and biodiesel samples.</i> Talanta, 81 (2010) 1572-1577.	161
4.3. Paper. <i>Sequential injection analysis for the determination of sulphate in water and biodiesel using second-order data.</i> Analytica Chimica Acta, 676 (2010) 28-33.	187
4.4. References	213
<b>Chapter 5. General conclusions</b>	215
Appendix	219

UNIVERSITAT ROVIRA I VIRGLI  
FAST ANALYTICAL METHODOLOGIES BASED ON MOLECULAR SPECTROPHOTOMETRIC TECHNIQUES  
AND MULTIVARIATE DATA ANALYSIS  
Vanessa del Rio Sánchez  
ISBN:978-84-693-9439-7/ DL:T.64-2011

1

# I Introduction



UNIVERSITAT ROVIRA I VIRGLI  
FAST ANALYTICAL METHODOLOGIES BASED ON MOLECULAR SPECTROPHOTOMETRIC TECHNIQUES  
AND MULTIVARIATE DATA ANALYSIS  
Vanessa del Rio Sánchez  
ISBN:978-84-693-9439-7/ DL:T.64-2011

## 1.1. BACKGROUND

One of the keys to achieving the goal of developing a fast analytical methodology is the establishment of analytical procedures in which the step related to the pre-treatment of the samples for isolating the analyte of interest before its identification or quantification could be minimized or even eliminated. The development of this kind of methodology is not only an issue of economic interest, but also of environmental and social interest. Environmental regulation, societal concerns and growing environmental awareness throughout the world have triggered the search for new products and processes that are compatible with the environment. The development of fast analytical methodologies accomplishes both the economic and environmental goals simultaneously through the minimization of the amount of reactants and waste, and the use of techniques that allow real-time monitoring and control, as reflected in principles 1, 5 and 11 of Green Chemistry [1].

As natural resources are being used up in the world, the use of raw materials and feedstocks that are renewable rather than depleting, e.g. vegetable oils, is one of the current challenges for the society, so it is of great significance and there is a patent need to develop fast, simple and low-cost methods for the analysis of these new products.

One interesting field of application for these methods is the evaluation of the possibilities that modified vegetable oils offer as precursors of pre-polymers. The chemical modification of vegetable oils, which is performed using the reactivity of the functional groups in their structure, enables the synthesis of designed monomers in such a way as to target polymeric materials [2,3]. The growing interest in the use of these substances is justified by the environmental



advantages compared with the use of polymers prepared from petroleum-based monomers.

Another remarkable field of application is the quality control of biodiesel, which is mostly obtained from vegetable oils by a process called transesterification [4,5]. To meet rising energy demands and to compensate for diminishing petroleum reserves, biodiesel used as neat diesel or in blends with petroleum-based diesel fuels is one of the alternative technologies.

The analytical methods developed in this thesis are characterized by the employment of molecular spectroscopic techniques such as infrared and UV-visible spectroscopy. The latter has been used integrating a diode array UV-visible detector into a flow-system, or more precisely into a sequential injection analysis (SIA) system.

These analytical techniques are robust and are commonly used in analytical laboratories for qualitative and quantitative analysis. The popularity of these techniques stems from their easy use and the speed of the analysis. However, their lack of selectivity makes it very difficult to gather complete analytical signals for every analyte of interest in multicomponent samples. In this thesis, this problem has been solved using methods based on the mathematical resolution of multivariate signals, which allow a rapid resolution and quantification of each chemical species in complex samples.

## 1.2. OBJECTIVES OF THE THESIS

The main objective of this thesis is to develop rapid analytical methodologies based on molecular spectrophotometric techniques and multivariate data analysis addressed to the quantitative monitoring of curing processes and to the control and characterization of products derived from vegetable oils. This main objective has given rise to other specific objectives:

- a) To develop analytical methodologies, based on infrared spectroscopy and second-order data treatment, for the quantitative study of the specific model polymer reactions of interest to obtain vegetable oil-based thermosetting polymers. Two kinds of reactions have been considered:
  - 1) The reaction between a derivative epoxidized oleic oil and aniline as a hardener. This reaction is taken as a model of the curing process in the manufacture of epoxy resins from triglycerides and diamines.
  - 2) The reaction between a modified fatty acid ester with  $\alpha,\beta$ -unsaturated ketone groups (enone-containing methyl oleate) and aniline as a hardener. This reaction is taken as an aza-Michael model of the curing process in the preparation of thermosets from triglycerides and diamines.
- b) To develop analytical methods, based on sequential injection analysis (SIA) and second-order data treatment, to determine the

specific parameters of interest for the characterization of biodiesel.

More specifically, two methods have been developed:

- 1) A method to determine the total acidity in biodiesel. This method has also been applied to total acidity determination in vegetable oils.
- 2) A method to determine sulphates in biodiesel. This method has also been applied to sulphate determination in natural and residual waters.

### 1.3. STRUCTURE OF THE THESIS

This thesis is based on papers published in international journals. These papers have been edited to give a uniform format. The contents have been structured in five chapters.

Chapter 1. **Introduction.** This chapter presents and defines the specific aims of the thesis detailing the application fields of the developed methodologies. The specific area of interest of the work carried out is highlighted.

Chapter 2. **Multivariate data analysis methods.** This chapter introduces the theoretical background of multidimensional spectroscopy and contains a brief description of the chemometric tools used in the treatment of the signal (multivariate curve resolution – alternating least squares method).

Chapter 3 and 4 contain the bulk of the work carried out for this thesis. Each of these chapters contains an introduction explaining the analytical problems we are going to look at and how they led to scientific papers. These papers describe the methods used, the results, the discussion and the conclusions.

Chapter 3. **Analytical methods based on infrared spectroscopy and second-order data treatment for the quantitative monitoring of model polymer reactions from vegetable oils.** This chapter deals with the experimentation and the analytical methodology used for studying quantitatively *in-situ* the specific model polymer reactions to obtain vegetable oil-based thermosetting polymers. Section 3.1 details the problem areas under study, offering the proper bibliographic review, and introduces the fundamentals of the developed

methodologies. Likewise, the experimental work carried out is described. Section 3.2 is addressed to the results obtained from these experiments and it is articulated in three published works introduced by a brief description of the main goal and the specific content. The first paper reports a spectroscopic and a quantitative chemometric study of the competitiveness between the oxirane functional group and the ester functional group present in the epoxidized methyl oleate (EMO) when this compound reacts with aniline as a hardener. The second paper analyses quantitatively and mechanistically the effect of the temperature on the model cure acid-catalysed reaction between the epoxidized methyl oleate (EMO) and aniline. The last paper describes the study of an aza-Michael model reaction between a modified fatty acid ester with  $\alpha,\beta$ -unsaturated ketone groups (enone-containing methyl oleate (eno-MO)) and aniline.

**Chapter 4. Analytical methods based on sequential injection analysis and second-order data treatment for determining parameters of interest in the characterization of biodiesel.** This chapter comprises two papers. Section 4.1 contains an introduction detailing considerations of a general and practical nature to develop the specific analytical methodologies under study. The study is carried out with data obtained from sequential injection analysis (SIA) with a diode-array spectrophotometric detector. The data matrices obtained are treated with multivariate curve resolution – alternating least squares (MCR-ALS) method and the concentration of the analyte of interest is determined without the need of selective data. Experimental design methodologies are employed to optimize and select the best conditions of the system. In section 4.2, a fast analytical methodology based on sequential injection analysis with a diode array UV-visible detector and second-order data treatment is developed for the determination of total acidity in plant oils and biodiesel. In section 4.3, a new spectrophotometric sequential injection analysis (SIA-DAD) method linked to

multivariate curve resolution – alternating least squares (MCR-ALS) to determine sulphates in aqueous (natural and residual waters) and organic (biodiesel) samples is developed.

Chapter 5. **General conclusions.** This chapter contains the general conclusions of the thesis.

The **Appendix** contains the list of papers and meeting presentations given by the author during the period of development of this thesis.

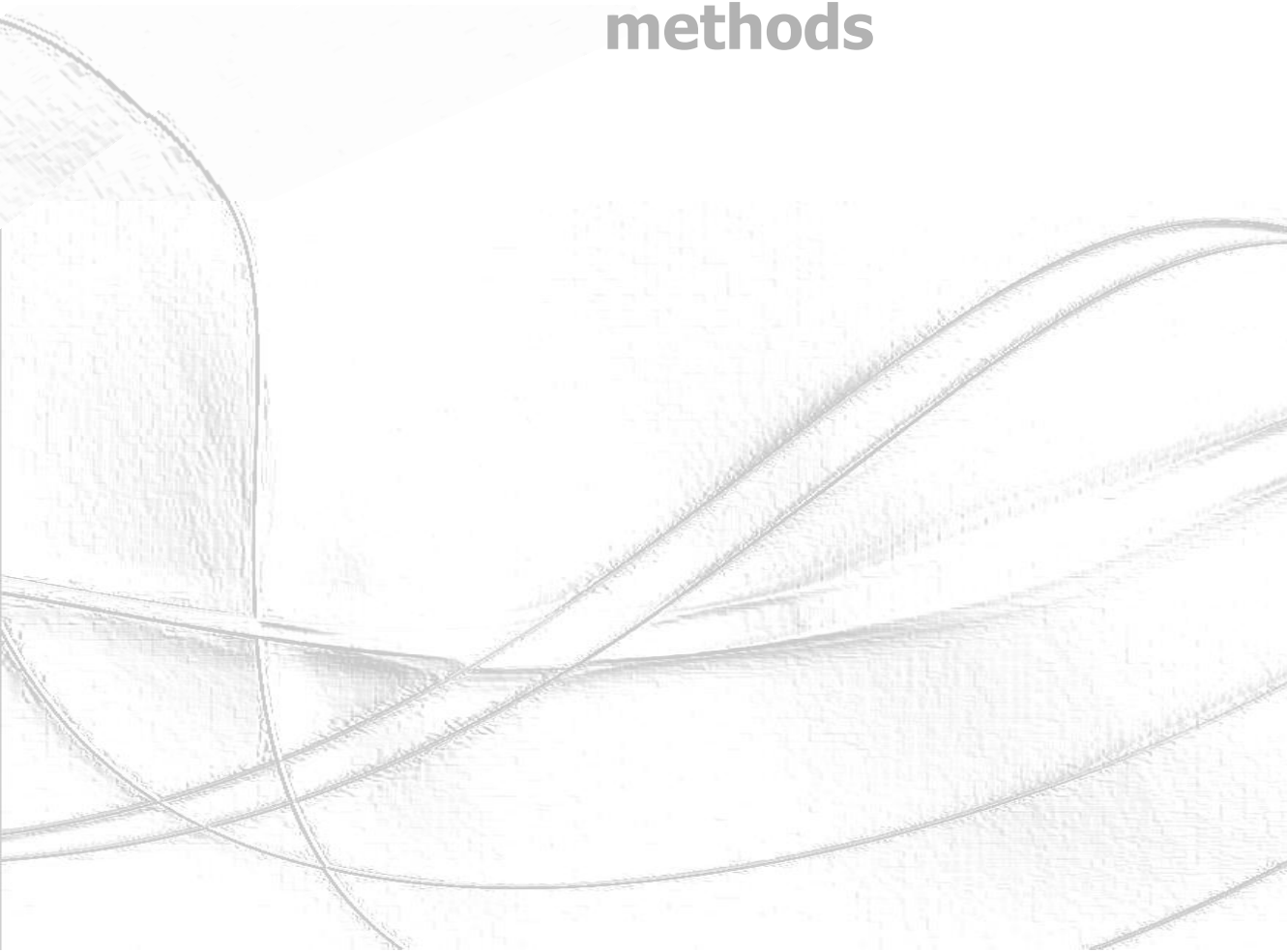
## 1.4. REFERENCES

- [1] R. Sanghi and M.M. Srivastava, *Green Chemistry. Environment Friendly Alternatives*, Alpha Science International Ltd., Pangbourne, 2003.
- [2] B.K. Sharma, Z. Liu, A. Adhvaryu and S.Z. Erhan, *J. Agric. Food Chem.* **56** (2008) 3049.
- [3] U. Biermann, W. Friedt, S. Lang, W. Lühs, G. Machmüller, J.O. Metzger, M.R. Klass, H.J. Schäfer and M.P. Schneider, *Angew. Chem. Int. Ed. Engl.* **39** (2000) 2206.
- [4] D.Y.C. Leung, X. Wu and M.K.H. Leung, *Appl. Energy* **87** (2010) 1083.
- [5] H. Fukuda, A. Kondo and H. Noda, *J. Biosci. Bioeng.* **92** (2001) 405.

UNIVERSITAT ROVIRA I VIRGILI  
FAST ANALYTICAL METHODOLOGIES BASED ON MOLECULAR SPECTROPHOTOMETRIC TECHNIQUES  
AND MULTIVARIATE DATA ANALYSIS  
Vanessa del Rio Sánchez  
ISBN:978-84-693-9439-7/ DL:T.64-2011

2

# Multivariate data analysis methods





UNIVERSITAT ROVIRA I VIRGLI  
FAST ANALYTICAL METHODOLOGIES BASED ON MOLECULAR SPECTROPHOTOMETRIC TECHNIQUES  
AND MULTIVARIATE DATA ANALYSIS  
Vanessa del Rio Sánchez  
ISBN:978-84-693-9439-7/ DL:T.64-2011

## 2.1. INTRODUCTION

Multivariate analysis, which is an important branch of chemometrics, comprises a set of techniques dedicated to the analysis of data sets characterized by multiple variables.

In this thesis, two groups of multivariate techniques have been applied:

- Multidimensional spectroscopic analysis, which has been applied to near infrared (NIR) data obtained from the monitoring of model curing polymer reactions.
- Multivariate curve resolution methods, which have been applied to near infrared (NIR) and infrared (IR) data obtained from the monitoring of model curing polymer reactions and to UV-visible data obtained from a sequential injection analysis (SIA) system.

## 2.2. MULTIDIMENSIONAL SPECTROSCOPIC ANALYSIS

An intriguing idea was put forward in the field of NMR spectroscopy almost three decades ago that, by spreading spectral peaks over the second dimension, one can simplify the visualization of complex spectra consisting of many overlapped peaks. Following this conceptual breakthrough, an impressive amount of progress has been made in the branch of science now known as *two-dimensional (2D) spectroscopy*.

Since its development, perturbation-based *generalized two-dimensional (2D) correlation spectroscopy* has evolved to become a powerful, versatile and broadly application technique for the detailed analysis of various spectroscopic data [1], which gained considerable popularity among scientists in many different areas of research activities [2-6].

### Generalized two-dimensional correlation spectroscopy

Two-dimensional correlation spectroscopy (2D-COS) was first developed in the late 1980s and in the early 1990s by Isao Noda in a series of papers in which he described the basic principles of this technique and its application to polymer systems using infrared spectroscopy [1,7-9].

The basic scheme used in 2D IR spectroscopy consists of applying an external perturbation, such as a change in concentration, temperature, pH, pressure, etc., and analysing the dynamic response of the system in the form of spectroscopic signals. Typical spectroscopic responses to external stimuli are observed in the form of changes in peak positions and intensities.

In a typical 2D experiment, a series of perturbation-induced dynamic spectra are collected in a sequential order during the process. Such a set of dynamic spectra is then transformed mathematically by cross-correlation analysis into a set of 2D correlation maps in which several peaks appear. The positions and signs of those peaks can be related to the effect of the applied perturbation.

The dynamic spectrum  $\tilde{y}(\nu, t)$  of a system induced by the application of an external perturbation is formally defined as

$$\tilde{y}(\nu, t) = \begin{cases} y(\nu, t) - \bar{y}(\nu) & \text{for } T_{min} \leq t \leq T_{max} \\ 0 & \text{otherwise} \end{cases} \quad (2.1)$$

where  $T_{min}$  and  $T_{max}$  define the finite observation interval and  $\bar{y}(\nu)$  is the reference spectrum of the system, which is commonly the averaged spectrum given by

$$\bar{y}(\nu, t) = \frac{1}{T_{max} - T_{min}} \int_{T_{min}}^{T_{max}} y(\nu, t) dt \quad (2.2)$$

In some applications, however, it is possible to select a different type of reference spectrum by choosing a spectrum observed at some fixed reference point. The selection of the reference spectrum depends on the specific type of 2D correlation analysis to be applied.

The fundamental concept governing 2D correlation spectroscopy is a quantitative comparison of the spectral intensity variations along the external perturbation ( $t$ ) observed at two different spectral variables,  $\nu_1$  and  $\nu_2$ , over

some finite interval between  $T_{min}$  and  $T_{max}$ . The 2D correlation spectrum can be expressed as

$$X(\nu_1, \nu_2) = \langle \tilde{y}(\nu_1, t) \cdot \tilde{y}(\nu_2, t') \rangle \quad (2.3)$$

where the symbol  $\langle \rangle$  denotes the cross-correlation function. The intensity of 2D correlation spectrum  $X(\nu_1, \nu_2)$  represents the quantitative measure of a comparative similarity or dissimilarity of spectral intensities variations  $\tilde{y}(\nu, t)$  measured at two different spectral variable,  $\nu_1$  and  $\nu_2$ , during a fixed interval.

In order to simplify the mathematical procedure,  $X(\nu_1, \nu_2)$  can be expressed as a complex number function

$$X(\nu_1, \nu_2) = \Phi(\nu_1, \nu_2) + \Psi(\nu_1, \nu_2) \quad (2.4)$$

comprising two orthogonal (real and imaginary) components, known respectively as the synchronous  $\Phi(\nu_1, \nu_2)$  and asynchronous  $\Psi(\nu_1, \nu_2)$  2D correlation intensities. The synchronous 2D correlation intensity represents the similarity or coincidental trends between two separate intensity variations at different spectral variables. The asynchronous 2D correlation intensity, on the other hand, may be regarded as a measure of out-of phase character of the spectral intensity variations.

The synchronous spectrum is symmetric and consists of autopeaks located along the main diagonal and cross-peaks appearing at off-diagonal positions. The autopeaks identify the signals that undergo changes during the experiment and they are always positive. The cross-peaks, on the other hand, are positive if the two signals change in the same direction (they both increase

or decrease) and are negative otherwise. The intensity of the peaks can be considered as a measure of the susceptibility of the relative signals to the external stimulus.

The asynchronous correlation spectrum is antisymmetric and it contains no autopeaks but only cross-peaks at off-diagonal positions, which develops only if the intensities of two spectral features change out of phase with each other. The sign of asynchronous peaks provides useful information about the sequential order of the intensity variations between  $\nu_1$  and  $\nu_2$ . According to the Noda and Ozaki publications [10], when  $\Phi(\nu_1, \nu_2) > 0$ , if  $\Psi(\nu_1, \nu_2) > 0$ , the intensity changes at  $\nu_1$  occurs predominantly before that at  $\nu_2$ . On the other hand, if  $\Psi(\nu_1, \nu_2) < 0$ , the change at  $\nu_1$  occurs predominantly after  $\nu_2$ . However, this sign rule is reversed if  $\Phi(\nu_1, \nu_2) < 0$ .

## 2.3. MULTIVARIATE RESOLUTION METHODS

Multivariate resolution methods make up a set of mathematical tools whose goal is the recovery of chemical and/or physical information from the experimental data.

There are different groups of multivariate resolution methods. Firstly, the soft-modeling approaches, which are meant to describe processes without using explicitly the underlying chemical model linked to them [11]. Among these different approaches, this thesis is focussed on the multivariate curve resolution - alternating least squares (MCR-ALS) method, which will be studied in depth later. Secondly, the hard-modeling approaches, which fit the results to an initially postulated physicochemical law [12]. Finally, an approach that mixes the qualities of hard-modeling and soft-modeling methods, which is called hard-soft modeling [13].

### **Multivariate curve resolution - alternating least squares (MCR-ALS)**

The main goal of multivariate curve resolution – alternating least squares (MCR-ALS) [14] is the decomposition of the initial data matrix into the product of two matrices that contain the pure concentration and response profiles of all the active species presents in the system (Figure 2.1), assuming that the experimental data follow a bilinear model of analogous structure to the generalized law of Lambert-Beer:

$$\begin{array}{c}
 \begin{array}{|c|} \hline \mathbf{D} \ (m \times n) \\ \hline \end{array} \\
 \begin{array}{c} n \\ m \end{array}
 \end{array}
 =
 \begin{array}{c}
 \begin{array}{|c|} \hline \mathbf{C} \ (m \times c) \\ \hline \end{array} \\
 \begin{array}{c} c \\ m \end{array}
 \end{array}
 \begin{array}{c}
 \begin{array}{|c|} \hline \mathbf{S}^T \ (c \times n) \\ \hline \end{array} \\
 \begin{array}{c} n \\ c \end{array}
 \end{array}
 +
 \begin{array}{c}
 \begin{array}{|c|} \hline \mathbf{E} \ (m \times n) \\ \hline \end{array} \\
 \begin{array}{c} n \\ m \end{array}
 \end{array}$$

**Figure 2.1.** Decomposition of matrix **D** by multivariate curve resolution - alternating least squares (MCR-ALS).

In matrix notation, the model can be written as

$$\mathbf{D} = \mathbf{C}\mathbf{S}^T + \mathbf{E} \quad (2.5)$$

where **D** is the original data matrix, **C** and **S<sup>T</sup>** are the matrices containing the concentration and response profiles, respectively, and **E** is the matrix of residuals not explained by the model and ideally it should be close to the experimental error. The dimensions of the four matrices are **D** ( $m \times n$ ), **C** ( $m \times c$ ), **S<sup>T</sup>** ( $c \times n$ ) and **E** ( $m \times n$ ), where  $m$  and  $n$  are the number of rows and the number of columns of the original data matrix, respectively, and  $c$  is the number of chemical components in the mixture or process. In spectroscopic measurements, the rows of **D** are the individual spectra measured for the different analysed samples and the columns are the absorbance values measured at each spectral wavelength.

To carry out the resolution process, the decomposition of the **D** matrix by MCR-ALS is performed in accordance to the following scheme:



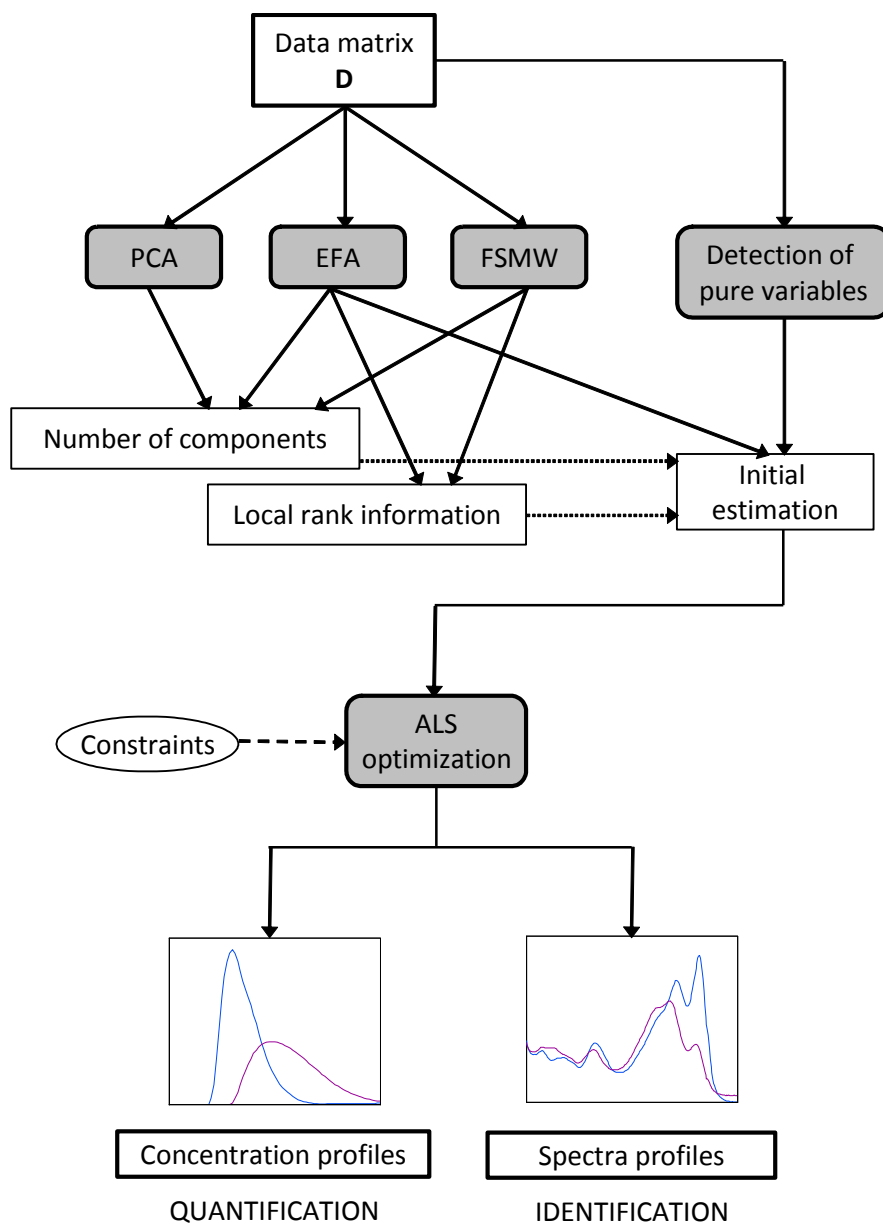


**Figure 2.2.** Scheme of the resolution process of the MCR-ALS method.

From a data matrix, firstly, it is necessary to determine how many principal components or sources of variation are present in the system, i.e. the chemical rank. In a second step, initial estimations of either the concentration profiles or the spectra profiles are created from the number of significant components previously found. Finally, from the initial estimation, alternating least squares (ALS) is applied to obtain a matrix of concentration and a matrix of spectra profiles in order to quantify (quantification analysis) or identify (qualitative analysis) the species. Although resolution does not require previous knowledge about the chemical system under study, additional knowledge, when existing, can be used to improve the results obtained and to tailor the sought pure profiles according to certain known features.

MCR-ALS is one of the curve resolution methodologies that have been proved to have high applicability in the study and resolution of second-order and three-way data matrices [15-17].

### ***Evaluation and determination of the number of components***

One of the main points in a curve resolution analysis is the determination of the number of components that make up the system. There are many exploratory procedures to determine the number of components [18]. Two of the most employed are Principal Component Analysis (PCA) and Evolving Factor Analysis (EFA).

#### a) Principal Component Analysis (PCA)

PCA is one of the most basic and widely used chemometric tool devoted to find the number and direction of the relevant sources of variation in a bilinear

data set [19]. PCA retain the main information contained in the original variables in a smaller number of variables, called principal components (PCs), which describe the most important variations in the data. These PCs are linear combinations of the original variables, they are orthogonal (i.e. uncorrelated to each other) and hierarchical (i.e. the first PC retains the maximum information of the data, the second PC retains the maximum information that is not included in the first one, and so on).

This method decomposes the experimental data matrix  $\mathbf{D}$  into the product of two matrices, which describes the original data in a more condensed way:

$$\mathbf{D} = \mathbf{UV}^T + \mathbf{E} \quad (2.6)$$

where  $\mathbf{U}$  is the score matrix that contains information about the samples and  $\mathbf{V}^T$  is the loading matrix that provides information about the importance of the variables. The residuals are collected in the  $\mathbf{E}$  matrix.

Principal component analysis can be performed using various algorithms. One of the most important is singular value decomposition (SVD) [20]. The easiest form to determine the number of components by a SVD analysis is the graphic representation of the singular values *versus* the number of components (Figure 2.3). The factors that have associate low singular values only gather information about the noise associated with the experimental measures.

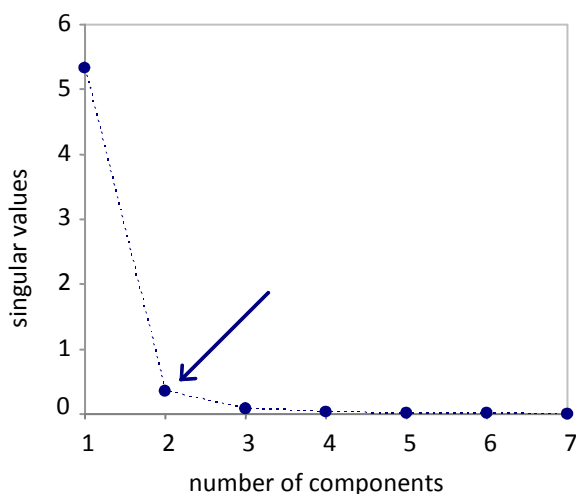


**Figure 2.3.** Singular value decomposition of a data matrix. The arrow indicates the number of significant principal components.

b) Evolving Factor Analysis (EFA)

EFA [21,22] aims to determine how many species there are at any time during an evolving system. The process starts applying singular value decomposition to a sub-matrix that contains only the first two rows of the initial data matrix  $\mathbf{D}$  and then adding the third spectra of the data matrix to the initial sub-matrix to calculate the rank. This process is repeated until singular value decomposition is applied to the whole matrices. It is performed in both directions: from top to bottom of the data set (forward EFA) and from bottom to top (backward EFA). The representation of eigenvalues logarithm *versus* row number is useful to investigate the emergence and the decay of the process contributions (see Figure 2.4).

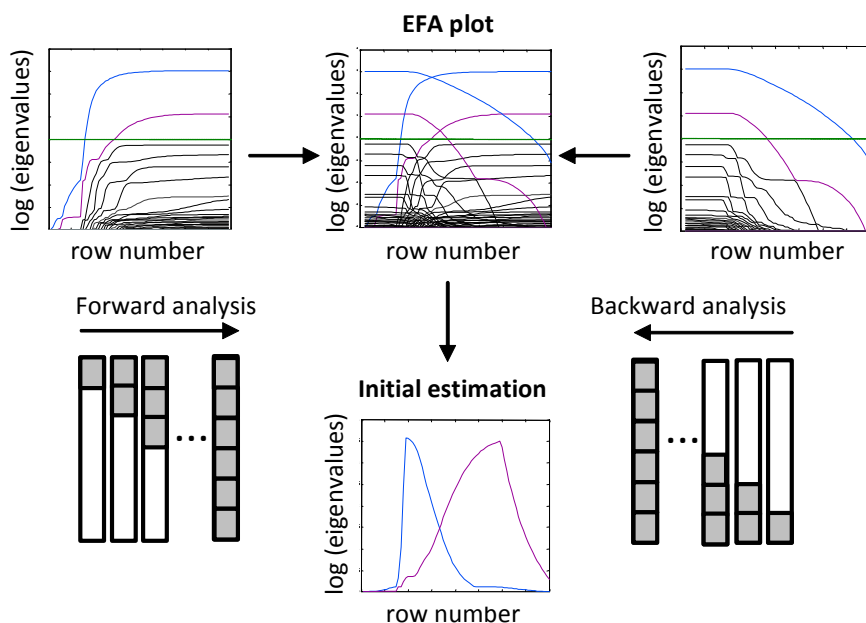


**Figure 2.4.** Steps in EFA method for a data matrix. The green line indicates the threshold selected.

Selecting a suitable threshold value, which delimits the noise level of the data, from the combination of the forward EFA and backward EFA analysis it is possible to estimate the number of components which contribute to the variability of the experimental data. In addition, EFA can be used as a tool for the exploratory analysis of the data matrix to looking for selectivity regions or localized rank information.

Nowadays, a modification of the EFA algorithm to be used with three-way data sets obtained from rank deficient systems, has been appeared [23,24]. The modified EFA algorithm is performed on a full rank augmented data set formed by column-wise appending a full rank matrix ( $\mathbf{D}_{fr}$ ) and the rank deficient matrix ( $\mathbf{D}_{rd}$ ). The EFA algorithm works according to the following steps:

1. Forward EFA on the augmented matrix  $[\mathbf{D}_{fr}, \mathbf{D}_{rd}]$ .
2. Backward EFA on the augmented matrix  $[\mathbf{D}_{rd}, \mathbf{D}_{fr}]$ .
3. Combined EFA plot taking into account the contributions present exclusively in  $\mathbf{D}_{rd}$ .

Applying this new tool and the appropriate augmentation strategy, local rank information of the contributions present in the rank-deficient matrix can be obtained. Fig. 2.5 shows graphically the procedure followed and the plots obtained when this algorithm is applied to a full rank augmented data set  $[\mathbf{D}_{fr}, \mathbf{D}_{rd}]$ . The forward and backward EFA are performed as in the classical algorithm, however the information in the plots is fundamentally different from the classical EFA analysis of  $\mathbf{D}_{rd}$ . Looking at the forward and backward EFA plots, the evolution of five significant contributions can be detected emerging from the noise level. A vertical line divides the plots in two sections, separating the information related to the rank-deficiency matrix  $\mathbf{D}_{rd}$  (three significant contributions) and the full-rank matrix  $\mathbf{D}_{fr}$  (two significant contributions).

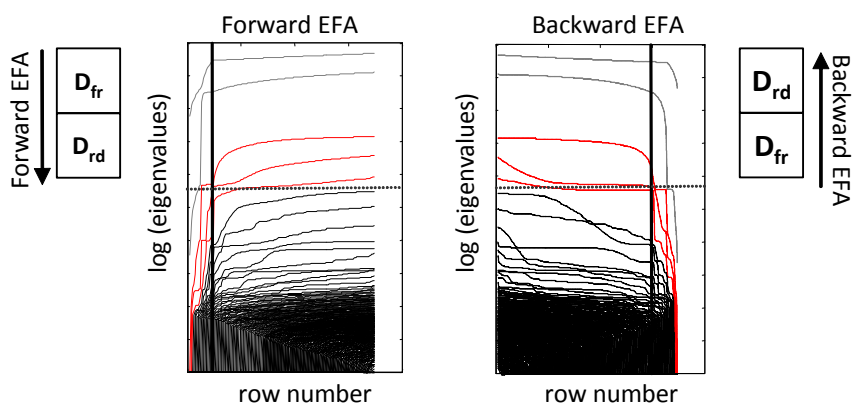


**Figure 2.5.** Graphical information of the modified EFA for full rank augmented data sets. (Red lines indicate the contributions exclusively present in the rank-deficient matrix  $\mathbf{D}_{rd}$ ).

The scheme of this new approach is based on the following strategy: first, rotational ambiguity is broken by matrix augmentation. Then, EFA is applied to the unfolded full rank augmented data set eventually providing information about contributions that are otherwise hidden.

### ***Search of the initial estimations***

Once the most appropriate number of factors that can be related to the chemical species presents in the system is determined, initial estimations of the concentration and/or the spectra profiles of these species are created. Good initial estimations help the alternating least squares (ALS) algorithm to achieve quickly the convergence towards the real solution.

In some cases, these estimations can be calculated from the previous known concentration or spectra profiles. Even so, initial estimates of the spectral and concentration profiles of the species present in a system are available from techniques based on evolving factor analysis (as EFA) [25-27] or from techniques based on the detection of purest variables (as Simple-to-use- Interactive Self-Modelling Mixture (SIMPLISMA)) [28-31].

SIMPLISMA is based on the search of pure variables. This information is obtained from the evaluation of the relative standard deviation of the column  $n$ , defined from equation (2.7)

$$p_n = \frac{s_n}{\bar{x}_n + \delta} \quad (2.7)$$

where  $s_n$  is the standard deviation of the column  $n$ ,  $\bar{x}_n$  is the average of the column  $n$  and  $\delta$  is a correction factor that is added in order to prevent columns with a low average value (generally associated with noise) from being the purest variables. A large relative standard deviation ( $p_n$ ) indicates a high purity of the column.

SIMPLISMA resolves sequentially the components. In a first step, the process involves finding the column with the highest value of relative standard deviation and then normalising this column. The process continues to select the successive columns on which it imposes the additional condition that they must have the least correlation with the previous ones.

### ***Optimization process by Alternating Least Squares (ALS)***

The third step in the multivariate curve resolution process is to optimize the initial estimations in order to obtain a result with chemical significance that corresponds satisfactorily to the experimental behaviour observed.

Equation (2.5) can be solved iteratively using an Alternating Least Squares (ALS) algorithm [32,33], which calculates concentration  $\mathbf{C}$  and pure spectra  $\mathbf{S}^T$  optimally fitting the experimental data matrix  $\mathbf{D}$ . When an initial estimation of the concentration matrix  $\mathbf{C}$  is available, the least squares solution for the spectra is estimated from:

$$\mathbf{S}^T = \mathbf{C}^+ \mathbf{D}^* \quad (2.8)$$



If, on the contrary, an initial estimation of the spectra matrix is known, the least squares solution for the concentration profiles can be calculated from the expression:

$$\mathbf{C} = \mathbf{D}^*(\mathbf{S}^T)^+ \quad (2.9)$$

where  $\mathbf{C}^+$  is the pseudoinverse of matrix  $\mathbf{C}$ ,  $(\mathbf{S}^T)^+$  is the pseudoinverse matrix of  $\mathbf{S}^T$  obtained from the initial estimation and  $\mathbf{D}^*$  is the data matrix reconstructed from the number of significant principal components selected in the principal component analysis.

Both steps can be implemented in an alternating least squares cycle so that in each iteration new matrices of  $\mathbf{C}$  and  $\mathbf{S}^T$  are then obtained. Convergence is achieved when in two consecutive iterative cycles, relative differences in standard deviations of the residuals between experimental and ALS calculated data values are lower than a previously selected value, usually chosen as 0.1%.

The final result of the iterative process can be improved using additional information based on physical and chemical knowledge of the system under study. The introduction of this information is carried out through the implementation of constraints [34,35].

A constraint can be defined as any chemical or mathematical property that is systematically satisfied by the whole system or by some parts of their pure contributions [36,37]. The constraints that can be applied for each iterative cycle are:

- *Non-negativity.* The concentrations of the chemical species and/or the values of the spectra must be positive or zero.

- *Unimodality*. This constraint imposes the existence of only one maximum in each response profile, which is common in the concentration profiles but not in the spectra profiles.
- *Closure*. It is applied in systems for which the quantity of matter is constant, i.e. when the sum of the concentrations of all the species involved in the reaction or the sum of some of them is forced to be constant at each stage of the reaction.
- *Selectivity*. It is used when zones are known to be totally selective for one of the species. It is the same as restricting the concentrations or signals of the other components to zero.

### ***Evaluation of the process quality***

There are different parameters from which it is possible to obtain information about the goodness of the model fit by MCR-ALS. One of them is the lack of fit (lof) of the model, expressed in equation 2.10:

$$lof = \sqrt{\frac{\sum (d_{ij}^* - d_{ij})^2}{\sum d_{ij}^2}} \quad (2.10)$$

where  $d_{ij}$  are each of the elements of the experimental matrix  $\mathbf{D}$  and  $d_{ij}^*$  are each of the elements of the reproduced data matrix  $\mathbf{D}$ , obtained by the MCR-ALS decomposition. Therefore, depending on the matrix used, either  $lof_{exp}$  or  $lof_{pca}$  is obtained.

Another parameter to evaluate the quality of the model is the percentage of explained variance, which is given by

$$R^2 = \frac{\sum_i \sum_j d_{ij}^{*2}}{\sum_i \sum_j d_{ij}^2} \quad (2.11)$$

When pure analyte is available, another way to check whether the model is well fit is to determine the correlation between the spectra obtained in the resolution process and the spectra of the pure species, calculated by (2.12)

$$r = \cos \gamma = \frac{s_i^T s_i^*}{\|s_i\| \|s_i^*\|} \quad (2.12)$$

where  $\gamma$  is the angle defined by the vectors associated to the spectrum recovered by MCR-ALS ( $s_i^*$ ) and the real spectrum ( $s_i$ ), for a particular species studied  $i$ .

### ***Simultaneous analysis of data from multiple experiments***

One of the main characteristics of the MCR-ALS method is the possibility of analyse data from different experiments simultaneously [32,33,38,39]. In this case, an augmented data matrix is created arranging the individual data matrices of each experiment. Several types of augmented data matrices can be obtained: a column-wise augmented data matrix (a), a row-wise augmented data matrix (b), or a column- and row-wise augmented data matrix (c) (see Figure 2.6).

This strategy is very useful to overcome intrinsic rotational ambiguities [40] and rank deficiency problems [41], i.e. when the number of significant principal components is lower than the number of chemical species of the system.

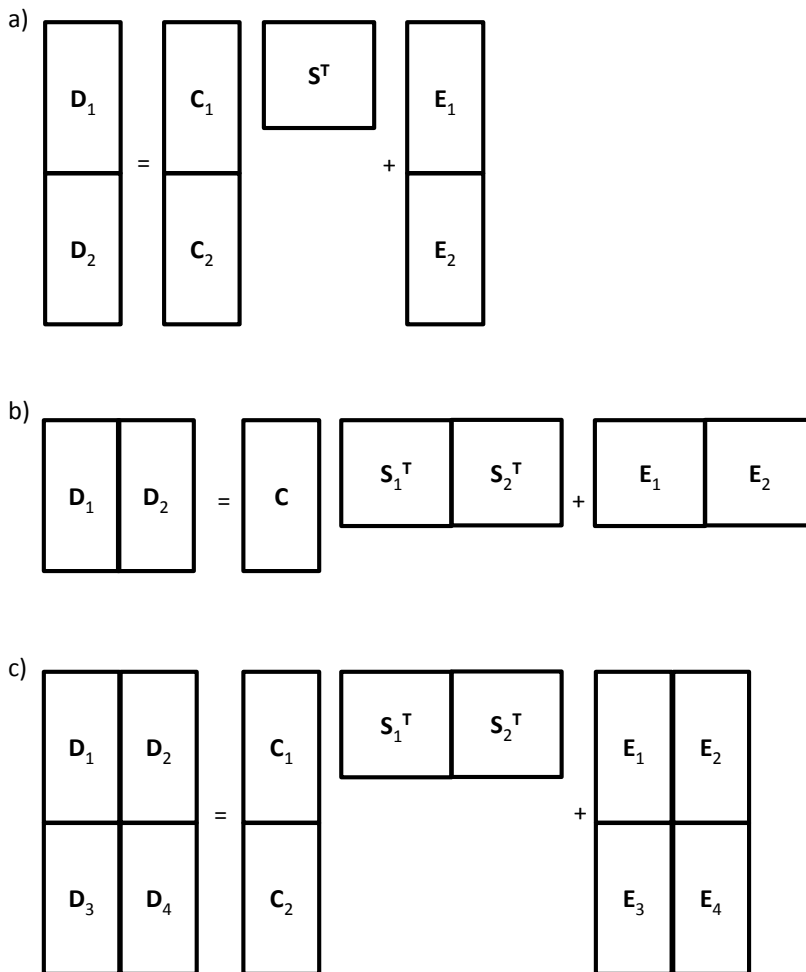


**Figure 2.6.** Arrangement of matrices and information obtained from MCR-ALS. (a) Column-wise augmented matrices, (b) row-wise augmented matrices and (c) row- and column-wise augmented matrices.

From an algorithmic and mathematical point of view, the complexity of the MCR-ALS resolution process does not change significantly. In the resolution of augmented matrices, augmented concentration and/or spectra profiles are generated, on which similar restrictions as the applied in the MCR-ALS analysis of a single matrix can be applied. In addition, there are two more constraints that only can be applied working with augmented matrices:

- Constraint related to the *correspondence of species*. This constraint fixes the species presents or absents in each sub-augmented matrix.
- *Trilinearity* (three-way structure). This condition imposes a unique response profile of one analyte in the various matrices used.

These constraints and the above described can be applied to all the sub-augmented matrices or only to some of them, i.e. only those in which the application of these constraints has sense.

## 2.4. REFERENCES

- [1] I. Noda, *Appl. Spectrosc.* **44** (1993) 1329.
- [2] H. Shinzawa, K. Awa, T. Okumura, S. Morita, M. Otsuka, Y. Ozaki and H. Sato, *Vibr. Spectrosc.* **51** (2009) 125.
- [3] I. Noda, *J. Molec. Struct.* **883** (2008) 2.
- [4] Y.M. Li, S.Q. Sun, Q. Zhou, J.X. Tao and I. Noda, *Spectrochim. Acta: Part A: Molec. and Biomolec. Spectrosc.* **63** (2006) 565.
- [5] I. Noda, *J. Molec. Struct.* **799** (2006) 2.
- [6] Y.M. Jung and I. Noda, *Appl. Spectrosc. Rev.* **41** (2006) 515-547.
- [7] I. Noda, *Bull. Am. Phys. Soc.* **31** (1986) 520.
- [8] I. Noda, *J. Am. Chem. Soc.* **111** (1989) 8116.
- [9] I. Noda, *Appl. Spectrosc.* **44** (1990) 550.
- [10] I. Noda and Y. Ozaki, *Two-Dimensional Correlation Spectroscopy*, Wiley, Chichester, 2004.
- [11] A. de Juan and R. Tauler, *Crit. Rev. Anal. Chem.* **36** (2006) 163.
- [12] G. Putxy, M. Maeder and K. Hungerbühler, *Chemom. Intell. Lab. Syst.* **81** (2006) 149.
- [13] A. de Juan, M. Maeder, M. Martínez and R. Tauler, *Chemom. Intell. Lab. Syst.* **54** (2000) 123.
- [14] R. Tauler, B. Kowalski and S. Flemming, *Anal. Chem.* **65** (1993) 2040.
- [15] M. Garrido, F.X. Rius and M.S. Larrechi, *Anal. Bioanal. Chem.* **390** (2008) 2059.
- [16] M. Esteban, C. Arino, J.M. Diaz-Cruz, M.S. Diaz-Cruz and R. Tauler, *Trends Anal. Chem.* **19** (2000) 49.
- [17] T. Azzouz and R. Tauler, *Talanta* **74** (2008) 1201.
- [18] E.R. Malinowski, *J. Chemom.* **13** (1999) 69.

- [19] D.L. Massart, B.G.M. Vandeginste, S.N. Deming, Y. Michotte and L. Kaufman, *Chemometrics: a textbook*, Part B, Elsevier, Amsterdam, 1988.
- [20] D.L. Massart, B. M. G. Vandeginste, L.M.C. Buydens, S. de Jong, P.J. Lewi and J. Smeyers-Verbeke, *Handbook of Chemometrics and Qualimetrics*, Part A, Elsevier, Amsterdam, 1997.
- [21] M. Maeder, *Anal. Chem.* **59** (1987) 527.
- [22] H. Gampp, M. Maeder, C.J. Meyer and A.D. Zuberbühler, *Talanta* **33** (1986) 943.
- [23] A. de Juan, S. Navea, J. Diework and R. Tauler, *Chemom. Intell. Lab. Syst.* **70** (2004) 11.
- [24] C. Ruckebusch, A. de Juan, L. Duponchel and J.P. Huvenne, *Chemom. Intell. Lab. Syst.* **80** (2006) 209.
- [25] C. Mason, M. Maeder and A. Whitson, *Anal Chem.* **73** (2001) 1587.
- [26] E.R. Malinowski, *J. Chemom.* **10** (1996) 273.
- [27] A.C. Whitson and M. Maeder, *J. Chemom.* **15** (2001) 475.
- [28] W. Windig and S. Markel, *J. Molec. Struct.* **292** (1991) 161.
- [29] W. Windig and J. Guilmet, *Anal. Chem.* **63** (1991) 1425.
- [30] W. Windig, *Chemom. Intell. Lab. Syst.* **36** (1997) 3.
- [31] W. Windig, N.B. Gallagher, J.M. Shaver and B.M. Wise, *Chemom. Intell. Lab. Syst.* **77** (2005) 85.
- [32] R. Tauler, A. Izquierdo-Ridorsa and E. Cassassas, *Chemom. Intell. Lab. Syst.* **18** (1993) 293.
- [33] A. Izquierdo-Ridorsa, J. Saurina, S. Hernández-Cassou and R. Tauler, *Chemom. Intell. Lab. Syst.* **38** (1997) 183.
- [34] R. Bro and S. De Jong, *J. Chemom.* **11** (1997) 393.
- [35] R. Tauler and E. Casassas, *Anal. Chim. Acta* **248** (1991) 447.
- [36] R. Gargallo, F. Cuesta-Sánchez, D.L. Massart and R. Tauler, *Trends Anal. Chem.* **15** (1996) 279.

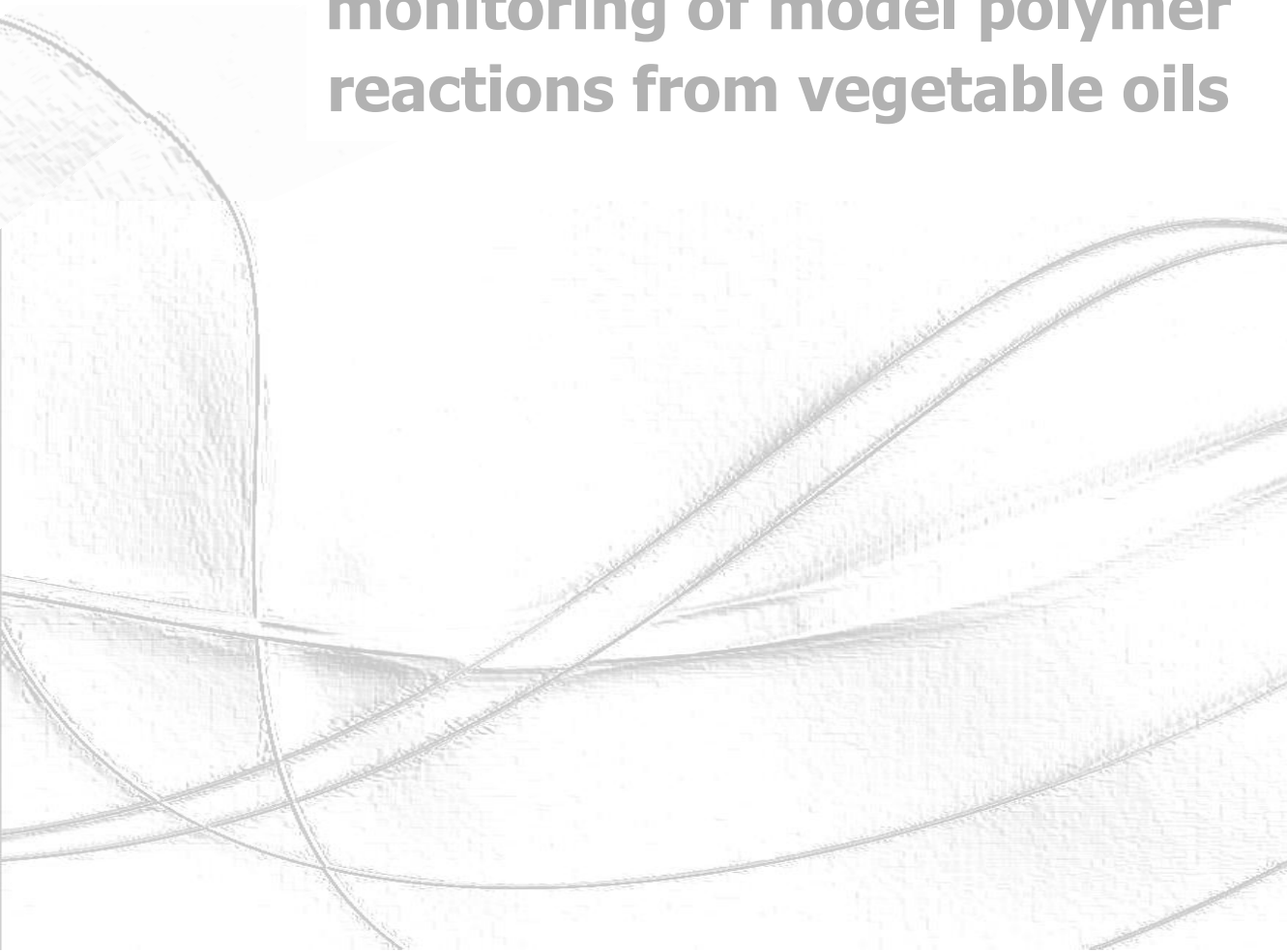
- [37] A. de Juan, Y. Vander-Hieden, R. Tauler and D.L. Massart, *Anal. Chim. Acta* **346** (1997) 307.
- [38] R. Tauler, A. Smilde and B. Kowalski, *J. Chemom.* **9** (1995) 31.
- [39] R. Tauler and D. Barceló, *Trends Anal. Chem.* **12** (1993) 319.
- [40] R. Tauler, B. Kowalski and S. Fleming, *Anal. Chem.* **65** (1993) 2040.
- [41] M. Amrhein, B. Srinivassan, D. Bonvin and M.M. Schumacher, *Chemom. Intell. Lab. Syst.* **33** (1996) 17.



UNIVERSITAT ROVIRA I VIRGLI  
FAST ANALYTICAL METHODOLOGIES BASED ON MOLECULAR SPECTROPHOTOMETRIC TECHNIQUES  
AND MULTIVARIATE DATA ANALYSIS  
Vanessa del Rio Sánchez  
ISBN:978-84-693-9439-7/ DL:T.64-2011

# 3

## **A** nalytical methods based on infrared spectroscopy and second-order data treatment for the quantitative monitoring of model polymer reactions from vegetable oils



UNIVERSITAT ROVIRA I VIRGLI  
FAST ANALYTICAL METHODOLOGIES BASED ON MOLECULAR SPECTROPHOTOMETRIC TECHNIQUES  
AND MULTIVARIATE DATA ANALYSIS  
Vanessa del Rio Sánchez  
ISBN:978-84-693-9439-7/ DL:T.64-2011

### 3.1. INTRODUCTION

This chapter includes, in three papers, the experimental part and the methodology for developing analytical methods based on infrared spectroscopy and second-order data treatment to study quantitatively *in-situ* the specific model polymer reactions of interest to obtain vegetable oil-based thermosetting polymers.

Among the polymerization processes, the curing of epoxy resins has been the most studied system [1-3]. The increasing interest in advanced composite materials based on epoxy resins matrices could be explained, in part, by the high performance of such thermosets. As important industrial materials, epoxy resins exhibit the attractive characteristics of heat and chemical resistance, excellent electrical insulating and mechanical properties and good adhesion to many substrates.

Nowadays, the depletion of the earth's limited petroleum reserves has heightened interest in using renewable resources as replacement materials for epoxy resins. The chemical transformation of triglycerides affords a wide variety of monomers for the synthesis of linear, hyperbranched or cross-linked structures. The modification of triglycerides is performed using the reactivity of the functional groups in their structure. Epoxidation is one of the most important functionalization reactions of the carbon - carbon double bond, which can be achieved by environmentally friendly procedures [4,5], and the opening of the epoxide ring is a versatile reaction that leads to numerous products [6,7].

The preparation of biobased epoxy resins from epoxidized vegetable oils has been the subject of many studies [8-10]. Nevertheless, epoxidized fatty oils, which contain oxirane groups that are hindered at both carbons, react sluggishly

with nucleophilic curing agents. On the other hand, the Michael addition reaction has received significant attention as a versatile tool in the synthesis of novel polymeric networks [11], which offer promise as high performance coatings, adhesives and laminates, and it is being used for the synthesis of biobased thermosets [12].

In this thesis, two chemical systems in which the pre-polymer used comes from vegetable oils have been studied:

- The model reaction between the epoxidized methyl oleate (EMO) and aniline. This system can be considered as a representative way to synthesize robust networks with good adhesive characteristics similar to those of conventional thermosets based on diglycidylether of Bisphenol A.
- The model reaction between a modified fatty ester with  $\alpha,\beta$ -unsaturated ketone groups (enone-containing methyl oleate (eno-MO)) and aniline. This system, which represents a variation of the common Michael reaction, permits the synthesis of sophisticated macromolecular structures with potential use in many applications such as drug delivery systems, high performance composites and coatings.

It is known that the final properties of the polymer are linked to the conditions of the curing process and the reaction pathway is affected by such characteristics of the experimental conditions, as the nature of the reactants and their concentration, the presence of catalysts and the temperature, among others. This dependence explains the numerous studies carried out to understand the mechanism better and to quantify the kinetics of these cure

reactions using several techniques such as differential scanning calorimetry (DSC) [13,14], thermogravimetric analysis (TGA) [15], fluorescence [16,17], Raman spectroscopy [18,19], nuclear magnetic resonance (RMN) [20], high-resolution liquid chromatography (HPLC) [21], Fourier transform infrared spectroscopy (FTIR) [22,23] and near infrared spectroscopy (NIR) [24-26].

Near Infrared (NIR) spectroscopy, as a consequence of the low molar absorptivities of the compounds, is a valuable tool for the *in-situ* monitoring of reactions. The most frequent bands in the NIR region are related to chemical bonds of hydrogen atoms, such as C-H, N-H, O-H and S-H. In general, the bands of the groups C=O, C-C, C-F or C-Cl, are weaker or do not appear in the NIR region. Moreover, in the NIR spectrum, the absorption bands are typically very broad and not so well defined due to the overlapping of overtones and combination bands, so spectral assignments to specific vibrational modes are not always possible and it is difficult to monitor each species involved in the process.

In the infrared (IR) spectral region, the spectral bands are related to fundamental vibrations and are relatively narrow and molecule specific, which allows more information for structural elucidation and compound identification to be extracted. Over the past decade, Fourier transform infrared (FTIR) spectroscopy has evolved rapidly and has become one of the techniques of choice to be used in both research and industry as a simple and reliable technique for measurement, quality control and dynamic measurements [27-29].

In this doctoral thesis, NIR and FTIR have been applied to monitor the reactions. The model curing reaction between the epoxidized methyl oleate (EMO) and aniline has been monitored in both regions, while the reaction between the modified fatty ester with  $\alpha,\beta$ -unsaturated ketone groups (enone-

containing methyl oleate (eno-MO)) and aniline has only been monitored in the NIR spectral region. Experimental details can be found in the particular works.

Usually, the information obtained from an FTIR or an NIR spectrum is analysed univariately, relating the changes in a characteristic band to the global advance reaction degree. However, this kind of analysis does not provide information about the number of steps involved in the process or about the concentration of each of the chemical species and their corresponding spectra.

One of the possibilities in order to obtain more information about the studied system is to use the curve resolution methods [30], which allow a multivariate analysis of the spectra data to be carried out. Since the implementation of these methods in multiple runs in an industrial process, few references to the application of quantitative resolution of reactions by NIR and FTIR spectrophotometric measurement have been found. Garrido et. al. [31-37] have worked extensively on the quantitative monitoring of epoxy resins by NIR and multivariate curve resolution – alternating least squares (MCR-ALS) method. The authors studied the epoxy-amine model curing reactions of phenylglycidylether (PGE) and silicon-based epoxy monomers with aniline, and established kinetic models with their corresponding kinetic constants for these reactions. Spegazzini et.al. [38-42] used FTIR and NIR spectroscopy combined with multidimensional correlation spectroscopic analysis and multivariate curve resolution – alternating least squares (MCR-ALS) method for the quantitative resolution of model cationic curing reactions of epoxy resins, e.g. the reactions of phenylglycidylether (PGE) and diglycidylether of Bisphenol A (DGEBA) with lactones. Blanco et. al. [43,44] have applied multivariate curve resolution methods to chemical process control of esterification reactions monitored by

near infrared (NIR) spectroscopy, with a view to establishing the effect of experimental variables on the reaction kinetics.

In this thesis, multivariate analysis methods were used to extract the desired information of the NIR and IR spectra. The model polymerization reactions studied use pre-polymers from vegetable oils synthesized by the Polymer Research Group of the Analytical and Organic Chemistry Department of the Universitat Rovira i Virgili. They are relatively new and constitute complex systems where several parallel and competitive reactions might take place. Because the final properties of the products in the polymerization reactions are related to the pathway through which the reaction takes place, the developed analytical methodologies were employed to detect the number of steps involved in the reaction, to identify the functional groups implicated in each step and to determine the concentration of each chemical species throughout the global reaction. Each one of these aspects gives useful information to evaluate the possibilities offered by vegetable oils as precursors of pre-polymers.

In general, factor analysis techniques, such as principal component analysis (PCA) and evolving factor analysis (EFA), have been used to determine the principal steps involved in the studied reactions. Classical spectroscopy and two-dimensional correlation spectroscopy (2D-COS) have been applied to identify the functional groups implicated in each step and to determine the sequential order of the reactions. Finally, multivariate curve resolution - alternating least squares (MCR-ALS) have been used to do the quantitative resolution of the concentration profiles of each chemical species.



Likewise, with regard to the reaction between the epoxidized methyl oleate (EMO) and aniline, the effect of the temperature on the kinetics of the reactions involved in the model curing system was evaluated.

### **Experimental part**

As mentioned previously, the systems studied in this thesis are reactions between pre-polymers from vegetable oils and amines. These reactions are model reactions that do not evolve into solid products, so the study of the chemical species involved throughout the reaction time can be done without considering the physical changes that take place during the polymerization process.

The pre-polymers used were synthesised by the Polymer Research Group of the Universitat Rovira i Virgili and are not commercially available. The catalysts and the aniline employed, which was distilled before its utilization, were supplied by Aldrich. All the compounds are liquid at room temperature. The experimental procedure involved weighing the necessary amounts of the reagents to obtain the desired molar ratio and mixing them until a homogenous mixture was obtained.

The near infrared (NIR) measurements were acquired using an InfraAlyzer 500 Bran-Luebbe spectrophotometer. The experimental procedure involves injecting 1 mL of the reacting mixture into the liquid cell of the spectrophotometer, which was previously thermostated at the desired temperature by a thermostatic bath PolyScience, USA (Figure 3.1). The pathlength of the liquid cell was adjusted to accommodate the sample being

analysed. The adjustment, which enables pathlengths of 0.1 to 0.5 mm, was made by rotating a dial on the liquid cell to the desired pathlength setting.

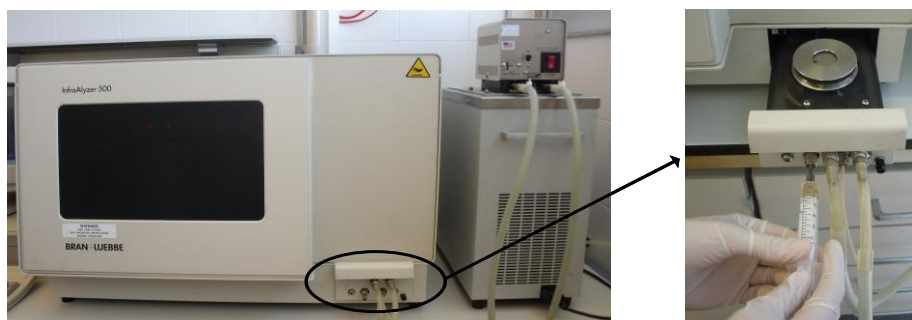


**Figure 3.1.** NIR measurements.

The Fourier transform infrared (FTIR) measurements, which were only done for the EMO/aniline system, were acquired using a FTIR 680 Plus Jasco spectrophotometer equipped with a 3000 Series<sup>TM</sup> High Stability Temperature Controller and a RS232 control to take the measurements. The reacting mixture was placed on a small diamond crystal on the spectrophotometer attenuated total reflection (ATR) cell (Figure 3.2).

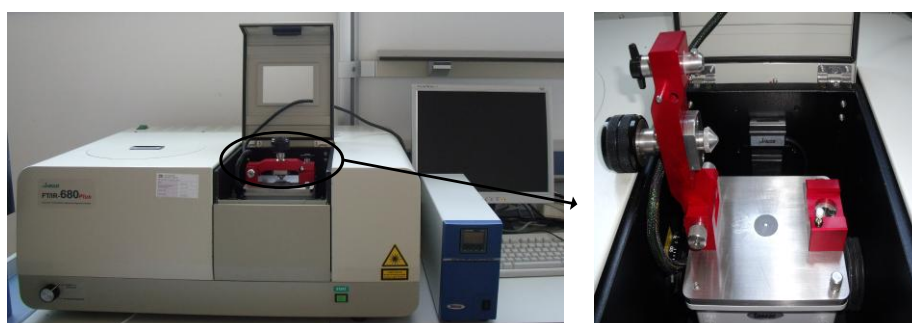


**Figure 3.2.** FTIR-ATR measurements.

The resonance magnetic nuclear (RMN) technique was employed to confirm the results found for the eno-MO/aniline system.  $^1\text{H}$  and  $^{13}\text{C}$  NMR spectra at the beginning and  $^1\text{H}$  and  $^{13}\text{C}$  NMR spectra of the mixture extracted from the NIR at the end of the experiment were recorded using a Varian Gemini 400 spectrometer with deuterated chloroform ( $\text{CDCl}_3$ ) as a solvent. A relaxation time delay of 10 seconds was used for obtaining a quantitative integration of the signals. This technique was also used to determine the purity of the synthesised pre-polymers.

## 3.2. RESULTS

### 3.2.1. A derivative epoxidized oleic oil, the epoxidized methyl oleate from high oleic sunflower oil, as pre-polymer in the curing of epoxy resins

The acid-catalysed reaction between a derivative epoxidized oleic oil (EMO) and aniline has been analysed in two works, using boron trifluoride etherate ( $\text{BF}_3 \cdot \text{OEt}_2$ ) as a catalyst. One of them has been published in *Journal of Near Infrared Spectroscopy* and the other has been submitted for publication. The EMO/aniline system studied is taken as a model of the curing process in the manufacture of epoxy resins from triglycerides and diamines.

Both works report a spectroscopic and a quantitative chemometric study of the competitiveness between the oxirane functional group and the ester functional group present in the derivative epoxidized oleic oil (EMO) when this compound reacts with aniline as a hardener. The presence of the ester group is associated with final products of poor quality [45,46]. Therefore, to analyse the competitiveness between the ring-opening reaction and the amidation reaction, which take place as a consequence of the nucleophilic attack of the aniline on the oxirane and on the ester functional groups of the epoxidized methyl oleate, respectively, it is of interest to evaluate the optimal experimental conditions of this system.

Two different experiments were performed. Initially, the EMO:aniline stoichiometric ratio was set at 1:1 and the reaction was monitored in the NIR region at 95 °C. It was observed that the system was extremely reactive and high conversion values were obtained from the beginning of the reaction. The NIR spectroscopic analysis of the results showed that the main important changes in the spectra were located in the wavelength regions where the primary and

secondary amines absorb and no specific bands of the epoxy vibrations were detected. The characterization by NIR of each species involved throughout the reaction was difficult due to the similarity between the characteristic functional groups of each compound, so the evaluation of the competitiveness between the oxirane ring and the ester group was complicated.

However, combining the conventional and two-dimensional spectroscopic analysis of the NIR data with the chemometric analysis, it was possible to detect the sequential order of both competitive reactions. Furthermore, a quantitative approximation of each species involved in the system was obtained.

The second study was performed using an EMO:aniline stoichiometric ratio of 2:1, the one habitually employed in the curing processes, and the reaction was monitored in the infrared region to avoid the drawbacks found in the previous study. To analyse the effect of the temperature on the model curing system quantitatively and mechanistically, taking into account the high conversion values obtained from the beginning of the reaction at 95 °C, the considered experimental temperatures for this study were set at 60 °C and 30 °C.

The spectroscopic analysis of the FTIR data obtained permitted the detection of specific bands of the species involved throughout the reaction and the characterization of each compound was easier. Moreover, by means of chemometric techniques, the curing kinetics and the reaction mechanism was evaluated and it was possible to obtain the quantitative resolution of each species that takes part in the system. This information permitted the analysis of the effect of the temperature on the reaction.

### **3.2.1.1. Paper**

## **Spectroscopic and quantitative chemometric analysis of the epoxidized oil/amine system**

Vanessa del Río, Nicolás Spegazzini, M. Pilar Callao, M. Soledad Larrechi

*Journal of Near Infrared Spectroscopy*, 18 (2010) 281-290

UNIVERSITAT ROVIRA I VIRGLI  
FAST ANALYTICAL METHODOLOGIES BASED ON MOLECULAR SPECTROPHOTOMETRIC TECHNIQUES  
AND MULTIVARIATE DATA ANALYSIS  
Vanessa del Rio Sánchez  
ISBN:978-84-693-9439-7/ DL:T.64-2011



## **Spectroscopic and quantitative chemometric analysis of the epoxidized oil/amine system**

**Vanessa del Río, Nicolás Spegazzini, M. Pilar Callao, M. Soledad Larrechi**

*Chemometrics, Qualimetrics and Nanosensors Research Group  
Analytical Chemistry and Organic Chemistry Department, Rovira i Virgili  
University  
Marcel·lí Domingo s/n, Campus Sescelades, 43007 Tarragona, Spain*

### **Abstract**

The competitiveness between the oxirane functional group and the ester functional group present in a derivative epoxidized oil was studied by monitoring a model system which involved epoxidized oleic oil and aniline (1:1). The reaction was carried out under isothermal conditions at 95°C and monitored *in situ* by near-infrared spectroscopy (NIR). This system is taken as a model of the curing process in the manufacture of epoxy resins from triglycerides and diamines.

Conventional spectroscopic analysis and generalized 2D NIR correlation spectroscopy analysis have led to the conclusion that, even though the formation of secondary amines by ring-opening of the oxirane group as a consequence of the nucleophilic attack of the aniline is prior, the formation of amides as a consequence of the ester group reactivity is a competitive reaction. The presence of the two aforementioned reactions is also in accordance with the significant number of factors found when the spectra data matrix was analyzed



by evolving factor analysis (EFA). By applying multivariate curve resolution-alternating least squares (MCR-ALS) to the NIR spectra obtained during the reaction, it has been possible to obtain the concentration and the spectra profiles of each chemical species involved in the reaction. The performance of the model was assessed by two parameters: ALS lack of fit (lof = 1.67 %) and explained variance ( $R^2 = 99.68$  %). The recovered spectra of the generated products have the characteristic bands associated with the two postulated reactions.

**Key words:** Near-infrared spectroscopy, Two-dimensional correlation spectroscopy, Evolving factor analysis, Multivariate curve resolution-alternating least squares, Epoxidized vegetable oil

## 1. Introduction

In recent years, the demand for green raw materials has been increasing because of the escalating price of petrochemicals and the high rate of depletion of natural mineral resources. Natural oils have therefore attracted renewed attention as alternatives to conventional petrochemicals for the manufacture of organic chemical and polymeric materials [1-6]. They can also be functionalized by epoxidation with organic peracids or  $H_2O_2$ , and epoxidized vegetable oils show excellent promise as inexpensive, renewable materials for industrial applications [7].

It is referenced in the literature [8,9] that the mechanical properties of the final products obtained from the curing processes between epoxidized vegetable oils and amines as hardeners, are of poor quality (low molecular weight and insufficient strength). This fact is attributable to the presence of the

ester group, which is characteristic of the initial fatty acid and can react with the amine group to form amides, competing with the ring-opening reaction of the oxirane ring. However, no research work is recorded where the competitiveness between these two reactions has been analyzed.

The present work focuses on the analysis of the reaction between an epoxidized derivative oleic oil, epoxidized methyl oleate (EMO), and aniline at 95 °C. The system is taken as a model of the curing process in the manufacture of epoxy resins from triglycerides and diamines. Most amine-cured epoxy resins are prepared under stoichiometric conditions or with a slight epoxy excess, which results in optimum properties. Thus, the experiment was done using an equimolar ratio (1:1).

To the best of our knowledge, this study reports the first attempt to offer a spectroscopic and a quantitative analysis of the reactions involved in the system and it represents a new work within one of the objectives of our research group, aimed at the quantitative resolution of polymer reactions using spectroscopic analysis and chemometric methods [10-13].

Near-infrared (NIR) spectroscopy, which has been shown to be a very useful technique for the *in-situ* monitoring of these kinds of processes [14-16], was used to monitor the reaction. Spectroscopic analysis of the spectral changes observed during the reactions was done using conventional spectroscopic analysis and generalized two-dimensional correlation analysis [17-21] (2D-CoS).

By and large, the spectral changes that take place during a reaction are analyzed in a univariate mode. This analysis provides information about the total degree of conversion, but does not explain how many steps are involved in the overall process, what their sequential order over time reaction is, how the

concentration of the species evolves over time (concentration profiles) or what the spectra profile of each compound is. In this work, the sequential order of the two studied reactions, the ring-opening reaction and the amidation reaction, was established by 2D correlation spectroscopy analysis and confirmed by the number of significant factors found by evolving factor analysis (EFA) [22]. These methods have led to the determination of when the amidation reaction can be considered noteworthy along the reaction time.

Rank deficiency was detected when the chemical rank of the spectra data matrix was analysed by singular value decomposition (SVD) [23]. This problem was solved by using the augmented matrices strategy [24] and the concentration and the spectra profiles of the chemical species over the reaction time were obtained using multivariate curve resolution – alternating least squares (MCR-ALS) method [25,26]. The quality of the results was evaluated by studying the residuals and such parameters as lack of fit and percentage of explained variance.

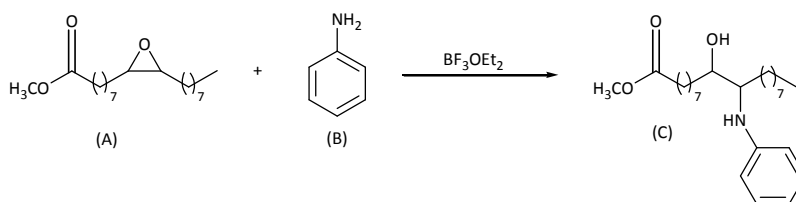
## **2. EXPERIMENTAL**

### **2.1. Materials**

The epoxidized derivative oleic oil, epoxidized methyl oleate (EMO), was synthesized and provided by the Polymer Research Group of our department [6]. Its purity was 97.89%, which was verified by elemental data analysis and  $^1\text{H}$  and  $^{13}\text{C}$  NMR spectra. Aniline reagent (Aldrich) and borontrifluoride etherate ( $\text{BF}_3 \cdot \text{OEt}_2$ ) (Aldrich) were used as received.

## 2.2. Reaction conditions and procedure

The reaction between the epoxidized derivative oleic oil (EMO, (A)) and aniline (B) in the presence of  $\text{BF}_3 \cdot \text{OEt}_2$  as a catalyst is depicted in Scheme 1. When EMO reacts with the curing agent aniline, the epoxide ring is opened and forms a new chemical chain with amine molecules (secondary amine, product C) [3,6].



**Scheme 1.** Ring-opening reaction between EMO and aniline at 95 °C. (A) EMO, (B) aniline, (C) secondary amine.

The experimental procedure involves mixing stoichiometric amounts of EMO and aniline and 2% of catalyser at room temperature to obtain the desired molar ratio and, immediately afterwards, injecting 1 mL of this mixture into the liquid cell of the NIR spectrophotometer, which is kept under the controlled temperature of 95 °C by recycling hot water-glycerine.

## 2.3. Data acquisition and data pretreatment

NIR transfectance spectra were acquired through the reaction every 4 nm at the 1100 - 2500 nm region using an Infra Analyzer 500 Bran-Luebbe spectrophotometer. This instrument has a closed liquid cell, whose pathlength was set to 0.3 mm, that allows the *in-situ* monitoring of the reaction. The software was programmed to acquire data at intervals of 5 minutes for a period

of 12 hours. After this time, no changes were observed in the spectra and a total of 144 spectra were obtained.

All the original spectra were corrected with an *off-set* correction to eliminate any vertical shift in the spectra during the course of the experiment caused by using a NIR spectrophotometer with only one light beam [27]. This pre-treatment involves subtracting from the values of reflectance, recorded at each wavelength, the lowest value of reflectance (the value at 1600 nm) for each individual spectrum.

Additionally, the wavelength range of interest was selected and those with no variations during the study period were ignored, because these provide no information about the reaction under study. The resulting, selected wavelengths ranged from 1350 to 2000 nm.

The recorded spectra were exported and converted into MATLAB binary files [28]. Pretreated experimental reaction data were arranged in a matrix **M** (144 x 163), whose rows were the number of recorded spectra and whose columns were the wavelengths.

Under the same conditions, the NIR spectra of the pure reactants (epoxidized oleic oil and aniline) were also recorded.

## 2.4. Data analysis

### 2.4.1. Spectroscopic analysis

Firstly, a conventional spectroscopic analysis of the evolution of the characteristic bands related to the functional groups involved in the reaction was carried out in order to obtain a global vision of the reaction process. From this analysis, the presence of two reactions was postulated.

Secondly, a two-dimensional correlation spectroscopic analysis using “2D shige” of Shigeaki Morita (Kwansei-Gakuin University) [29] was performed to obtain information about the sequential order of the two postulated reactions. This technique gives two different correlation spectra/maps: synchronous and asynchronous maps, which provide complementary information about the spectral bands. In these maps, white regions indicate positive correlation intensities, while grey regions indicate negative correlation intensities. In the synchronous spectrum correlation, the cross peaks  $\phi(\nu_1, \nu_2)$  indicate the correlation between spectroscopic variables (wavelength). Under the same perturbation, the increase or decrease is simultaneous. More information can be obtained from the corresponding asynchronous correlation spectrum  $\psi(\nu_1, \nu_2)$ , where the cross peaks appear only if the intensities of two dynamic bands change asynchronously, i.e. when two spectral intensities vary out of phase with each other. The sign of an asynchronous correlation peak provides information about the sequential order of intensity variations between band  $\nu_1$  and  $\nu_2$ . According to the Noda and Ozaki [20] publications, when  $\phi(\nu_1, \nu_2) > 0$ , if  $\psi(\nu_1, \nu_2)$  is positive, change at  $\nu_1$  occurs predominantly earlier than at  $\nu_2$  and if  $\psi(\nu_1, \nu_2)$  is negative, change at  $\nu_1$  occurs predominantly later than at  $\nu_2$ . However, the sign rule is reversed if  $\phi(\nu_1, \nu_2)$  is negative [18].

#### 2.4.2. Evolving factor analysis

Evolving Factor Analysis (EFA) [22] is a valuable technique to detect when a chemical change happens throughout a reaction. The idea on which EFA is based is to follow the change or the evolution of the rank of the total matrix with progressing elution by rank analysis of the submatrices. The appearance of each new component at the threshold is intrinsically associated with a different chemical situation in the system. In this work, the second singular value of the reagents matrix data was considered as the threshold value associated with the instrumental noise and the experimental error.

In this study, singular value decomposition (SVD) [23] was firstly applied to a sub-matrix that contains only the first two spectra and then adding the third spectrum of the data matrix to the initial sub-matrix to calculate the rank. This process was repeated until singular value decomposition was applied to the whole matrix **M** (144 x 163) and performed in the two directions (forward and backward).

#### 2.4.3. Multivariate curve resolution-alternating least squares (MCR-ALS)

Multivariate resolution of the concentration (**C**) and spectra (**S<sup>T</sup>**) profiles of the chemical species involved in the two reactions was carried out by MCR-ALS, which is an iterative method intended to minimize the residual matrix **E** [25,26] in the model equation

$$\mathbf{D} = \mathbf{CS}^T + \mathbf{E} \quad (1)$$

where  $\mathbf{D}$  is the data matrix obtained experimentally,  $\mathbf{C}$  is the matrix that describes the changes in the concentration of the species in the system,  $\mathbf{S}^T$  is the matrix that contains the response profiles of these species and  $\mathbf{E}$  is the residual matrix with the data variance unexplained by  $\mathbf{CS}^T$ .

This process involves the following steps:

1) Determination of the number of factors that contribute to the chemical information contained in the experimental spectra data matrix (chemical rank). Rank analysis was performed by singular value decomposition (SVD) [23]. In order to overcome the rank deficiency of matrix  $\mathbf{M}$  found, a column-wise augmented matrix [24]  $\mathbf{D}$  was built appending the NIR spectra recorded for the epoxidized oil and aniline to the experimental data matrix  $\mathbf{M}$ .

2) Construction of the initial estimate, either of the spectra in  $\mathbf{S}^T$  or of the concentration profiles associated with these spectra. In this study, the initial estimate of  $\mathbf{S}^T$  consisted of the experimentally recorded pure spectra of the reactants, i.e., epoxidized oil (EMO) and aniline, and the spectra of secondary amine and amide found when the ALS algorithm optimized the initial EFA estimate.

3) Optimization by alternating least squares (ALS). The ALS algorithm was iterated by applying a series of constraints [30,31] in order to obtain a sound solution to the chemical problem and to restrict the number of possible solutions. These constraints were: a) non-negativity to the values of the spectra and concentration profiles of each component; b) the system must be closed with respect to the total analytic concentration (closure); c) selectivity in the concentration profile of the amide compound.



### 3. Results and discussion

To clearly evidence the evolution of the spectra recorded during the reaction, three spectra were isolated and represented in Figure 1. As can be seen, all spectra are also inserted in the figure and the characteristic bands of the functional groups involved in the reaction are marked: the primary amine combination band<sup>32</sup> (bending and stretching vibration) located at 1976 nm and corresponding to the aniline reagent; the combined absorption band (combination of symmetric and asymmetric stretching vibrations) of primary and secondary amines [32] located at 1500 nm, related to the aniline reagent and to the product (C) of the reaction; and the characteristic bands of the O-H functional group [33,34], located at 1412 (O-H first overtone) and 1900 nm (O-H stretching and deformation vibrations), respectively. The wavelength region between 1650 nm and 1750 nm is related to the C-H combination bands characteristics of the aromatic ring of the aniline reagent and to the C-H stretching bands characteristics of the carbonated chain of the oil reagent. These functional groups are present in all the products formed during the reaction and the variations observed in this region can be attributed to the different chemical environment of the vibrations in each product.

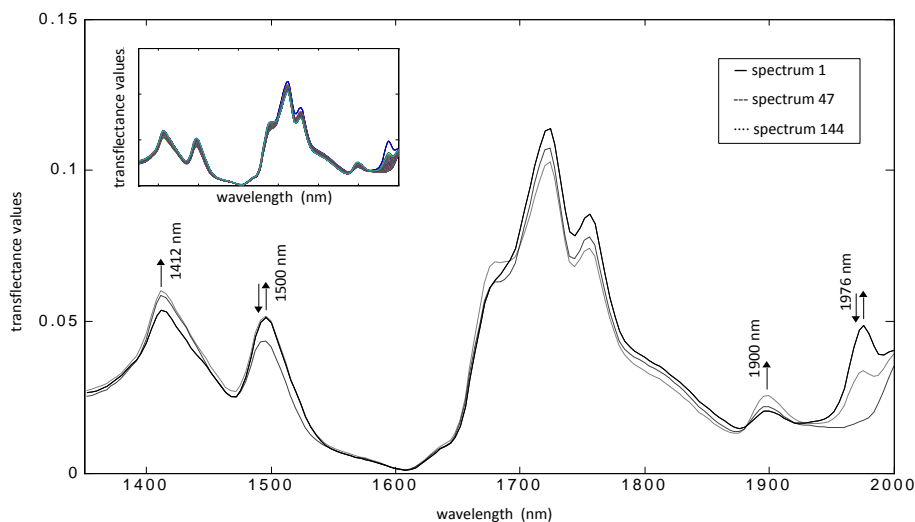


**Figure 1.** NIR spectra of EMO/aniline 1:1 obtained every 5 min at 95 °C. The arrows indicate the evolution over time of the spectral bands (see the text). (solid line) spectrum Nº 1, (dashed line) spectrum Nº 47, (dotted line) spectrum Nº 144.

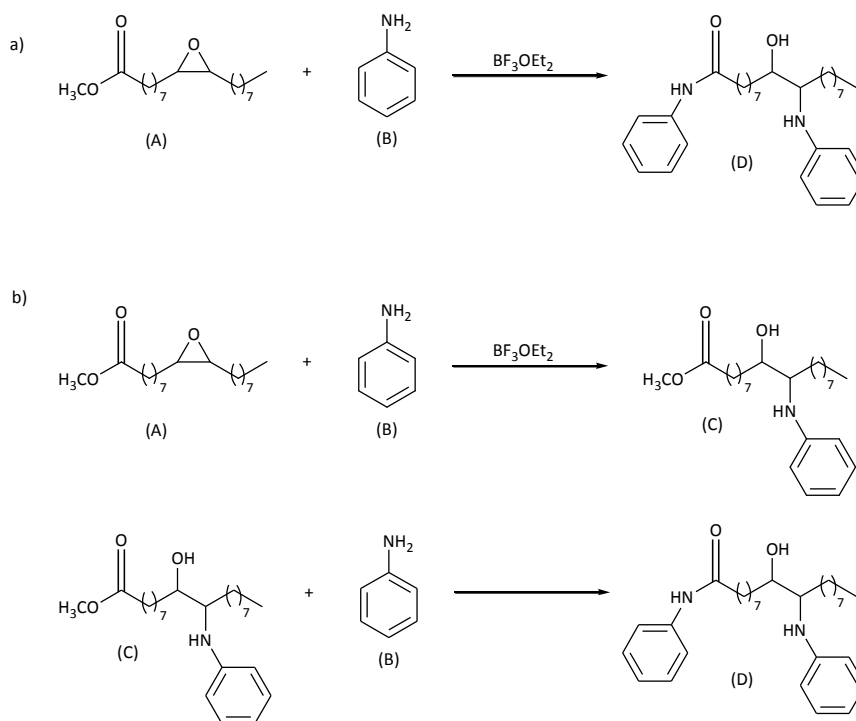
A detailed and independent analysis of the evolution of the bands leads to the following observations: a) no specific bands of the epoxy vibrations, b) absorption values at 1412 and 1900 nm from the first spectrum not observed in the reagents spectra and c) a change in the intensity evolution at 1500 and 1976 nm. To further investigate these observations, the first spectrum, the spectrum where the changes in the evolution of the bands at 1500 nm and 1976 nm were observed (spectrum 47, approximately 4 hours of reaction) and the last spectrum of the reaction, were isolated (Fig. 1).

It was found in the literature [34,35] that epoxy vibrations of terminal oxirane rings are located around 1645 nm and the absorption bands are weak, of low intensity and they can be overlapped with the absorption bands corresponding to the  $-CH$  and  $-CH_2$  stretching vibrations of the carbonated

chain. In this study, the oxirane ring is located in an internal position and no references about its corresponding absorption bands in the NIR region were found. Due to the position of this group in the oil, its absorption bands would be weaker and of lower intensity than the absorption bands of a terminal epoxy group. Therefore, it would not be strange not to find a characteristic band of this epoxy group in the NIR spectra acquired. The second observation indicates that the ring-opening reaction (scheme 1) is very fast and, as a consequence, the product contribution (secondary amine (C), which contains O-H functional groups) in the first spectra is significant. The behaviour of the primary amine group at 1500 and 1976 nm is more difficult to explain if the only chemical species involved in the reaction are the species shown in Scheme 1.

Near infrared spectroscopy is based on molecular overtone and combination vibrations and the NIR spectra are characterised by broad bands with small intensities. Therefore, in the pertinent literature it is common to find wavelength intervals assigned to the vibrations of the functional groups. Specifically, the interval between 2100 – 1900 [36-38] nm and the region around 1500 [36,37,39] nm, associated with combination bands of N-H amide groups, and the interval between 1900 – 1930 [38] nm, related to the second overtone of the amide C=O stretching vibration are described. In the EMO/aniline system under study, amide groups could be formed if amidation reactions between the aniline and the ester group present in the epoxidized oleic oil take place, according to the two possibilities depicted in Scheme 2: a) where the amidation reaction is simultaneous with the ring-opening reaction and b) where there is a sequential order of the two reactions. In both cases, if this reaction takes place, it is possible to imagine that, at some time during the reaction, when the quantity of primary amine is low, an increase in the absorption values of the N-H characteristic bands, at 1500 and 1976 nm, would be observed. Bearing this

possibility in mind, a detailed inspection of the intensity values evolution at 1900 nm, which is referenced as amide C=O and O-H vibrations, was done. It was possible to detect that the increment of the absorbance values at 1900 nm from the spectrum 47 to the last spectrum is higher than the increment of the absorbance values between these two spectra at 1412 nm, which is only characteristic of the hydroxyl group formed in the ring-opening reaction. If the absorption band at 1900 nm was only related to the ring-opening reaction, its intensity increment would be always constant and of the same magnitude as the observed one at 1412 nm. This fact is not observed and, therefore, it can be assumed that amide C=O stretching vibrations are contributing to the absorption values at 1900 nm, which implies that an amidation reaction is taking place. Nevertheless, it seems as if this amidation reaction was only revealing from the spectrum 47, when variations due to the ring-opening reaction do not practically exist. The sequentiality of both reactions was confirmed by 2D correlation spectroscopy.



**Scheme 2.** Amidation competitive reaction in the EMO/aniline system under study.

a) Situation where the amidation reaction is done simultaneously with the ring-opening reaction; b) Situation where there is a sequential order of the two reactions. (A) EMO, (B) aniline, (C) secondary amine, (D) amide.

The wavelength-wavelength correlation spectra are shown as contour plots in Figure 2. As expected, in the synchronous correlation map (Fig. 2a), autocorrelation peaks of different intensities appear at (1412, 1412) nm, (1500, 1500) nm, (1900, 1900) nm and (1976, 1976) nm. The intensity of the correlation peaks is related to the absorption coefficients of the compounds in the NIR region. The intensity correlation peak related to the absorption band at 1976 nm is the highest. Positive synchronous correlation cross peaks are also detected at (1500, 1412) nm and (1976, 1412) nm, which are characteristic bands of the N-H

bonds and of the hydroxyl group present in the product of the ring-opening reaction (Scheme 1), respectively. Because in the synchronous maps negative correlation cross peaks between the characteristic bands from the reagents and products are expected, this positive correlation can be attributed to the fact that the amidation reaction is taking place (Scheme 2), so the amide compound (D) is being generated throughout the reaction, as we stated for the one-dimensional spectral analysis.

In the asynchronous map (Fig. 2b), correlation cross peaks between two dynamic bands develop only if the intensity changes are sequential. In Figure 2b, positive correlation peaks can be observed between the same bands mentioned in the synchronous spectra, at (1500, 1412) nm and (1976, 1412) nm. According to the Noda rules (Table 1), it is possible to indicate that the intensity variations at 1500 and 1976 nm are prior to the changes at 1412 nm. Obviously, intensity changes at the 1500 and 1976 nm bands associated with the reagent aniline must be occur before the intensity changes at 1412 nm band, which is associated with the secondary amine (C) and amide product (D).

More interesting information about the sequentiality can be extracted analysing the correlation peaks assigned to the characteristic bands of the two products generated. In the synchronous correlation map (Fig. 2a), a positive correlation cross peak at (1900, 1412) nm appears, which indicates that the two intensity variations occur simultaneously in the same direction, in agreement with the observed increase (Figure 1). In the asynchronous map (Fig. 2b), a positive correlation peak between these absorption bands is detected. The appearance of this asynchronous peak points out that the intensity variations of these bands are not simultaneous, in agreement with the sequentiality of both reactions above discussed. However, in this case, the application of the Noda

rules to establish the sequential order of the two reactions is not straightforward. A positive asynchronous peak between (1900, 1412) nm is obtained because the intensity changes at 1900 nm are globally higher than the intensity changes at 1412 throughout the reaction (from spectrum 47 to spectrum 144). Hence, the straight combination of the sign of the synchronous and asynchronous peak indicates that the intensity changes at 1900 nm occurs predominantly before the intensity changes at 1412 nm, which means that the starting time of the intensity changes at 1900 nm is *prior* to that at 1412 nm. In our experimental conditions, important intensity absorption values are observed from the first spectrum at 1412 nm. We therefore postulated that the sequential order of both reactions, the ring-opening reaction and the amidation reaction, is the indicated in *b* of Scheme 2.

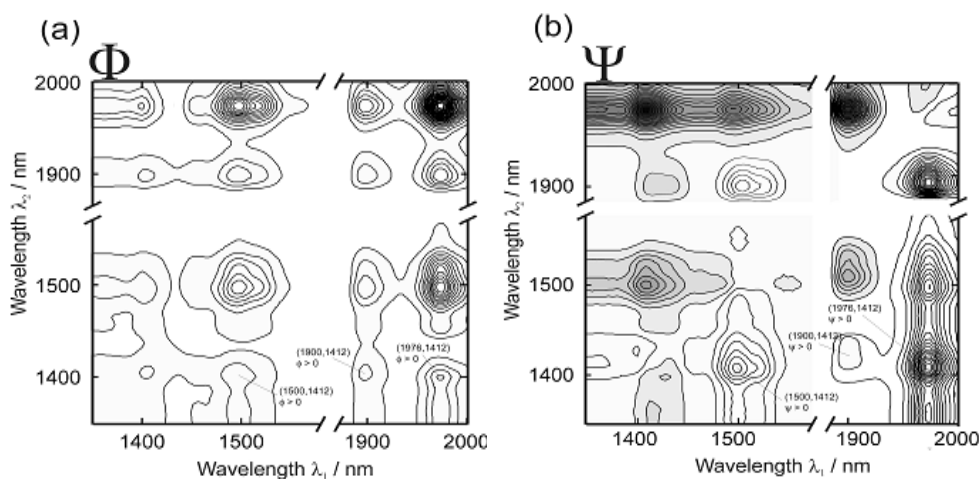


**Figure 2.** Synchronous (a) and asynchronous (b) spectra 2D NIR correlation map.

Positive cross peaks in white contour, negative cross peaks in grey contour.

**Table 1.** Synchronous, asynchronous 2D correlation intensities and order of intensity variations between bands for the experimental spectra data matrix **M**.

Number	$\phi$	$\psi$	Order
1	(1500, 1412) > 0	(1500, 1412) > 0	1500 before 1412 nm
2	(1900, 1412) > 0	(1900, 1412) > 0	1900 before 1412 nm
3	(1976, 1412) > 0	(1976, 1412) > 0	1976 before 1412 nm

The sequentiality of the reactions is supported by evolving factor analysis (EFA) applied to the experimental spectra data matrix. In this study, the second singular value calculated with the matrix data of the EMO and aniline reagents was considered as the threshold value associated with the noise (log eigenvalues = -2.4). The forward EFA plot (Figure 3) suggests that, at the end of the reaction, at least three singular values should be necessary to describe the reaction. This is in agreement with Amrhein [40], who reports that the number of significant factors corresponds to the number of independent reactions plus one. Therefore, the reactions are coming about as depicted in Scheme 2b. It is also possible to observe that until 4 hours of reaction (spectrum 47) only two factors, which are associated with only one reaction, can be distinguished from the noise. Considering the above discussion, this reaction is the ring-opening reaction, because it is more favoured than the amidation reaction. Furthermore, the reaction time when the third factor begins to be significant matches up with the spectrum number shown in Figure 1 (spectrum 47), when the intensity values of the absorption bands at 1500 and 1976 nm change their evolution.



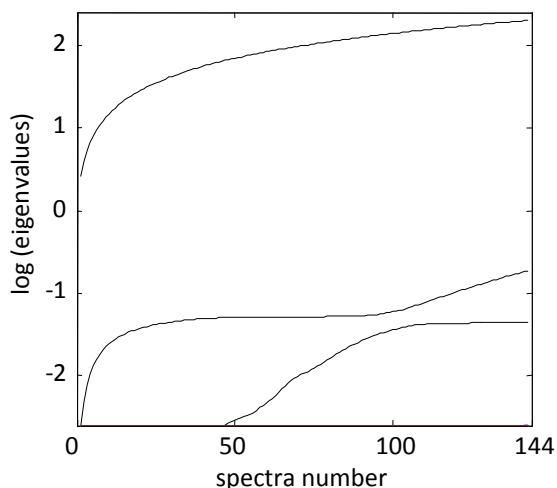


**Figure 3.** Forward EFA plot of the experimental spectra data matrix **D**.

At this point of the discussion it is possible to summarize that: a) four chemical species are involved in the studied reaction between the epoxidized oleic oil with aniline; b) in the NIR region, the spectra of the two products generated in the reactions and the aniline reagent have very similar characteristic NIR absorption bands; c) no specific bands of the epoxidized oleic oil were detected; and d) the contribution of the secondary amine product (C) generated by the ring-opening reaction is noteworthy from the beginning. According to these statements, these conditions are not the most favourable to carry out the quantitative resolution of the concentration and spectra profiles of the chemical species involved in the reaction, but in order to probe the potentiality of the multivariate curve resolution method - alternating least squares (MCR-ALS), this method was applied to the experimental data matrix.

To overcome the rank deficiency problem found in the experimental spectra data matrix **M**, a column-wise augmented matrix **D** (146 x 163) was built

appending to the experimental data matrix **M** the NIR spectra recorded for the epoxidized oil and aniline. Thus, the rank deficiency was broken and an attempt could be made to resolve the system satisfactorily.

Initial estimates of the pure spectra to be used in the optimization process were obtained in three stages. First, the evolving factor analysis algorithm was applied to the corresponding matrix to search for concentration estimates of the various reaction components. Second, the ALS algorithm optimized the EFA initial estimates and led to a set of spectra and concentration profiles for each reaction component. Finally, initial spectral estimates were obtained for the secondary amine and the amide products as described above. For the epoxidized oleic oil and aniline, however, the previously recorded spectra of the pure compounds were used.

In the optimization process, in which ALS is applied to the new **D** matrix, two constraints were imposed in order to improve the resolution and to limit the number of possible solutions: non-negativity for the concentration profiles to be resolved in matrix **C** and the spectra profiles in matrix **S<sup>T</sup>**, and closure for the concentration profiles. Likewise, a local rank constraint of selectivity zones was imposed from the starting point to 4 hours (spectrum 47) into the reaction so that the concentration of the amide product was zero. This constraint is an approximation of reality because very probably the amide product is generated once the secondary amine exists on the reaction medium. Rather, it is an approximation, which, if imposed according with the EFA results, can be considered to be appropriate. What is more, in the optimization process, the correspondence between the pure spectra of the individual matrices that constitute the augmented matrix **D** has been established.

The MCR-ALS optimization of the augmented NIR data matrix gave rise to two matrices: a matrix  $\mathbf{C}$  (146 x 4) that contained the concentration profiles for the four compounds involved in the reaction (Figure 4) and a matrix  $\mathbf{S}^T$  (4 x 163) which consisted of the spectra recovered for each of the four species (Figure 5). The quality of the fitting was evaluated by means of two parameters: the lack of fit (1.67%) and the percentage of explained variance (99.68 %), which in quantitative terms means that it explains practically all the variability of the experimental data as a product of both matrices.

Figure 4 shows the concentration evolution of the chemical species, recovered in % w/w. As rotational ambiguity exists, the depicted MCR-ALS solution is one of a number of possible solutions. However, in overall terms, this is a good reflection of the one expected. The recovered concentration profile associated with the secondary amine product (dashed line) shows an elevated value at the starting point of the reaction (the conversion is almost 60%) and begins to diminish when the recovered concentration profile of the amide product (dash-dot line) is noteworthy. On the other hand, at the beginning of the reaction, the epoxidized oil and aniline concentrations (solid and dotted line, respectively) are equal and diminish thorough the reaction time.

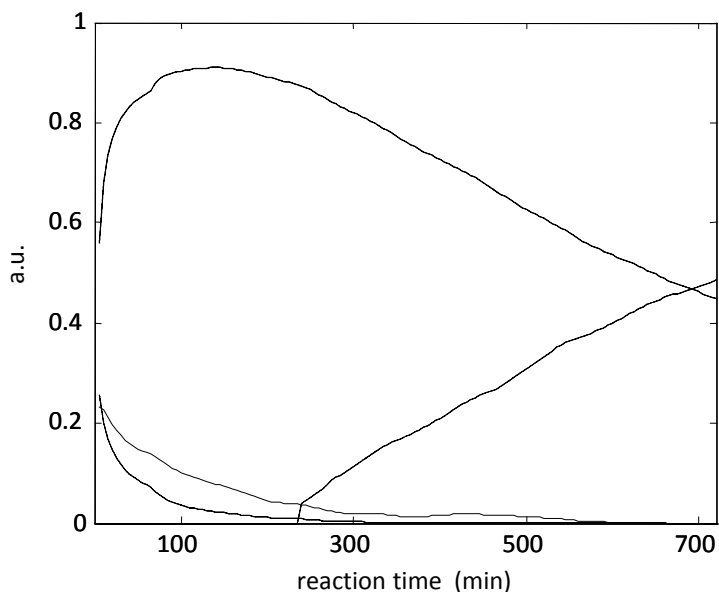


**Figure 4.** Concentration profiles of the species recovered by MCR-ALS. (solid line) EMO, (dotted line) aniline, (dashed line) secondary amine, (dash-dotted line) amide.

Figure 5 shows the recovered spectra profiles for the species that are involved in the chemical reaction. It should be pointed out the information obtained from the recovered spectra related to the secondary amine and amide products. As expected, the NIR spectra assigned to the secondary amine product, which is generated in the ring-opening reaction, has the characteristic absorption bands of the secondary amine functional group (1500 nm) and of the O-H functional group (1412 and 1900 nm). On the other hand, the NIR spectra assigned to the amide product, which is generated in the amidation reaction, has the characteristic absorption bands of the secondary amine functional group (1500 nm), of the O-H functional group (1412 and 1900 nm) and of the amide group (1500, 1900 and 1976 nm). The goodness of the spectra profiles of the reagents was determined, in quantitative terms, using the similarity coefficient

( $r$ ) between the recovered spectra and the experimental spectra. The  $r$  values calculated were: 0.9998 for the epoxidized oleic oil and 0.9938 for the aniline, indicating that the recovered profiles have a high degree of concordance with the originals.

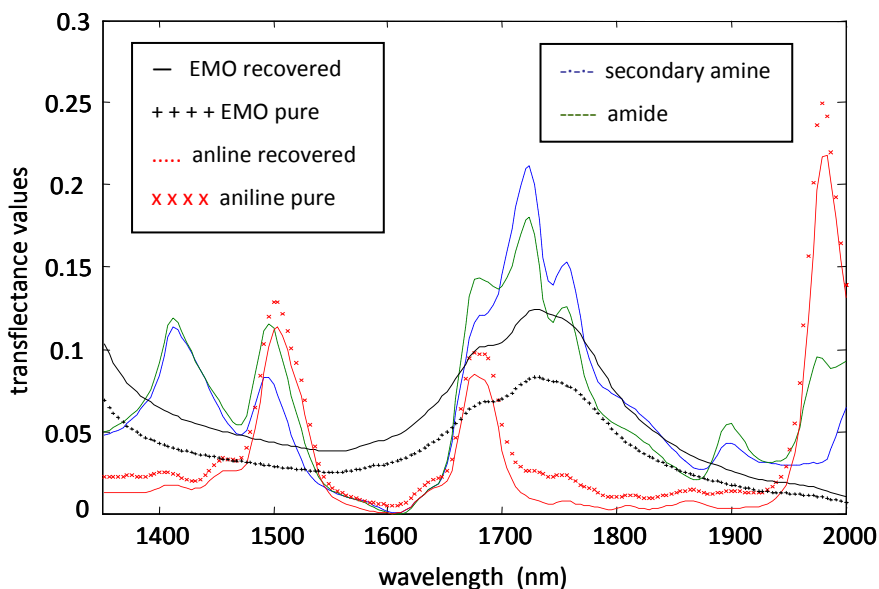


**Figure 5.** Superposition of the spectra of the species recovered by MCR-ALS and the pure spectra of the reactants EMO and aniline. For the MCR-ALS spectra profiles: (black solid line) EMO, (red dotted line) aniline, (blue dash-dotted line) secondary amine, (green dashed line) amide. For the pure reactants: (black + line) EMO, (red x line) aniline.

#### 4. Conclusions

The present contribution has demonstrated the usefulness of NIR instrumentation combined with spectroscopic and chemometric analysis for the study of polymer reactions where different and competitive processes can occur.

Conventional spectroscopic analysis and generalized 2D NIR correlation spectroscopic analysis of the intensity changes observed during the ring-opening reaction between an epoxidized oleic oil with aniline, have shown that a competitive amidation reaction is also taking place. From the analysis, it has been concluded that there is a sequential order between the reactions, being favored the nucleophilic attack of the aniline to the epoxy group *versus* the attack to the ester group, both present in the epoxidized oleic oil.

Evolving factor analysis applied to the experimental spectra data matrix has confirmed the existence of both reactions and has allowed the detection of the reaction time when the amidation reaction can be considered noteworthy.

The overall results of applying MCR-ALS to the augmented data matrix give a first solution to the evolution of the concentration profiles of the compounds that participate in the reaction studied. Also, the recovered spectra for the four species are in good agreement with the expected spectra.

The main final product of the reaction between the epoxidized oleic oil with aniline is the secondary amine. Nevertheless, the amide product is also present and it can affect the end-properties of the products obtained when epoxidized vegetable oils are cured with amines.

**Acknowledgments.** We would like to thank Virginia Cádiz from the Polymer Research Group of the Rovira i Virgili University, for their collaboration in the preparation of this paper. Likewise, we would like to acknowledge the Spanish Ministry of Science and Innovation (Project CTQ2007-61474/BQU) for economic support and the Universitat Rovira i Virgili, for providing Vanessa del Río with a doctoral fellowship.

## 5. References

- [1] V. Sharma and P.P. Kundu, *Prog. Polym. Sci.* **33** (2008) 1199.
- [2] V. Sharma and P.P. Kundu, *Prog. Polym. Sci.* **31** (2006) 983.
- [3] F.S. Güner, Y. Yagci and A.T. Erciyas, *Prog. Polym. Sci.* **31** (2006) 633.
- [4] M.A.R. Meier, J.O. Metzger and U.S. Schubert, *Chem. Soc. Rev.* **36** (2007) 1788.
- [5] L. Montero de Espinosa, J.C. Ronda, M. Galià and V. Cádiz, *J. Polym. Sci.: Part A: Polym. Chem.* **47** (2009) 1159.
- [6] L. Montero de Espinosa, J.C. Ronda, M. Galià and V. Cádiz, *J. Polym. Sci.: Part A: Polym. Chem.* **46** (2008) 6843.
- [7] D.L. Kaplan, *Biopolymers from Renewable Resources*, Springer, Berlin, p. 267, 1998.
- [8] N. Boquillon and C. Fringant, *Polymer* **41** (2000) 8603.
- [9] F.T. Wallenberger and N. Weston, *Natural Fibers, Plastics and Composites*, Kluwer Academic Publisher, USA, p. 171, 2004.
- [10] M. Garrido, F. X. Rius and M.S. Larrechi, *Anal. Bioanal. Chem.* **390** (2008) 2059.
- [11] V. del Río, M.P. Callao, M.S. Larrechi, L. Montero de Espinosa, J.C. Ronda and V. Cádiz, *Anal. Chim. Acta* **642** (2009) 148.
- [12] N. Spegazzini, I. Ruisánchez, M.S. Larrechi, V. Cádiz and J. Canadell, *Analyst* **133** (2008) 1028.
- [13] N. Spegazzini, I. Ruisánchez and M.S. Larrechi, *Anal. Chim. Acta* **642** (2009) 155.
- [14] J. Mijovic and S. Andjelic, *Macromolec.* **28** (1995) 2787.
- [15] K. Dean, W. Cook, L. Rey, J. Galy and H. Sautereau, *Macromolec.* **34** (2001) 6623.
- [16] D.J.T. Hill, G.A. George and D.G. Rogers, *Polym. Adv. Technol.* **13** (2002) 353.

- [17] I. Noda, *Appl. Spectrosc.* **47** (1993) 1329.
- [18] I. Noda, A.E. Dowrey, C. Marcott, G.M. Story, Y. Ozaky, *Appl. Spectrosc.* **54** (2000) 236A.
- [19] I. Noda, *Appl. Spectrosc.* **54** (2000) 994.
- [20] I. Noda and Y. Ozaki, *Two-Dimensional Correlation Spectroscopy*, Wiley & Sons, Chichester, West Sussex, 2004.
- [21] I. Noda, *J. Molec. Struct.* **883-884** (2008) 2.
- [22] M. Maeder, *Anal. Chem.* **59** (1987) 527.
- [23] D.L. Massart, B. Vandeginste, L. Buydens, S de Jong, P. Lewi and J. Smeyers-Verbeke, *Handbook of Chemometrics and Qualimetrics*, Part A, Elsevier, Amsterdam, 1997.
- [24] J. Saurina, S. Hernández-Cassou, R. Tauler and A. Izquierdo-Ridorsa, *J. Chemom.* **12** (1998) 183.
- [25] R. Tauler, *Chemom. Intell. Lab. Syst.* **30** (1995) 133.
- [26] A. de Juan and R. Tauler, *Anal. Chim. Acta* **500** (2003) 195.
- [27] M. Garrido, I. Lázaro, M.S. Larrechi and F.X. Rius, *Anal. Chim. Acta* **515** (2004) 65.
- [28] The Mathworks, MATLAB Version 6.5, Natick, MA, 2004.
- [29] 2Dsigue (c) Shigeaki Morita, Kwansei-Gakuin University, 2004-2006. All rights reserved.
- [30] R. Bro and S. de Jong, *J. Chemom.* **11** (1997) 393.
- [31] R. Tauler and E. Cassassas, *Anal. Chim. Acta* **248** (1991) 447.
- [32] M. Garrido, M.S. Larrechi and F.X Rius, *Anal. Chim. Acta* **585** (2007) 277.
- [33] L. Xu and J.R. Schlup, *J. Appl. Polym. Sci.* **67** (1997) 895.
- [34] J. Mijovic, S. Andjelic and J.M. Kenny, *Polym. Adv. Technol.* **7** (1995) 1.
- [35] G. Lachenal, I. Stevenson, A. Duran, G. Seytre and D. Bertrand, *Macromolec. Symp.* **265** (2008) 249.
- [36] Y. Xu and P. Wu, *J. Mol. Struct.* **833** (2007) 145.



- [37] P. Wu, Y. Yang and H.W. Siesler, *Polymer* **42** (2001) 10181.
- [38] L. Moghaddam, D.J. Martin, P.J. Halley and P.M. Fredericks, *Vibr. Spectrosc.* **51** (2009) 86.
- [39] P. Wu and H.W. Siesler, *J. Molec. Struct.* **521** (2000) 37.
- [40] M. Amrhein, B. Srinivasan, D. Bonvin and M.M. Schumacher, *Chemom. Intell. Lab. Syst.* **33** (1996) 17.

### **3.2.1.2. Paper**

**Quantitative analysis of the influence of the  
temperature on a model curing reaction of epoxy  
resins from vegetable oils using FTIR  
spectroscopy and MCR-ALS**

Vanessa del Río, M. Pilar Callao, M. Soledad Larrechi

Submitted

UNIVERSITAT ROVIRA I VIRGLI  
FAST ANALYTICAL METHODOLOGIES BASED ON MOLECULAR SPECTROPHOTOMETRIC TECHNIQUES  
AND MULTIVARIATE DATA ANALYSIS  
Vanessa del Rio Sánchez  
ISBN:978-84-693-9439-7/ DL:T.64-2011

**Quantitative analysis of the influence of the temperature on a model  
curing reaction of epoxy resins from vegetable oils using FTIR  
spectroscopy and MCR-ALS**

**Vanessa del Río, M. Pilar Callao, M. Soledad Larrechi**

*Chemometrics, Qualimetrics and Nanosensors Research Group  
Analytical Chemistry and Organic Chemistry Department, Rovira i Virgili  
University  
Marcel·lí Domingo s/n, 43007 Tarragona, Spain*

**Abstract**

Quantitative analysis of the temperature effect on the model cure acid-catalysed reaction between the epoxidized methyl oleate (EMO), obtained from high oleic sunflower oil, and aniline is reported. The study was carried out analysing the kinetic profiles of the chemical species involved in the reactions, which were found applying multivariate curve resolution – alternating least squares to the Fourier transform infrared spectra data obtained from the reaction monitoring at two different temperatures (60°C and 30°C).

The reactions involved in this system are the amine addition to the oxirane ring of the epoxidized methyl oleate and the amidation reaction between the ester group of the oil and the amine group. The results have revealed that the formation of the amide compound competes significantly at high temperatures with the first amine addition reaction and plays an important role in the reaction mechanism.

At both experimental temperatures, two mechanisms were postulated: non- autocatalytic and autocatalytic. The different behaviour was discussed considering not only the influence of the temperature on the amidation reaction kinetic, but also the presence of the homopolymerization of the EMO reagent. The homopolymerization conversion degrees (1.88 % and 0.17 % at 60 °C and 30 °C, respectively) have shown that this reaction can be considered quantitatively neglected *versus* the extension of the amine-amide reactions. However, its contribution in the non-autocatalytic mechanism observed at 60°C is relevant.

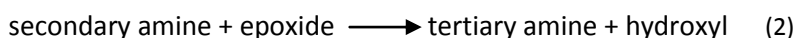
The present study contributes to better evaluation of the possibilities that vegetable oils offer as precursors of pre-polymers.

**Key words:** Infrared spectroscopy; Temperature influence; Reaction mechanism; Multivariate curve resolution – alternating least squares; Epoxidized vegetable oil.

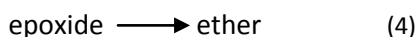
## 1. Introduction

The development of environmentally compatible polymers is one of the current challenges in polymer chemistry. In this sense, epoxy resins from vegetable oils are extremely promising as environmentally friendly polymers for industrial applications because they share many of the characteristics of conventional petro-chemical based epoxy resins [1]. The curing process of the epoxy resins affects the chemical structure of the network and hence, its mechanical properties. This dependence explains the numerous studies carried out to better understand the mechanism and to quantify the kinetics of cure reactions [2-9].

It is generally admitted that, when epoxide monomers are cured with aromatic amines, the two main reactions that take place are related to the addition of the amine to the oxirane ring, in which the involved functional groups are:



According to the type of the epoxide/amine system and to the experimental conditions, etherification reaction (3) can be done [4]. With an excess of epoxide, at high temperature and in the presence of Lewis bases, inorganic bases or Lewis acids catalysts, homopolymerization of epoxides (4) also takes place [3]. These two parallel reactions promote the presence of ether groups.



If the epoxide monomers (or pre-polymers) contain an ester functional group, as occurs in the epoxidized oils, it is possible to consider that an amide is also formed (5) as a consequence of the reaction between the amine and the ester group.



The existence of the homopolymerization and etherification reactions is related to such characteristics of the experimental conditions, as the temperature, the concentration of the reagents and the presence of catalysts. However, the amidation reaction is only related to the ester-containing

monomer used and the presence of this kind of reaction result in cured products of poor quality [10,11]. Thus, to optimize the process, knowledge of the effect of the temperature on the kinetics of the reactions involved in these kinds of systems is required, which is the main purpose of this work.

In the present study, a model reaction between an epoxidized methyl oleate (EMO), obtained from high oleic sunflower oil, and aniline using borontrifluoride etherate ( $\text{BF}_3 \cdot \text{OEt}_2$ ) as catalyst, has been monitored at two temperatures.

Infrared spectroscopy is by far the most utilized characterization method to monitoring *in situ* a reaction [12-16] and, in this work, FTIR-ATR was selected. The experimental considered molar ratio EMO:aniline (2:1) reproduces the habitually employed in the curing processes. To analyze the temperature effect the experiment was carried out at 60 °C and at 30 °C. These values were selected considering that, in a previous work [17] in which the temperature was 95 °C, conversion values higher than 50 % were observed from the beginning of the reaction, which does not allow the accurate analysis of the system. In addition, the homopolymerization of the EMO reagent at the two experimental temperatures was also monitored in order to evaluate the extension of this reaction.

Spectra and concentration profiles of the chemical species involved in the two experiments were obtained applying multivariate curve resolution - alternating least squares (MCR-ALS) to the FTIR data recorded during the reaction. Analysis of the reaction rate *versus* epoxy conversion throughout the reaction time was employed to identify the nature of the reaction mechanism involved at the two experimental temperatures.

This report aims at characterizing quantitatively and mechanistically by FTIR-ATR the effect of the temperature on the polymerization reaction between the epoxidized methyl oleate (EMO) and aniline, which can be considered as a model of the curing reactions using epoxy derivatives obtained from vegetable oils. These reactions are relatively new systems and, to the best of our knowledge, no studies of these characteristics are referenced in the literature. Therefore, the present study of epoxy resins contributes to better evaluation of the possibilities that vegetable oils offer as precursors of pre-polymers.

## **2. Experimental**

### **2.1. Materials**

The epoxidized methyl oleate (EMO) was synthesized and provided by the Polymer Research Group of our department [18]. Its purity was 97.89%, which was verified by elemental data analysis and  $^1\text{H}$  and  $^{13}\text{C}$  NMR spectra. Aniline reagent (Aldrich) and borontrifluoride etherate ( $\text{BF}_3\cdot\text{OEt}_2$ ) (Aldrich) were used as received.

### **2.2. Reaction conditions and procedure**

The reaction was performed at two different temperatures: 60 °C and 30 °C. The reaction samples were prepared by directly mixing the necessary amounts of EMO and aniline and 2% of catalyst ( $\text{BF}_3\cdot\text{OEt}_2$ ) at room temperature to obtain the desired molar ratio of 2:1. The mixture was placed immediately on a small diamond crystal in the spectrophotometer ATR cell (FTIR 680 Plus JASCO), which was equipped with a 3000 Series™ High Stability Temperature Controller



and a RS232 Control to take the measurements, and it was continuously purged with N<sub>2</sub> during the FTIR analysis. The FTIR spectra of the reacting mixture were obtained *in-situ* at equal time intervals during the isothermal cure.

In the same conditions, at 60 °C and 30 °C, the homopolymerization of the EMO reagent was monitored. The FTIR spectra of the pure reactant aniline was also recorded during 8 hours in order to evaluate the noise.

### **2.3. Data acquisition and data pretreatment**

The data correspond to the FTIR spectra recorded throughout the reaction every 0.964 cm<sup>-1</sup>, between 4000 and 600 cm<sup>-1</sup> in a FTIR 680 Plus JASCO spectrophotometer.

For each experiment, data at intervals of 5 minutes were acquired until the end of the reaction. The reaction was considered to be completed until no changes over time were observed in the spectra. In this way, the spectra were recorded for 250 min for the experiment at 60 °C and for 480 min for the experiment at 30 °C. Therefore, 50 and 96 spectra were recorded, respectively. Also, 50 and 96 FTIR spectra were recorded during the homopolymerization of the EMO reagent and 96 FTIR spectra were acquired for the pure reactant aniline.

All spectra were exported and converted into MATLAB binary files to carry out their mathematical treatment [19].

The experimental data of each experiment were arranged in matrices whose rows were the recorded spectra and whose columns were the absorbance

values at different wavenumbers: Thus, the matrices obtained were:  $\mathbf{M}_1$  (50 x 3528) for the experiment at 60 °C,  $\mathbf{M}_2$  (96 x 3528) for the experiment at 30 °C and  $\mathbf{M}_3$  (50 x 3528) and  $\mathbf{M}_4$  (96 x 3528) for the homopolymerization reaction at 60 °C and 30 °C, respectively, and  $\mathbf{M}_5$  (96 x 3528) for the pure reactant aniline.

### 3. Results and discussion

First, FTIR absorption spectra were analyzed and their characteristic absorption bands were assigned. Then, the concentration and spectral profiles of the chemical species involved in the reactions were solved and the conversion of the epoxide reagent was evaluated. Finally, the quantitative analysis as well as the conversion of the epoxide in the homopolymerization of the EMO reagent was discussed and the mechanism of the studied system was investigated.

For better exposition of the results, the first and the last spectra recorded throughout the reaction between EMO and aniline at 60 °C are displayed in the graphs (Figure 1(a,b)). The two wavenumber regions of particular interest in the FTIR spectra are: 1800-1100  $\text{cm}^{-1}$  and 4000-2600  $\text{cm}^{-1}$ . In order, these will be referred to as regions A and B, and are shown in Fig. 1a and Fig. 1b, respectively. The absorption bands characteristics of the functional groups that participate in the EMO/aniline system are summarized in Table 1 [20].

In region A, Figure 1a, it is possible to observe that, throughout the reaction time, the intensity of the characteristics absorption bands of the N-H bending vibrations at 1624  $\text{cm}^{-1}$  characteristic of the aniline reagent and of the C-O- vibrations of the oxirane ring at 1276  $\text{cm}^{-1}$  characteristic of the EMO reagent, decreases. On the other hand, an increase in the intensities of the absorptions

bands associated with some of the functional groups present in the products generated by the reactions described in equations (1)-(5) can be observed: between 1600 – 1500  $\text{cm}^{-1}$  the absorption bands of the N-H bending vibrations of the secondary amine, between 1700 – 1650  $\text{cm}^{-1}$  the absorption bands of the C=O stretching vibrations of the amide and at 1364  $\text{cm}^{-1}$  and 1310  $\text{cm}^{-1}$  the absorption bands of the C-N vibrations of the tertiary amine.

In region B, Figure 1b, as the reaction progresses, it is possible to observe a decrease in the intensity of the two bands at 3460 and 3370  $\text{cm}^{-1}$ , which are associated with the N-H stretching vibrations of the aniline reagent, and an increase in the intensity of the bands between 3650  $\text{cm}^{-1}$  and 3500  $\text{cm}^{-1}$ , which are related to the O-H stretching vibrations of the hydroxyl group present in all the products generated.

**Table 1.** Assignment of the absorption bands in the FTIR-ATR spectra (see Figure 1).

Origin	Wavenumber ( $\text{cm}^{-1}$ )	Assignment
C-O	1276	Epoxy and oxirane ring
C-N	1310	Aromatic tertiary amine, CN stretching
C-N	1364	Aromatic tertiary amine, CN stretching
N-H	1500 – 1600	Secondary amine, NH bending
N-H	1624	Primary amine, NH bending
C=O	1650 – 1700	Amide, CO stretching
C=O	1740	Ester, CO stretching
CH <sub>2</sub> -	2800 – 3050	Methylene, CH stretching
N-H	3370	Primary amine, NH stretching
N-H	3460	Primary amine, NH stretching
O-H	3500 -3650	Hydroxy group, OH stretching

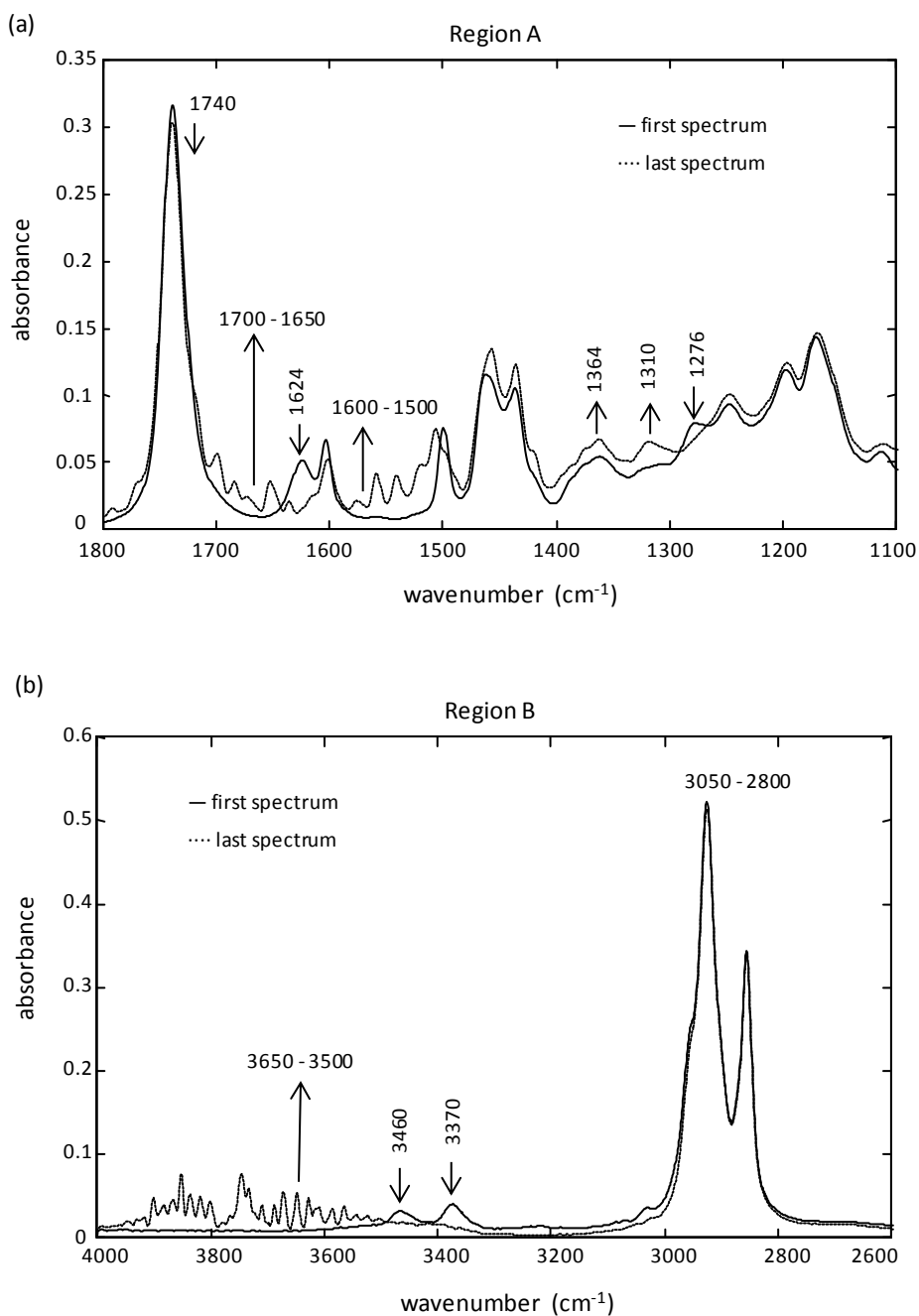


**Figure 1.** First and last FTIR-ATR of EMO/aniline system 2:1 recorded at  $T^{\text{a}} = 60$  °C. (a) region between 1800 – 1100  $\text{cm}^{-1}$  (A); (b) region between 4000 - 2600  $\text{cm}^{-1}$  (B).

Similar spectral changes were observed when the analysis of the spectra recorded at 30 °C was carried out, although it should be said that, at this experimental temperature, the intensities of the absorption bands between 1700 cm<sup>-1</sup> and 1650 cm<sup>-1</sup> associated with the amide compound were significantly lower.

The spectroscopic analysis reflects that, at the two experimental temperatures, the main amine addition reactions to the oxirane ring (Eq. 1 and 2) and the amidation reaction (Eq. 5) have taken place.

Before carrying out the quantitative resolution of the concentration and spectral profiles of the chemical species involved in the reactions, the number of independent contributions to the variation present in the individual matrices **M**<sub>1</sub> and **M**<sub>2</sub> was evaluated analysing the chemical rank of both matrices by singular value decomposition (SVD) [21]. In this work, the threshold value (0.095) was obtained from the singular value decomposition of the spectra data matrix of the aniline reagent (**M**<sub>5</sub>). The value of the second singular value of this matrix is related to the instrumental noise and the experimental error. The results (Table 2) show that only five singular values are significant in both matrices, which according to Amrhein [22] means that four independently reactions can be present.

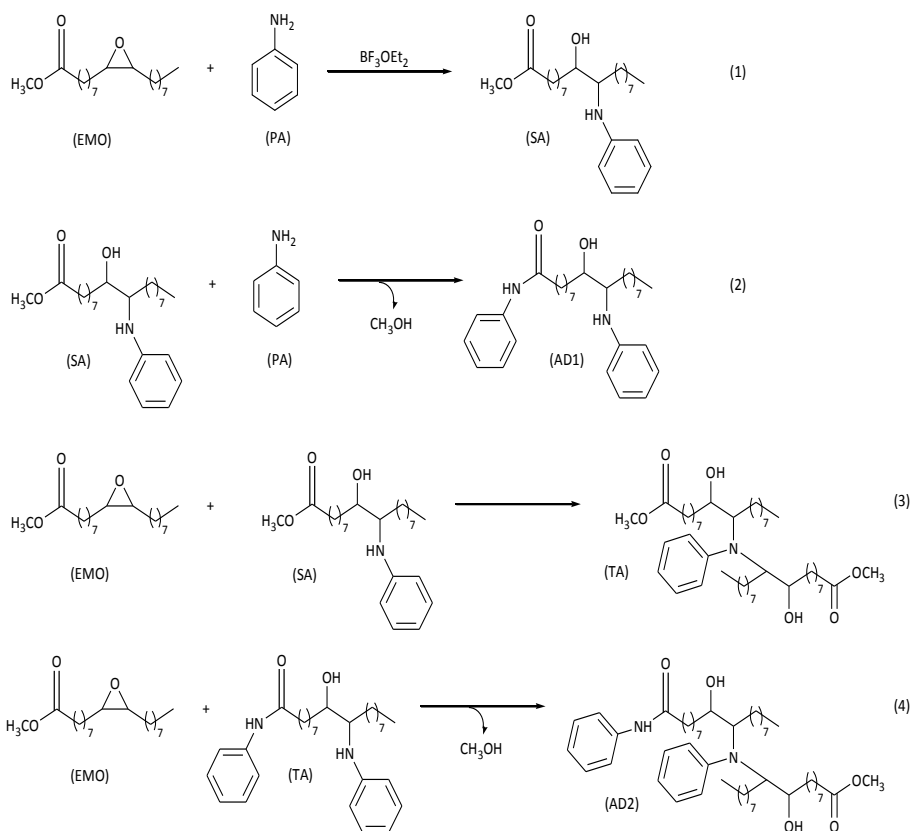
**Table 2.** Rank analysis of matrices **M** and **D**.

Number of factor	<b>M</b> <sub>1</sub>	<b>D</b> <sub>1</sub>	<b>M</b> <sub>2</sub>	<b>D</b> <sub>2</sub>
1	29.0408	29.3428	37.6861	37.9182
2	1.954	5.4823	2.9207	5.8910
3	0.5727	1.9385	2.0849	2.8395
4	0.2867	0.7053	0.3270	1.9131
5	0.2129	0.2779	0.2461	0.5935
6	0.0845	0.2263	0.0930	0.2912
7	0.0374	0.0579	0.0492	0.0706
8	0.0295	0.0339	0.0424	0.0473

Considering the results obtained in the previous work [17], where the sequential order of the primary amine addition to the oxirane ring and of the amidation reaction was established by two-dimensional spectroscopy correlation and chemometric techniques, it can be postulated that, in the experimental conditions, these four reactions correspond to those indicated in Scheme 1. Formally, in these reactions, seven chemical species are involved but, taking into account the experimental temperatures and that the system was monitored without interrupting the N<sub>2</sub> purge of the FTIR-ATR spectrometer, it can be assumed that the methanol formed is displaced from the cell. Therefore, the number of chemical species that can be expected throughout the reaction is six. In any case, regarding the significant values (Table 2) it is evidenced that rank deficiency exists in both matrices.

To overcome this problem and to obtain the evolution of the concentration profiles along the reaction time of the six chemical species, the multivariate curve resolution – alternating least squares method was applied to the column-wise augmented data matrices **D**<sub>1</sub> and **D**<sub>2</sub>, which were constructed

with the data corresponding to the  $M_1$  and  $M_2$  experimental data matrices, respectively, and the pure spectra of the EMO and aniline reagents. In these augmented matrices the number of significant singular values was six, as is exposed in Table 2. The variance associated with the solutions found by MCR-ALS for the augmented matrices  $D_1$  and  $D_2$  was 99.92 % and 99.94 %, respectively.



**Scheme 1.** Reaction between EMO and aniline using  $BF_3 \cdot OEt_2$  as catalyst: (1) primary amine addition to the oxirane ring; (2) amidation reaction; (3) secondary amine addition to the oxirane ring; (4) amidation reaction. (EMO) epoxidized derivative oleic oil; (PA) aniline; (SA) secondary amine; (AD1) amide; (TA) tertiary amine; (AD2) tertiary amine.

As example, Figure 2 shows the spectra for each of the six species recovered by MCR-ALS from the  $\mathbf{D}_1$  matrix and to obtain a better visualization, a restricted spectral zone where the characteristic spectral bands of each compound appear is amplified. The first and the second recovered spectra (A and B) contain the characteristic bands of the epoxy group at  $1276\text{ cm}^{-1}$  and of the primary amine group at  $3460$ ,  $3372$  and  $1624\text{ cm}^{-1}$ , respectively. For these spectra, their similarity with the pure spectra recorded for EMO and aniline reagents was evaluated throughout the correlation coefficient, founding  $r$  values of  $0.9939$  and  $0.9998$ , respectively. Thus, the first and the second spectra were assigned to the EMO and aniline reagents, respectively.

The other four recovered spectra are very similar, as expected considering the chemical structure of the compounds. In all of them there are no signals from either the primary amine or from the oxirane group in any of the representative zones and, on the other hand, it is possible to detect the bands associated with the OH functional group ( $3650 - 3500\text{ cm}^{-1}$ ). The two recovered spectra C and D were assigned to the secondary amine (SA) and to the amide compound (AD1) formed in reactions (1) and (2) of Scheme 1, respectively. These two spectra show the characteristic spectral bands of the secondary amine functional group between  $1600$  and  $1500\text{ cm}^{-1}$  and the only difference between them is observed in the wavelength range characteristic of an amide compound between  $1700$  and  $1650\text{ cm}^{-1}$ , where absorbance values appear in spectra D. Finally, the last two recovered spectra (E and F) can be related to the tertiary amine compounds (TA and AD2) formed in reactions (3) and (4) of Scheme 1, respectively. These two spectra show the characteristic bands of tertiary amines, located at  $1364$  and  $1310\text{ cm}^{-1}$ . The difference between them falls on the spectral zones related to the secondary amine functional group ( $1600\text{-}1500\text{ cm}^{-1}$ )



and to the amide functional group ( $1700\text{-}1650\text{ cm}^{-1}$ ), in where absorbance values can be only distinguished in spectrum F, as expected.

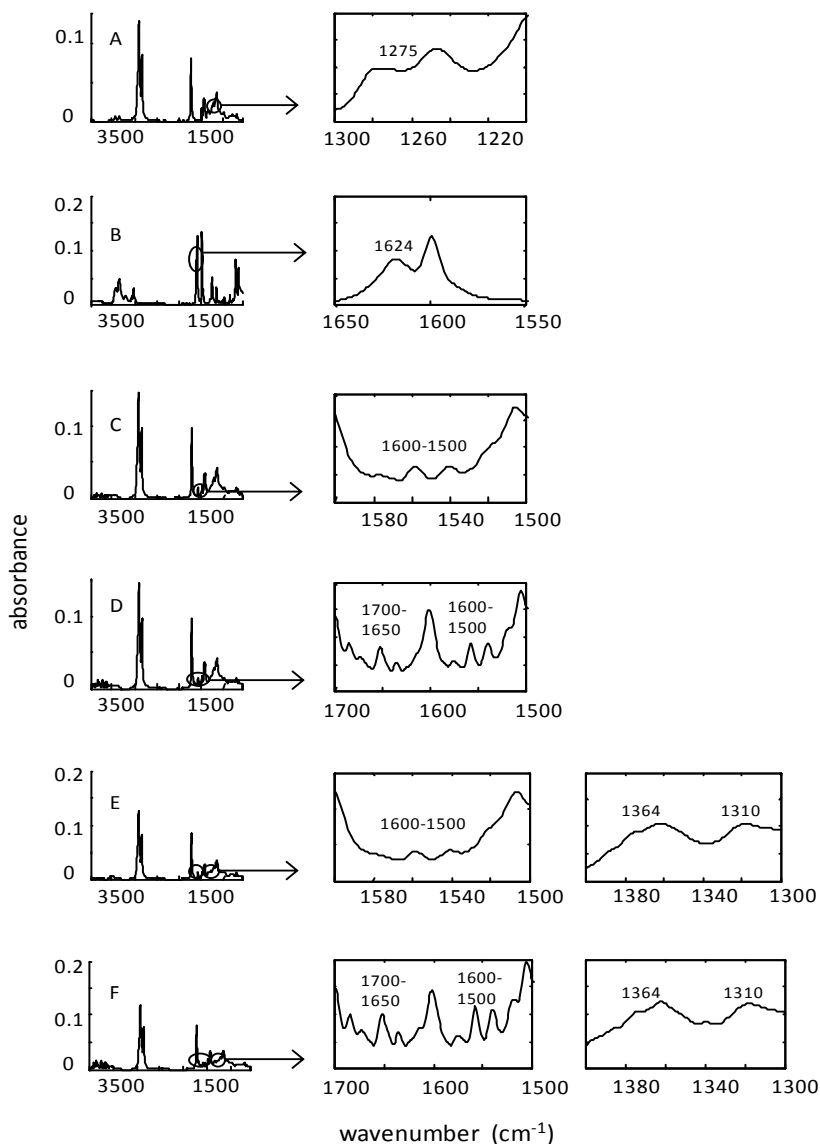


**Figure 2.** Spectral profiles of the species recovered by MCR-ALS: (A) EMO; (B) aniline; (C) secondary amine (SA); (D) amide (AD1); (E) tertiary amine (TA); (F) tertiary amine (AD2).

The concentration profiles obtained by MCR-ALS for the EMO/aniline system at the two experimental temperatures (60 °C and 30 °C) are shown in Figure 3(a,b). The concentration profiles recovered by the ALS algorithm were expressed in mass units, so the corresponding values in moles were obtained by dividing each concentration profile by the corresponding molecular weight, assuming that each species and their molecular weight are known. It is known that the solutions obtained by MCR-ALS are not unique and around each profile exist band boundaries which contain the possible solutions that fit the experimental data equally well [23]. Therefore, the concentration profiles shown are only one of the possible solutions. However, in overall terms, these solutions seem a good reflection of the expected behaviour and they were considered useful to compare the effect of the temperature on the amine addition/amidation reactions involved in the process.

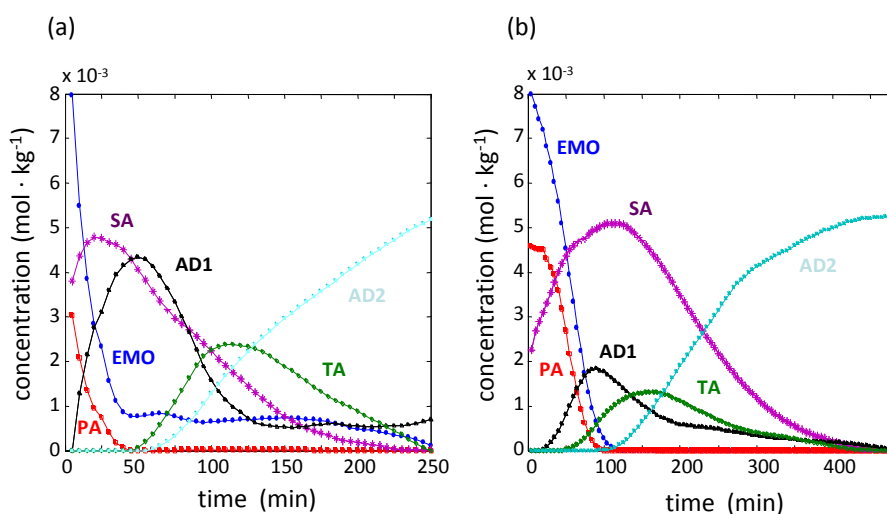


**Fig 3.** Concentration profiles of the species recovered by MCR-ALS: (a)  $T^a = 60\text{ }^\circ\text{C}$ ; (b)  $T^a = 30\text{ }^\circ\text{C}$ . (●) EMO; (■) aniline; (\*) secondary amine (SA); (▲) amide (AD1); (◆) tertiary amine (TA); (★) tertiary amine (AD2).

In Figure 3 it is observed that in both experiments, from the beginning of the reaction, the concentration value of the secondary amine compound (SA) formed in the first amine addition to the oxirane ring is noteworthy and higher at 60 °C than at 30 °C, as can be expected in agreement with the Arrhenius equation.

The effect of the temperature on the behaviour of the amide concentration profile (AD1) generated in the amidation reaction is worthy of note. In the experiment at 60 °C (Figure 3a), a significant change in its concentration is observed from the beginning and it achieves a maximum value at 50 minutes. However, at this time in the experiment at 30 °C (Figure 3b), the change in AD1 concentration value is lower and, at no time along the reaction does it achieve the maximum observed at 60°C. In addition, comparing the evolution of these AD1 profiles with the evolution of the concentration profiles of the other chemical species in both experiments, it can be considered that at 60 °C the kinetics of the amidation reaction ((2) in scheme 1) competes with the kinetics of the primary amine addition reaction ((1) in scheme 1), while at 30 °C the kinetics of the amidation reaction is relatively similar to the kinetics of the second amine addition reaction ((3) in scheme 1).

From these results, it can be supposed that the pathway of the process is not the same at the two experimental temperatures. In order to provide a basis for understanding this consideration, the epoxy conversion ( $\alpha = 1 - \frac{[EMO]_t}{[EMO]_{t=0}}$ ) throughout the reaction time was calculated using the concentration values ( $[EMO]_t$ ) of the EMO recovered concentration profiles shown in Figure 3(a,b) and it was plotted *versus* the reaction rate ( $d[EMO]/dt$ ) in Figure 4(a,b). The plot corresponding to the values obtained at 30 °C (Figure 4b) shows the

characteristic behaviour of the autocatalytic reactions [24]: the reaction rate increases initially as the reaction advances, passes through a maximum, and progressively slows down tending to zero. The initial increase in the reaction rate is associated with the formation of hydroxyl groups, which acts as catalyst of the reaction. The maximum rate is observed at conversion between 40 - 50 %, as expected for autocatalytic reactions. However, at 60 °C the maximum rate appears at conversion extremely low (< 0.1) and decreases along the reaction time, which led to the conclusion that in this case the mechanism is non-autocatalytic.

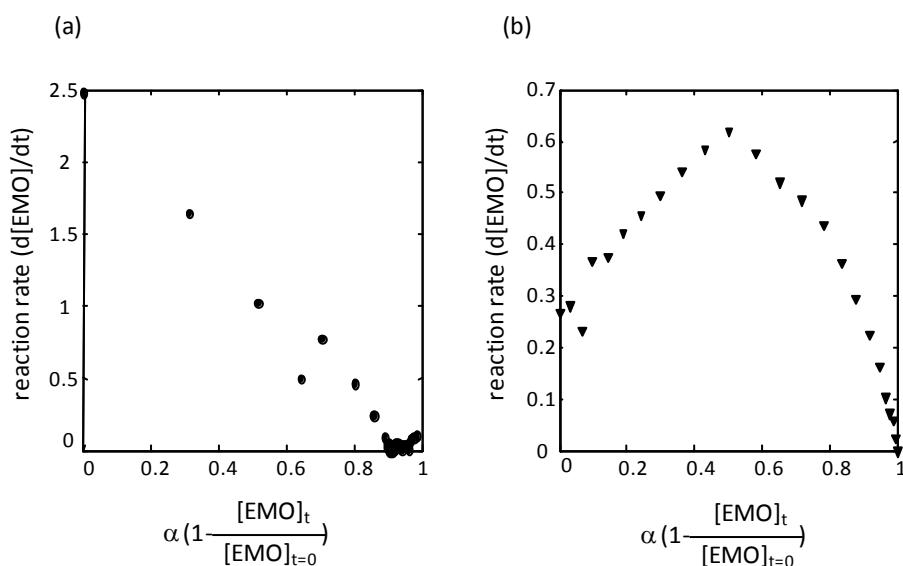


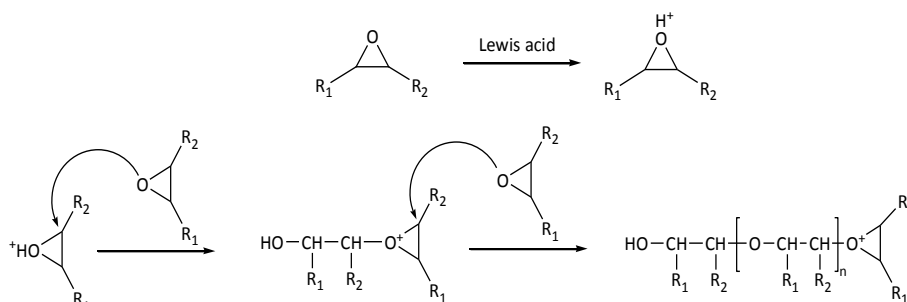
**Fig 4.** Reaction rate *versus* conversion ( $\alpha$ ): (a) 60 °C; (b) 30 °C.

Two possibilities can explain the different behaviour of the system at the two experimental temperatures. Firstly, as the authors commented above, the methanol formed in the amidation reaction can be evaporated at 60 °C faster

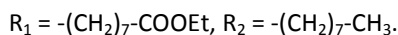
than at 30 °C, so the amidation reaction takes place more easily and it is favored at higher temperatures.

Secondly, as was indicated in the introduction, although the main reactions involved in the cure process are the amine additions to the oxirane ring, when the reaction takes place in presence of a Lewis acid as catalyst, homopolymerization reaction is also reported [3]. To evaluate this possibility, the epoxide conversion was calculated from the spectra recorded during homopolymerization of the EMO reagent, whose data was arranged in matrices  $M_3$  and  $M_4$ . At the reaction time of 50 minutes and 100 minutes, where the concentration of the amide compound (AD1) was maximum for the two temperatures (Figure 3), 60 °C and 30 °C respectively, the conversion values obtained were 1.88 % at 60 °C and 0.17 % at 30 °C, in agreement with the consideration that this reaction is less favoured than the amine addition reaction. However, although quantitatively this reaction can be considered neglected in the working experimental conditions, it may play an important role in the behaviour of the amide reaction and therefore, in the pathway of the process.

In the homopolymerization of EMO, the cationic ring opening of the epoxide could follow the activate chain end (ACE) mechanism [25], as indicated in Scheme 2. The ACE mechanism involves nucleophilic attack of the heteroatom of the monomer to the growing chain end, which is a cationic species. As a result, polyether with pendant ester groups is formed. The presence of these ester groups could explain the high and fast increase in the concentration profile of the amide compound shown in Figure 3a.



**Scheme 2.** Homopolymerization of epoxide by activate chain end (ACE) mechanism.



These expounded likelihoods are not mutually exclusive and, in any case, from all these considerations, it is reasonable to assume that the formation of the amide compound plays an important role in the mechanism of the reaction.

#### 4. Conclusions

The importance of the effect of the temperature on a model curing reaction of epoxy resins from vegetable oils was successfully demonstrated by the combination of infrared spectroscopy and multivariate curve resolution – alternating least squares. The corresponding concentration and spectral profiles of the species involved in the EMO/aniline system monitored were successfully drawn and the first ones were a valuable guide for analysing the mechanism of the process.

Two different mechanisms depending on the temperature for the EMO/aniline system were postulated: at low temperatures the mechanism was autocatalytic and at high temperatures was non-autocatalytic.

It has been evidenced that higher temperatures favour the amidation reaction in the model system studied. As epoxidized vegetable oils contain ester groups, when they are cured with amine hardeners, the amidation reaction will take place in some extent, what could lead to products of poor quality.

**Acknowledgments.** The authors gratefully acknowledge the collaboration in the preparation of this paper of Virginia Cádiz from the Polymer Research Group of the Universitat Rovira i Virgili. Likewise, we would like to thank the Spanish Ministry of Science and Innovation (Project CTQ2007-61474/BQU) for economic support and the Universitat Rovira i Virgili, for providing Vanessa del Río with a doctoral fellowship.

## 5. References

- [1] J.D. Earls, J.E. White, L.C. López, Z. Lysenko, M.L. Dettloff and M.J. Null, *Polymer* **48** (2007) 712.
- [2] J. Mijovic, S. Andjelic, C.W. Yee, F. Belluci and L. Nicolais, *Macromolec.* **28** (1995) 2797.
- [3] L. Xu, J.H. Fu and J.R. Schlup, *Ind. Eng. Chem. Res.* **35** (1996) 963.
- [4] L. Xu and J.R. Schlup, *J. Appl. Polym. Sci.* **67** (1998) 895.
- [5] J.C. Ronda, A. Serra and V. Cádiz, *Macromolec. Chem. Phys.* **200** (1999) 221.
- [6] L. Matejka, *Macromolec.* **33** (2000) 3611.
- [7] S. Swier and B.V. Mele, *Termochim. Acta* **41** (2000) 149.
- [8] S. Swier, G.V. Assche and B.V. Mele, *J. Appl. Polym. Sci.* **91** (2004) 2814.
- [9] M. Garrido, M.S. Larrechi and F.X. Rius, *Appl. Spectrosc.* **60** (2006) 174.
- [10] N. Boquillon and C. Fringant, *Polymer* **41** (2000) 8603.

- [11] F.T. Wallenberger and N. Weston, *Natural Fibers, Plastics and Composites*, Kluwer Academic Publisher, USA, 2004.
- [12] J. Mijovic, S. Andjelic and J.M. Kenny, *Polym. Adv. Technol.* **7** (1995) 1.
- [13] J.R. Schoonover, R. Marx and W.R. Nichols, *Vibr. Spectrosc.* **35** (2004) 239.
- [14] B. Czarnik-Matuszewicz and S. Pilorz, *Vibr. Spectrosc.* **40** (2006) 235.
- [15] M. Garrido, M.S. Larrechi and F.X.Rius, *J. Chemom.* **21** (2007) 263.
- [16] N. Spegazzini, I. Ruisánchez, M.S. Larrechi, V. Cádiz and J. Canadell, *Analyst* **133** (2008) 1028.
- [17] V. del Río, N. Spegazzini, M.P. Callao and M.S. Larrechi, *J. Near Infrared Spectrosc.* doi: 10.1255/jnirs.880.
- [18] L. Montero de Espinosa, J.C. Ronda, M. Galià and V. Cádiz, *J. Polym. Sci.: Part A: Polym. Chem.* **46** (2008) 6843.
- [19] The Mathworks, MATLAB Version 6.5, Natick, MA, (2004)
- [20] J. Coates, *Interpretation of Infrared Spectra, A Practical Approach in Encyclopedia of Analytical Chemistry*. R.A. Meyers (Ed.), John Wiley & Sons Ltd, Chichester, 2000.
- [21] D.L. Massart, B. Vandeginste, L. Buydens, S. de Jong, P. Lewi and J. Smeyers-Verbeke, *Handbook of Chemometrics and Qualimetrics*, Part A, Elsevier, Amsterdam, 1997.
- [22] M. Amrhein, B. Srinivasan, D. Bonvin and M.M. Schumacher, *Chemom. Intell. Lab. Syst.* **33** (1996) 17.
- [23] R. Tauler, A. Smilde and B.R. Kowalski, *J. Chemom.* **9** (1995) 31.
- [24] M. Ghaemy, M. Barghamadi and H. Behmadi, *J. Appl. Polym. Sci.* **94** (2004) 1049.
- [25] S. Penczek, P. Kubisa and K. Matyjaszewski, *Adv. Polym. Sci.* **37** (1980) 1.



### **3.2.2. A new enone-containing triglyceride derivative, the enone-containing methyl oleate from high oleic sunflower oil, as pre-polymer in the curing aza-Michael reaction**

This work, which have been published in *Analytica Chimica Acta*, analyses the reaction between a modified fatty acid ester with  $\alpha,\beta$ -unsaturated ketone groups (enone-containing methyl oleate (eno-MO)) and aniline. This reaction is taken as an aza-Michael model of the curing process in the preparation of thermosets from triglycerides and diamines.

The aza-Michael reaction, a variation in which an amine acts as the nucleophile, has been used in the synthesis of improved bismaleimide networks [47] and it has recently been applied to the synthesis of crosslinked polymers derived from vegetable oils [12]. The acid-catalysed aza-Michael reaction can be affected by a retro-Mannich-type fragmentation [48] and the cleavage of the aza-Michael addition product would mean the breakage of the forming network and a deterioration of the mechanical properties. Therefore, to determine the optimal experimental conditions of the system, it is important to evaluate the extension of the fragmentation and to study the evolution of each chemical species involved in the reaction of interest.

In this study, the model aza-Michael reaction was monitored by NIR spectroscopy at 95 °C, using an eno-MO:aniline stoichiometric ratio of 1:1. The reaction comprises several steps. First, the aza-Michael adduct is formed by the addition of the primary amine to the double bond of the eno-MO reagent. Then, the retro-Mannich-type fragmentation takes place, which leads to the formation of two products whose main functional groups are similar to the functional groups of the reagents. More details of the reaction can be found in the paper.

Local rank factor analysis of the NIR data showed that, although the retro-Mannich side reaction took place from the beginning, it has no relevance compared to the aza-Michael addition. This was confirmed by  $^1\text{H}$  NMR. Moreover, in the experimental conditions, the evolution of the concentration of the chemical species involved throughout the aza-Michael reaction was obtained by means of multivariate curve resolution - alternating least squares.

UNIVERSITAT ROVIRA I VIRGLI  
FAST ANALYTICAL METHODOLOGIES BASED ON MOLECULAR SPECTROPHOTOMETRIC TECHNIQUES  
AND MULTIVARIATE DATA ANALYSIS  
Vanessa del Rio Sánchez  
ISBN:978-84-693-9439-7/ DL:T.64-2011

### **3.2.2.1. Paper**

**Chemometric resolution of NIR spectra data of a model aza-Michael reaction with a combination of local rank exploratory analysis and multivariate curve resolution – alternating least squares (MCR-ALS) method**

Vanessa del Río, M. Pilar Callao, M. Soledad Larrechi  
Lucas Montero de Espinosa, J. Carles Ronda, Virginia Cádiz

*Analytica Chmica Acta*, 642 (2009) 148-154

UNIVERSITAT ROVIRA I VIRGLI  
FAST ANALYTICAL METHODOLOGIES BASED ON MOLECULAR SPECTROPHOTOMETRIC TECHNIQUES  
AND MULTIVARIATE DATA ANALYSIS  
Vanessa del Rio Sánchez  
ISBN:978-84-693-9439-7/ DL:T.64-2011

**Chemometric resolution of NIR spectra data of a model aza-Michael reaction with a combination of local rank exploratory analysis and multivariate curve resolution - alternating least squares (MCR-ALS) method**

**Vanessa del Río<sup>a</sup>, M. Pilar Callao<sup>a</sup>, M. Soledad Larrechi<sup>a</sup>**

**Lucas Montero de Espinosa<sup>b</sup>, J. Carles Ronda<sup>b</sup>, Virginia Cádiz<sup>b</sup>**

*(a) Chemometrics, Qualimetrics and Nanosensors Research Group*

*(b) Polymer Research Group*

*Analytical Chemistry and Organic Chemistry Department, Rovira i Virgili University*

*Marcel·li Domingo s/n, Campus Sescelades, 43007 Tarragona, Spain*

**Abstract**

The aza-Michael reaction, a variation of the Michael reaction in which an amine acts as the nucleophile, permits the synthesis of sophisticated macromolecular structures with potential use in many applications such as drug delivery systems, high performance composites and coatings. The aza-Michael product can be affected by a retro-Mannich-type fragmentation. A way of determining the reactions that are taking place and evaluate the quantitative evolution of the chemical species involved in the reactions is presented. The aza-Michael reaction between a modified fatty acid ester with  $\alpha,\beta$ -unsaturated ketone groups (enone containing methyl oleate (eno-MO)) and aniline (1:1) was studied isothermally at 95 °C and monitored *in-situ* by near-infrared

spectroscopy (NIR).

The number of reactions involved in the system was determined analyzing the rank matrix of NIR spectra data recorded during the reaction. Singular value decomposition (SVD) and evolving factor analysis (EFA) adapted to analyze full rank augmented data matrices have been used. In the experimental conditions, we found that the resulting aza-Michael adduct undergoes a retro-Mannich-type fragmentation, but the final products of this reaction were present in negligible amounts. This was confirmed by recording the  $^1\text{H}$  NMR spectra of the final product. Applying multivariate curve resolution – alternating least squares (MCR-ALS) to the NIR spectra data obtained during the reaction, it has been possible to obtain the concentration values of the species involved in the aza-Michael reaction. The performance of the model was evaluated by two parameters: ALS lack of fit ( $lof = 1.31\%$ ) and explained variance ( $R^2 = 99.92\%$ ). Also, the recovered spectra were compared with the experimentally recorded spectra for the reagents (aniline and eno-MO) and the correlation coefficients ( $r$ ) were 0.9997 for the aniline and 0.9578 for the eno-MO.

**Keywords:** Near-infrared spectroscopy; Evolving factor analysis; Multivariate curve resolution; Alternating least squares; Aza-Michael reaction; Ester fatty acid.

## 1. Introduction

The challenge to progressively replace fossil feedstocks by materials arising from plant-derived renewable sources implies not only the development of new original reactions and catalysts but also the application of environmentally friendly well established reactions to the production of new

tailor made compounds capable to produce competitive performance materials [1]. The Michael addition reaction permits the synthesis of sophisticated macromolecular structures with potential use in many applications such as drug delivery systems, high performance composites and coatings. The aza-Michael reaction, a variation in which an amine acts as the nucleophile, is a key transformation which enables the preparation of these compounds [2,3]. The end-user properties of the product depend not only on the extent of the reaction but also on the possible presence of secondary reactions. Thus, the study of the evolution of the chemical species involved in the reaction is of interest.

Plant oils can be polymerized directly through autoxidation or peroxide formation and subsequent radical polymerization. However, the functionalization of the alkyl chains towards the introduction of polymerizable groups gives rise to a variety of monomers that can be used in the preparation of crosslinked materials [4,5]. The crosslinking reactions are difficult to follow because once the system has reached the gelation point, few characterization techniques can be used. For this reason, a previous step to the synthesis of new plant oil derivatives is the study of the crosslinking reaction on monofunctional model compounds.

Near-infrared spectroscopy (NIR) in combination with multivariate analysis methods has demonstrated to be a useful technique in many analytical applications due to the combination of an instrumental technique that allows to obtain easily the analytical signal with a powerful chemometric technique able to achieve the necessary spectral resolution [6-8]. Soft-modelling methods, in particular multivariate curve resolution - alternating least squares method (MCR-ALS), have a great potentiality when they are applied to spectroscopic data



obtained from monitoring a chemical reaction, because they allow to obtain the concentration profiles and the corresponding pure spectra of each species involved in the reaction [9-11].

This work is focused on the on-line study of different reactions which can take place between a modified fatty acid ester with  $\alpha,\beta$ -unsaturated ketone groups (enone containing methyl oleate (eno-MO)) and aniline at 95 °C. These reactions are taken as an aza-Michael model of the curing process in the preparation of thermosets from triglycerides and diamines.

The possibility of studying the reaction considered in the present work using these methodologies represents a challenge because the efficiency of the studied aza-Michael reaction can be affected by a retro-Mannich-type fragmentation [12]. One of the products generated by this fragmentation is the reagent aniline. The other new products generated have similar functional groups and, therefore, similar spectral behavior. As the cleavage of the aza-Michael addition product would mean a loss in the crosslinking density of the final thermosetting material, knowing the moment in which the fragmentation takes place and its extent is of great interest.

The purpose of the present study is to demonstrate the potential of the combination of a local rank analysis technique to analyze full rank augmented data matrices, with multivariate curve resolution methods to calculate the concentration and spectra profiles of each compound involved in the aza-Michael reaction.

Rank information, i.e. the determination of the total number of components and their evolution, is crucial in the resolution of dynamic multicomponent systems [13,14]. The chemical rank is the number of controlling

factors responsible for the data in absence of noise and it can be estimated neglecting the non-significant singular values and their corresponding singular vectors calculated by singular value decomposition (SVD) [15].

Evolving factor analysis [16] adapted to analyze full rank augmented data matrices has been used to detect the evolution of the singular values as the measurement is carried out and to obtain information about the number of the reactions that are taking place. The rank-deficiency problem detected has been solved by a matrix augmentation process [14]. In this study, a column-wise data matrix has been constructed appending at the data matrix recorded during the studied reaction, the two sets of data obtained when the pure reactants has been monitored independently in the same conditions.

Considering as representative of the variability of experimental error the value of the second singular value calculated by SVD in the data matrix obtained when the spectra of the reagents in the experimental conditions was monitored, we have found that as consequence of the reaction that is taking place, five singular values were significant. Analyzing the reaction time where they appear and their values, we have postulated that, in the experimental conditions, the most important reaction is the aza-Michael reaction, which is taking place quickly, but from the beginning the retro-Mannich-type fragmentation was also detected. However, regarding the values of the singular values and the EFA plot, it has been considered insignificant. This approximation has been confirmed by NMR analysis.

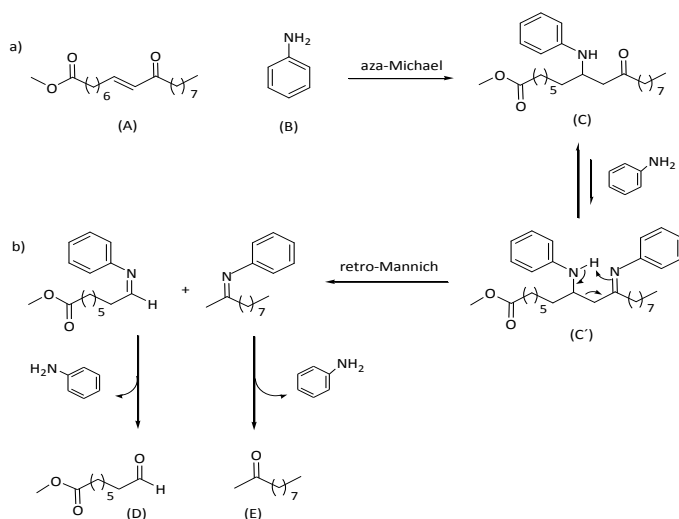
The quantitative resolution of the data of the aza-Michael reaction was performed by MCR-ALS and in the optimization process only non-negativity constraint was applied [17]. The lack of fit (*lof*) of the model, the explained

variance and the correlation coefficients between the recovered spectra and the spectra of the pure species ( $r$ ) were used to assess the quality of the results.

## 2. Experimental

### 2.1. Reaction conditions and procedure

Scheme 1 shows the reaction that takes place between eno-MO (A) and aniline (B) (reaction a). The primary amine reacts with eno-MO to form a secondary amine through an aza-Michael addition reaction. The condensation of the resulting aza-Michael adduct (C) with aniline (B) gives the intermediate C' which undergoes a retro-Mannich reaction to form a mixture of products (D and E) (reaction b).



**Scheme 1.** Reaction between eno-MO and aniline at 95 °C: (a) aza-Michael reaction, (b) retro-Mannich-type fragmentation. (A) eno-MO, (B) aniline, (C) resulting aza-Michael adduct, (C') retro-Mannich intermediate, (D) and (E) retro-Mannich-type fragmentation products.

The temperature for the isothermal reaction was 95 °C. Initial molar ratio between eno-MO and aniline was 1:1 (eno-MO:aniline). The experimental procedure involved mixing of the necessary amounts of aniline and eno-MO at room temperature to obtain the desired molar ratio and immediately injecting 1 mL of this mixture into the liquid cell of the NIR spectrophotometer.

The eno-MO was synthesized as previously reported [18].

## 2.2. Data acquisition and data pre-treatment of NIR spectra

The data obtained correspond to the NIR spectra recorded every 4 nm between 1352 and 2256 nm in an Infra Analyzer 500 Bran-Luebbe spectrophotometer. The instrument is designed to measure the reflectance of the samples when the radiation is reflected over a stainless steel disk. For each experiment, data at intervals of 5 min were acquired.

The band at 1976 nm [19], which is characteristic of the primary amine group, was chosen as a reference. Thus, the reaction was considered to be completed when absorbance changes at this band were not observed. In this way, we consider that the reaction ended after 12.5 h. At this time, 150 spectra were obtained. Therefore, we obtained a matrix **M** (150 x 227), whose rows were the number of recorded spectra and whose columns were the wavelengths. In the same conditions, the NIR spectra of the pure reactants were also recorded during 1 h (**A** (12 x 227) and **B** (12 x 227)) in order to evaluate the noise and to perform the local rank analysis using modified evolving factor analysis.

The spectra recorded in the InfraAnalyzer 500 were exported and converted into MATLAB binary files [20].

All the original spectra were corrected to eliminate the vertical shift caused by using a NIR spectrophotometer with only one light beam [21].

## 2.3. Chemometrics analysis

### 2.3.1. Rank analysis

The rank of the **M** matrix has been calculated by singular value decomposition (SVD) [15]. In this study, we are considering the second singular value of the data matrix of the reagent aniline (**B** matrix) as threshold value associated to the noise. To overcome the rank deficiency detected on **M** matrix, an augmented matrix **D** was constructed appending the full rank matrices **A** and **B** (Fig. 1). The rank of the new data set calculated by SVD and the number of significant values detected are the same of possible absorbing species in **M**.

The modified EFA algorithm [16] was applied to this augmented matrix **D**. The EFA algorithm works according to the following steps:

1. Forward EFA on the augmented matrix [**A;B;M**].
2. Backward EFA on the augmented matrix [**M;B;A**].
3. Combined EFA plot taking into account the contribution present exclusively in **M**.

The aim of this algorithm is to extract the information about the contributions present in **M** and their evolution along the reaction time.

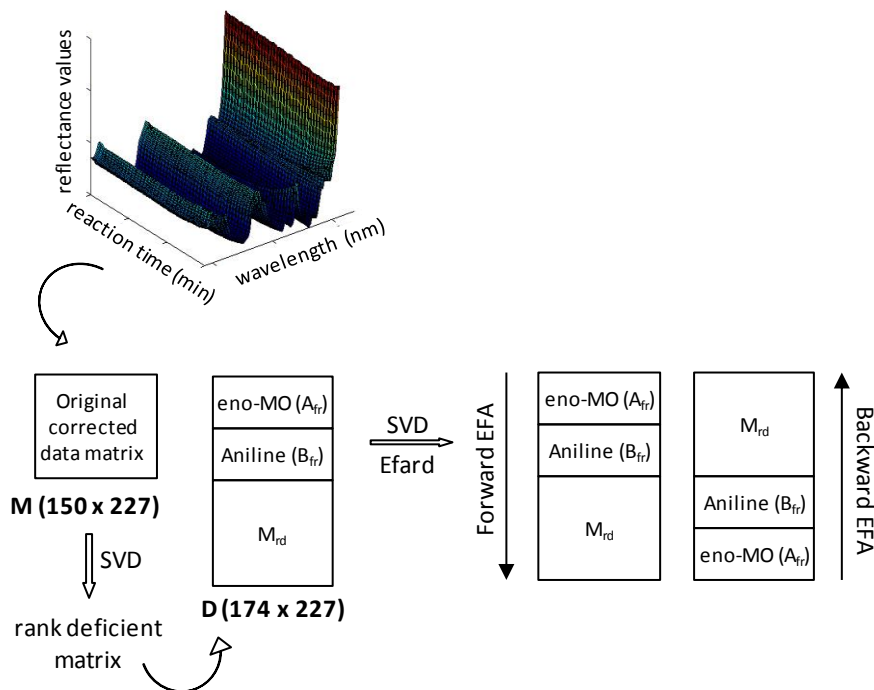


**Figure 1.** Data matrix. (**M**) Rank-deficient data matrix containing the spectra recorded during the reaction. (**D**) Augmented matrix in the direction of columns which contains additional chemical information supplied to the system.

### 2.3.2. Multivariate curve resolution-alternating least squares (MCR-ALS)

The aim of MCR-ALS [22] method is the bilinear decomposition of the experimental data set **D** in order to obtain matrices **C** and **S<sup>T</sup>**, which have a real chemical significance, according to Eq. (1):

$$\mathbf{D} = \mathbf{CS}^T + \mathbf{E} \quad (1)$$

where the dimensions of the matrices are: **D** ( $n \times m$ ), **C** ( $n \times c$ ), **S<sup>T</sup>** ( $c \times m$ ), **E** ( $n$

$x$   $m$ ); and  $c$  is the number of components considered (chemical species contributing to the signal),  $n$  is the number of spectra and  $m$  is the number of wavelengths in data matrix  $\mathbf{D}$ .  $\mathbf{C}$  is the matrix that describes the changes in the concentration of the species in the system under study.  $\mathbf{S}^T$  is the matrix that contains the response profile of these species (spectra profiles) and  $\mathbf{E}$  is the residual matrix with the data variance unexplained by the product  $\mathbf{CS}^T$ .

First, the number of compounds present in  $\mathbf{D}$  that have chemical information is estimated from the chemical rank associated with the data matrix  $\mathbf{D}$ . This determination is performed according to expose above in section 2.3.1.

In the optimization process, in which ALS is applied to the matrix  $\mathbf{D}$ , constraint of non-negativity for the concentrations ( $\mathbf{C}$ ) and spectral ( $\mathbf{S}^T$ ) profiles was imposed [17].

The percentage of explained variance by the product of  $\mathbf{CS}^T$ , the lack of fit and the coefficient of similarity between the recovered spectra and the spectra of the pure species were used as parameters to evaluate the goodness of the model.

The software used in this work has been written by Chemometrics Group of Barcelona University and has been downloaded from the Web page [23].

## 2.4. NMR spectra

$^1\text{H}$  NMR spectra at the beginning and  $^1\text{H}$  NMR spectra of the mixture extracted from the NIR at the end of the experiment (12.5 hours) was recorded using a Varian Gemini 400 spectrometer with  $\text{CDCl}_3$  as the solvent.

A relaxation time delay of 10 seconds was used for obtaining a quantitative integration of the signals.

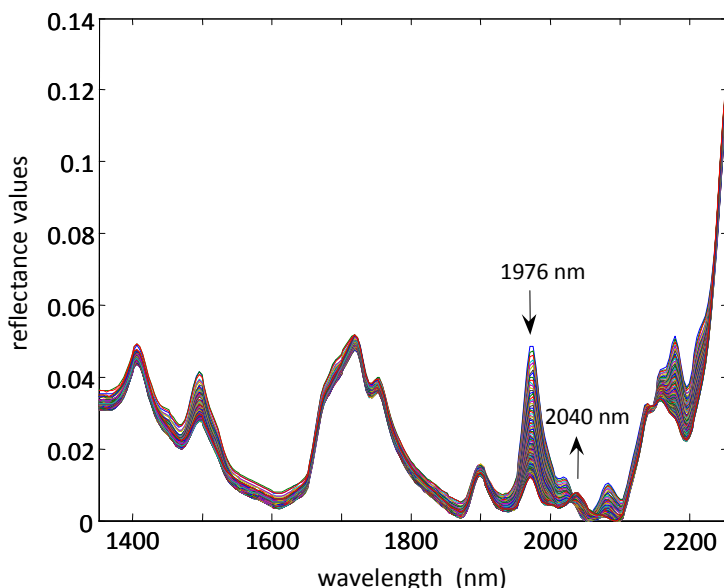
## 3. Results and discussion

Fig. 2 shows the NIR spectra obtained by monitoring the experiment with eno-MO/aniline molar ratio 1:1 at 95 °C, after an off-set correction. The bands of interest, including primary and secondary amine and carbonyl group are identified in the spectra and their assignments are listed in Table 1. The assignments of the bands generally agree with those reported in the literature [19,24,25].

**Table 1.** Assignment of the absorption bands in the NIR spectra (see Fig. 2).

	Wavelength (nm)	Assignment
1	1500	NH and $\text{NH}_2$ group
2	1676	CH aromatic
3	1900	C=O group
4	1976	$\text{NH}_2$ group
5	2020	NH and C=O group
6	2040	C=O group
7	2084	C=O group
8	2160	CH aromatic
9	2180	C=O group
10	2256	CH





**Figure 2.** NIR transfectance spectra of eno-MO/aniline 1:1 obtained every 5 min at 95 °C, after the application of the *off-set* correction. The arrows indicate the evolution over time of the spectral bands (see the text).

The principal changes correspond to the following vibrations. The band at 1976 nm associated with primary amine group present in the reagent aniline (B), decreases constantly during the reaction time. However, it is possible to observe that through the reaction the disappearance of this band changes the velocity in the temps unit. At the end of the recorded spectra this band is present and this fact indicates that the reaction is very low or that the other reactions postulated in scheme 1 are taking place.

The same happens with the absorption bands at 2020, 2084 and 2180 nm, characteristic of stretching vibrations of the C=O group present in the initial reagent A and in the resulting aza-Michael adduct C. The intensity of these bands decreases throughout the reaction, indicating that they are mainly characteristic of the C=O group present in reagent A. Also, during the reaction time, an increase in the absorption at 2040 nm is observed. This band is also characteristic of C=O groups and, as consequence of its increase, it can be assigned to product C.

The main bands typically observed in the NIR region correspond to overtones and combination bands containing hydrogen and other light atoms (namely C-H, N-H O-H and S-H) [26,27]. For this reason, in the experimental data it is not easy to find characteristic bands of the different compounds that have been postulated in the scheme 1.

Table 2 shows the values of the first six singular values calculated by means of SVD procedure of data matrix **M**. The number of chemical components was estimated by inspecting of the size of the singular values. It is assumed that the singular values associated to the chemical components are much larger than other possible contributions such as instrumental drift or experimental error. Even though some test to evaluate the number of significant factors exist [28], in this study we are considering the second singular value calculated with the data matrix of the reagents aniline (B) as threshold value associated to the noise (0.066). Therefore, the number of significant factors in individual matrix **M** is 3. However, the value associated to the last singular value is near to the limit established.

**Table 2.** Rank analysis of matrices **M** and **D**.

Number of factor	Singular values of the M matrix	Singular values of the D matrix
1	5.3234	6.9916
2	0.3538	3.5431
3	0.0852	0.3776
4	0.0348	0.1931
5	0.0157	0.0925
6	0.0089	0.0548
7	0.0063	0.0322

If the only reaction that was taking place was the postulated aza-Michael reaction in scheme 1, in which the number of species that intervene in the process and absorb in the spectral zone is 3, the number of significant values it will be 2, in agreement with Amhrein et al. [29]. The existence of three significant values indicates that the evolution of the reagents along the reaction is not the same. This fact can be interpreted by the presence of the other chemical reactions postulated in scheme 1. Then, matrix **M** would be present rank deficiency.

A strategy to detect the rank deficiency implicit in individual matrix **M** is to add chemical knowledge available to the experimental data [14]. In this study, to overcome the possible rank deficiency, a column-wise data matrix was constructed with the two sets of data corresponding to the two reagents (**D** = [**A**;**B**;**M**]). The singular values associated to the SVD for the augmented matrices are shown in Table 2. When we calculated the singular values for the augmented matrix, there was a considerable increase in the fifth singular value, whose magnitude was similar to the third singular value of the individual data matrix. This fact indicates that there is added information (variability) not contained in

the matrix **M** and, therefore, the original matrix presents rank deficiency.

In the new augmented matrix **D** the number of singular values is 5. Thus, the rank deficiency is broken because the rank of the new matrix matched the number of absorbing species that intervene in the reactions postulated in scheme 1.

A step further into the search for the right number of variability sources in the spectral data is to apply modified EFA [16] to augmented full rank matrix. The performance of the modified EFA algorithm will be shown on the full rank augmented data set formed by column-wise appending **A**, **B** and **M** (matrix **D**). The new data set has now rank 5, the number of absorbing species.

As in the classical EFA algorithm, the analysis is performed forward and backward, plotting eigenvalues as a function of the number of rows included in the submatrix grown inside the augmented data set [30]. Forward EFA applied to the full rank matrix provides the results presented in Fig. 3, where the evolution of five significant contributions can be detected emerging from the noise level (log eigenvalue = -2.4). A vertical line divides the plot in two sections to separate the information from samples windows related to rank-deficiency matrix **M** and full-rank matrices **A** and **B**, on the left and right side of the forward and backward plot, respectively.

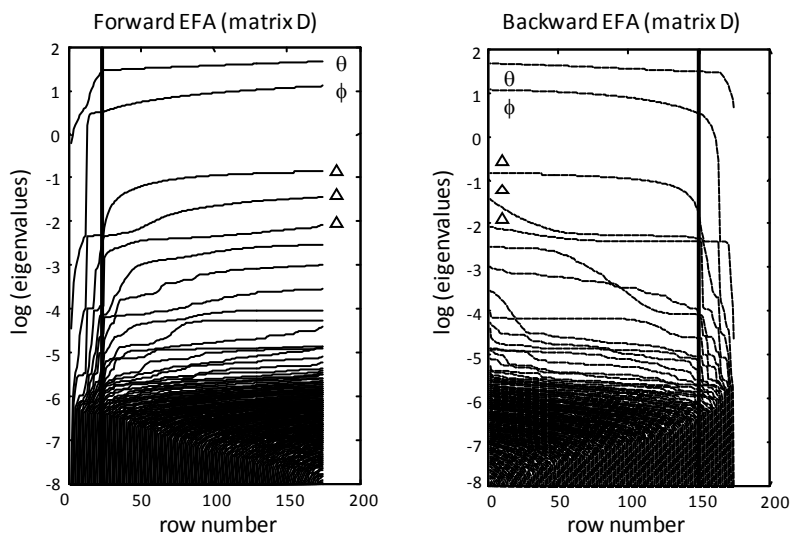


**Figure 3.** EFA plots of full rank  $\mathbf{M}$  matrix; forward EFA (left) and backward EFA (right); the lines marked “ $\theta$ ” and “ $\phi$ ” indicated reagent contributions and the lines “ $\Delta$ ” denote additional contributions emerging in  $\mathbf{D}$ .

As was to be expected, two components are present from the beginning to the row 24, related to the pure reagents present in full-rank matrices  $\mathbf{A}$  and  $\mathbf{B}$ , respectively. The corresponding emerging lines are marked “ $\theta$ ” and “ $\phi$ ”, respectively. The major interest of the modified EFA appears once the vertical line has been crossed. At row 25, rows of rank-deficiency  $\mathbf{M}$  start to form part of the submatrices analyzed. At the noise level considered, the right part of the plot shows now the five real contributions in  $\mathbf{M}$ . From these contributions, two are common to the full-rank matrices and three new ones (marked “ $\Delta$ ”) are only present in  $\mathbf{M}$ . At the first spectrum of  $\mathbf{M}$ , a new factor emerges significantly. The second and third are detected later and the values reached by these factors are smaller than the values of the previous factors. This is in agreement with the hypothesis raised of that in the experimental conditions, besides the aza-Michael reaction, the retro-Mannich reaction can be taking place.

This was confirmed by NMR. Fig. 4 shows the  $^1\text{H}$  NMR spectra of a mixture of eno-MO and aniline at 0 min and at 12.5 h. The signals assignments are shown together with the molecular formulas. At the beginning of the reaction (spectra a) eno-MO and aniline have still not significantly reacted. After 12.5 h (spectra b), A and B signals have almost totally disappeared. As was predicted, the retro-Mannich-type fragmentation takes place as it can be observed by the presence of a singlet at 2.13 ppm. This signal belongs to the three protons of the methyl group of methyl ketone E. The presence of D (see scheme 1) could be followed by the appearance of the aldehyde proton around 10 ppm, but this kind of signals are broad and in this case is too weak as it belongs to one proton. However, D must be present since E is observed. In spectra b, by-product E signal has not significantly increase, confirming that the retro-Mannich side reaction has not relevance compared to the aza-Michael addition.

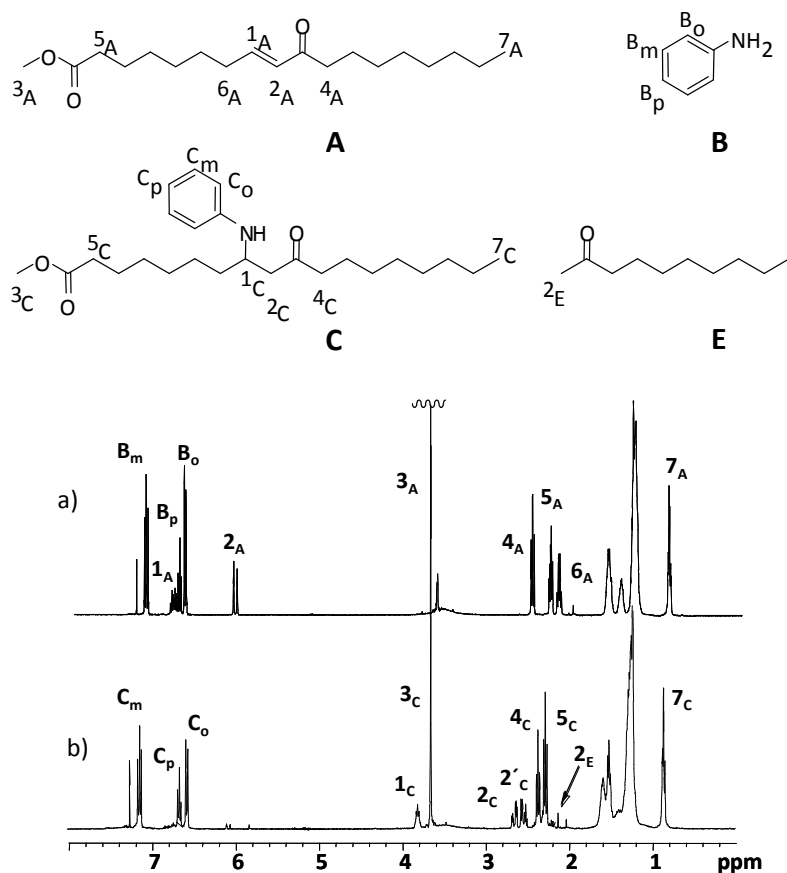


**Figure 4.**  $^1\text{H}$  NMR spectra and signal assignments of the reacting mixture at different reaction times: (a) 0 min and (b) 12.5 h.

MCR-ALS was applied to the augmented data matrix **D**. As the value associated to the last singular values considered representatives of the evolution of the compound associated to retro-Mannich reaction are near the limit established and according to the results found by  $^1\text{H}$  NMR, that show that the products **D** and **E** are present in insignificant amounts, only the aza-Michael reaction has been considered. Therefore, only three factors were considered in the optimization process by MCR-ALS.

The MCR-ALS optimization of the augmented NIR data matrix gave two matrices: a matrix **C** that contains the concentration profiles for the three compounds involved in the aza-Michael reaction and a matrix **S<sup>T</sup>** which consists of the spectra recovered for each of the three species. The product of both matrices accounts for 99.92 % of the variance associated with the augmented experimental data matrix **D** and the lack of fit is 1.31 %, which in quantitative terms means that it explains practically all the variability of the experimental data.

Fig. 5 shows the recovered spectra profiles by MCR-ALS for the chemical species involved in the aza-Michael reaction and the pure spectra of the reactants eno-MO and aniline. Their goodness was evaluated quantitatively by calculating the similarity coefficients between the recovered spectra and the pure spectra recorded for the reactants (eno-MO and aniline), respectively. The values were 0.9578 for the eno-MO and 0.9997 for the aniline, indicating that the recovered profiles have a high degree of concordance with the original ones. In the recovered spectra associated to product C it is possible to observe that the typical primary amine signal at 1976 nm does not appear and a signal at 1500 nm appear but less intense than the signal attributed to aniline. Also, a band not observed in the other spectra at 2040 nm associated with stretching vibration of the functional group C=O can be observed. All these characteristics make it possible to assign this profile as characteristic of the resulting aza-Michael adduct (C) because it presents a secondary amine group and the C=O group that it presents is different from the C=O group present in eno-MO (A) because it is not conjugated.



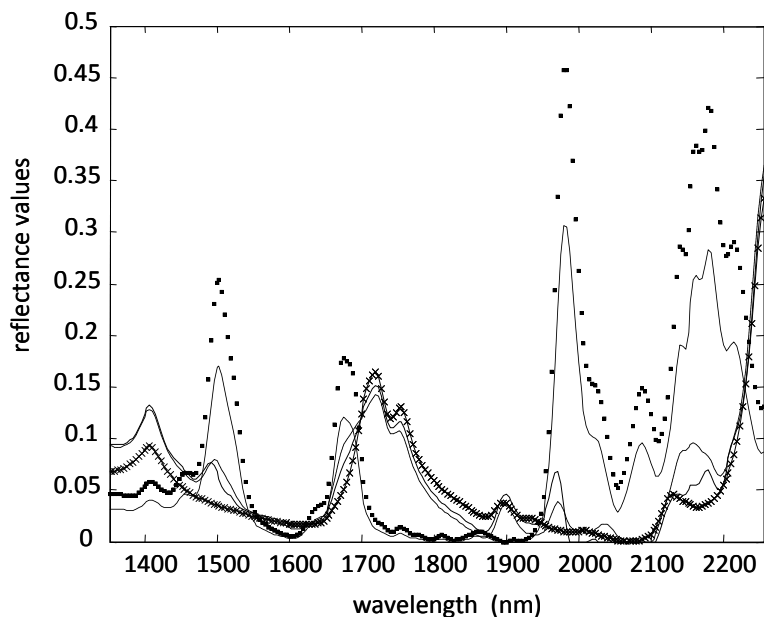


**Figure 5.** Superposition of the spectra of the species recovered by MCR-ALS that intervene in the chemical reaction and the pure spectra of the reactants eno-MO and aniline. For the MCR-ALS spectra profiles: (—) eno-MO, (···) aniline and (---) resulting aza-Michael adduct. For the pure reactants: (\*) eno-MO and (■) aniline.

Fig. 6 shows the evolution of the concentrations in moles of the chemical species involved in the aza-Michael reaction. As consequence to the approach considered during the resolution by MCR-ALS in the optimization process, the closure constraint has not been applied. It is necessary to say that this solution is one of the possible solutions that can be obtained by MCR-ALS, but we have considered that this results are in agreement with the results found by  $^1\text{H}$  NMR. At the beginning of the reaction, the eno-MO and aniline concentrations (solid and dotted line for eno-MO and aniline, respectively) are equal, and the concentration of the product C (dashed line) is zero. At the end of the reaction, the concentration of reagents is zero and the concentration value for adduct C

represents almost 72% of the initial concentration of the reagents. These results are in agreement with the spectra 4b, in which the characteristic signals of aniline can not be detected.

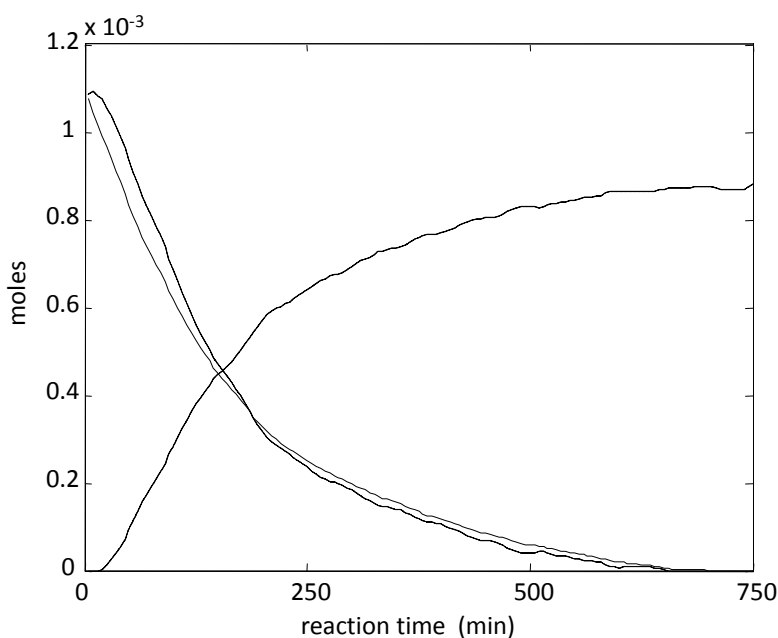


**Figure 6.** Concentration profiles of the species recovered by MCR-ALS that intervene in the chemical reaction: (solid line) eno-MO; (dotted line) aniline; (dashed line) resulting aza-Michael adduct.

#### 4. Conclusions

The properties of products obtained in the polymerization reactions are condition by the reaction mechanism. To determine the optimal experimental conditions is necessary to know the concentration of the species involved in the process. It has been demonstrated that near-infrared spectroscopy (NIR) with multivariate curve resolution methods, such as MCR-ALS, is a useful tool to

obtain this information.

An aza-Michael reaction between a modified fatty acid ester with  $\alpha,\beta$ -unsaturated ketone groups (enone containing methyl oleate (eno-MO)) and aniline at 95 °C has been monitored by NIR. The efficiency of the studied reaction can be affected by a retro-Mannich-type fragmentation, which has been detected from the beginning of the aza-Michael reaction applying local rank exploratory analysis to the NIR spectra.

By inspection of the values it has been possible to consider that the extension of the retro-Mannich reaction in the experimental conditions is not significant. This conclusion has been validated by  $^1\text{H}$  NMR analysis of the final product, as its spectrum shows the complete disappearance of the signals corresponding to free aniline.

Assuming a value of lack of fit of 1.31% during the resolution of the NIR spectra using MCR-ALS, a quantitative study of this reaction allow to conclude that, at the end of the reaction, the majority product is the resulting aza-Michael adduct.

## 5. References

- [1] U. Biermann, W. Friedt, S. Lang, W. Lühs, G. Machmüller, J.O. Metzger, M.R. Klass, H.J. Schäfer and M.P. Schneider, *Angew. Chem. Int. Ed.* **39** (2000) 2206.
- [2] B.D. Mather, K. Viswanathan, K.M. Miller and T.E. Long, *Prog. Polym. Sci.* **31** (2006) 487.
- [3] B.D. Mather, K.M. Miller and T.E. Long, *Macromolec. Chem. Phys.* **207** (2006) 1324.

- [4] M.A.R. Meier, J.O. Metzger and U.S. Schubert, *Chem. Soc. Rev.* **36** (2007) 1788.
- [5] F.S. Güner, Y. Yagci and A.T. Erciyas, *Prog. Polym. Sci.* **31** (2006) 633.
- [6] M. Garrido, M.S. Larrechi and F.X. Rius, *Anal. Chim. Acta* **585** (2007) 277.
- [7] S. Navea, A. de Juan and R. Tauler, *Anal. Chem.* **75** (2003) 5592.
- [8] M.S. Larrechi and M.P. Callao, *Trends Anal. Chem.* **22** (2003) 634.
- [9] L.A. Mercado, M. Galià, J.A. Reina, M. Garrido, M.S. Larrechi and F.X. Rius, *J. Polym. Sci.: Part A: Polym. Chem.* **44** (2006) 1447.
- [10] M. Garrido, M.S. Larrechi and F.X. Rius, *Appl. Spectrosc.* **60** (2006) 174.
- [11] M. Blanco, M. Castillo and R. Beneyto, *Talanta* **72** (2007) 519.
- [12] S.G. Lim and C.H. Jun, *Bull. Korean Chem. Soc.* **11** (2004) 1623.
- [13] A. Izquierdo-Ridorsa, J. Saurina, S. Hernández-Cassou and R. Tauler, *Chemom. Intell. Lab. Syst.* **38** (1997) 183.
- [14] J. Saurina, S. Hernández-Cassou, R. Tauler and A. Izquierdo-Ridorsa, *J. Chemom.* **12** (1998) 183.
- [15] D.L. Massart, B. Vandeginste, L. Buydens, S. de Jong, P. Lewi and J. Smeyers-Verbeke. *Handbook of Chemometrics and Qualimetrics*, Part A, Elsevier, Amsterdam, 1997.
- [16] A. de Juan, S. Navea, J. Diewok and R. Tauler, *Chemom. Intell. Lab. Syst.* **70** (2004) 11.
- [17] A. de Juan and R. Tauler, *Anal. Chim. Acta* **500** (2003) 195.
- [18] E.D. Mihelich and D.J. Eickhoff, *J. Org. Chem.* **48** (1983) 4135.
- [19] J. Mijovic, S. Andjelic and J.M. Kenny, *Polym. Adv. Technol.* **7** (1995) 1.
- [20] The Mathworks, MATLAB Version 6.5, Natick, MA, 2004.
- [21] M. Garrido, I. Lázaro, M.S. Larrechi and F.X. Rius, *Anal. Chim. Acta* **515** (2004) 65.
- [22] A. de Juan and R. Tauler, *Anal. Chim. Acta* **500** (2003) 195.
- [23] Available at: [http://www.ub.es/gesq/eq1\\_eng.htm](http://www.ub.es/gesq/eq1_eng.htm)

- [24] E.D. Tenenbaum, G.C. Clayton, M. Asplund, C.W. Engelbracht, K.D. Gordon, M.M. Hanson, R.J. Rudy, D.K. Lynch, S. Mazuk, C.C. Venturini and R.C. Puetter, *Astron. J.* **130** (2005) 256.
- [25] M. Garrido, M.S. Larrechi and F.X. Rius, *Anal. Chim. Acta* **585** (2007) 277.
- [26] H. Huang, H. Yu, H. Xu and Y. Ying, *J. Food Eng.* **87** (2003) 303.
- [27] M. Blanco and I. Villarroya, *TrAC, Trends Anal. Chem.* **21** (2002) 240.
- [28] M. Wasin and R.G. Brereton, *Chemom. Intell. Lab. Syst.* **72** (2004) 133.
- [29] M. Amrhein, B. Srinivasan, D. Bonvin and M.M. Schumacher, *Chemom. Intell. Lab. Syst.* **33** (1996) 17.
- [30] C. Ruckebusch, A. de Juan, L. Duponchel and J.P. Huvenne, *Chemom. Intell. Lab. Syst.* **80** (2006) 209.

### 3.5. REFERENCES

- [1] J.H. Fu and J.R.Schlup, *J. Appl. Polym. Sci.* **49** (1993) 219.
- [2] G.A. George, P. Cole-Clarke, N. ST. John and G. Friend, *J. Appl. Polym. Sci.* **42** (1992) 643.
- [3] J. Mijovic and S. Andjelic, *Macromolec.* **28** (1995) 2787.
- [4] B.S. Lane and K. Burgess, *Chem. Rev.* **103** (2003) 2457.
- [5] H. Uyama, M. Kuwabara, T. Tsujimoto and S. Kobayashi, *Biomacromolec.* **4** (2003) 211.
- [6] J.D. Earls, J.E. White, L.C. López, Z. Lysenko, M.L. Dettloff and M.J. Null, *Polymer* **48** (2007) 712.
- [7] G. Lligadas, J.C. Ronda, M. Galià and V. Cádiz, *Biomacromolec.* **8** (2007) 686.
- [8] F.L. Jing and S.J. Park, *Polym. Int.* **57** (2008) 577.
- [9] G. Lligadas, J.C. Ronda, M. Galià and V. Cádiz, *Biomacromolec.* **7** (2006) 3521.
- [10] Y. Situ, J. Hu, H. Huang, H. Fu, H. Zeng and H. Chen, *Chin. J. Chem. Eng.* **15** (2007) 418.
- [11] B.D. Mather, K. Viswanathan, K.M. Miller and T.E. Long, *Prog. Polym. Sci.* **31** (2006) 487.
- [12] L. Montero de Espinosa, J.C. Ronda, M. Galià and V. Cádiz, *J. Polym. Sci.: Part A: Polym. Chem.* **46** (2008) 6843.
- [13] V.L. Zvetkov, R.K. Krastev and V.I. Samichkov, *Thermochim. Acta* **478** (2008) 17.
- [14] J.M.E. Rodrigues, M.R. Pereira, A.G. de Souza, M.L. Carvalho, A.A. Dantas Neto, T.N.C. Dantas and J.L.C. Fonseca, *Thermochim. Acta* **427** (2005) 31.
- [15] F.P. Bradner and J.S. Shapiro, *Polymer* **33** (1992) 4366.
- [16] F. Mikes, F. González-Benito, B. Serrano, J. Bravo and J. Baselga, *Polymer* **43** (2002) 4331.
- [17] Ö. Pekcan, D. Kaya and M. Erdogan, *Polymer* **42** (2001) 645.

- [18] G.F. Ghesti, J.L. de Macedo, V.S. Braga, A.T.C.P. de Souza, V.C.I. Parente, E.S. Figueredo, I.S. Resck, J.A. Dias and S.C.L. Dias, *J. Am. Chem. Oil Soc.* **83** (2006) 597. [19] S. Parnell, K. Min and M. Cakmak, *Polymer* **44** (2003) 5137.
- [20] R.E. Challis, M.E. Unwin, D.L. Chadwick, R.J. Freemantle, I.K. Partridge, D.J. Dare and P.I. Karkanis, *J. Appl. Polym. Sci.* **88** (2003) 1665.
- [21] M. Fedtke, J. Haufe, E. Kahler and G. Müller, *Angew. Makromolec. Chem.* **255** (1998) 53.
- [22] H. Madra, S.B. Tantekin-Ersolmaz and F.S. Guner, *Polym. Test.* **28** (2009) 773.
- [23] K. Sahre, T. Hoffmann, D. Pospiech, K.J. Eichhorn, D. Fischer and Brigitte Voit, *Eur. Polym. J.* **42** (2006) 2292.
- [24] L.A. Rodríguez-Guadarrama, *Eur. Polym. J.* **43** (2007) 928.
- [25] M. Garrido, M.S. Larrechi, F.X. Rius, L.A. Mercado and M. Galià, *Anal. Chim. Acta* **583** (2007) 392.
- [26] G. Lachenal, A. Pierre and N. Poisson, *Micron* **27** (1996) 329.
- [27] O. Abbas, C. Rebufa, N. Dupuy and J. Kister, *Talanta* **77** (2008) 200.
- [28] M.J. Adams, M.J. Romeo and P. Rawson, *Talanta* **73** (2007) 629.
- [29] K. Pöllänen, A. Häkkinen, S.P. Reinikainen, J. Rantanen, M. Karjalainen, M. Louhi-Kultanen and L. Nyström, *J. Pharm. Biomed. Anal.* **38** (2005) 275.
- [30] R. Tauler, *Anàlisi de Mescles mitjançant Resolució Multivariant de Corbes*, Institut d'Estudis Catalans, Barcelona, 1997.
- [31] M. Garrido, M.S. Larrechi and F.X. Rius, *Anal. Chim. Acta* **585** (2007) 277.
- [32] M. Garrido, M.S. Larrechi and F.X. Rius, *J. Chemom.* **21** (2007) 263.
- [33] M. Garrido, I. Lázaro, M.S. Larrechi and F.X. Rius, *Anal. Chim. Acta* **515** (2004) 65.
- [34] M. Garrido, M.S. Larrechi and F.X. Rius, *Appl. Spectrosc.* **60** (2006) 174.
- [35] M. Garrido, M.S. Larrechi, F.X. Rius and R. Tauler, *Chemom. Intell. Lab. Syst.* **76** (2005) 111.

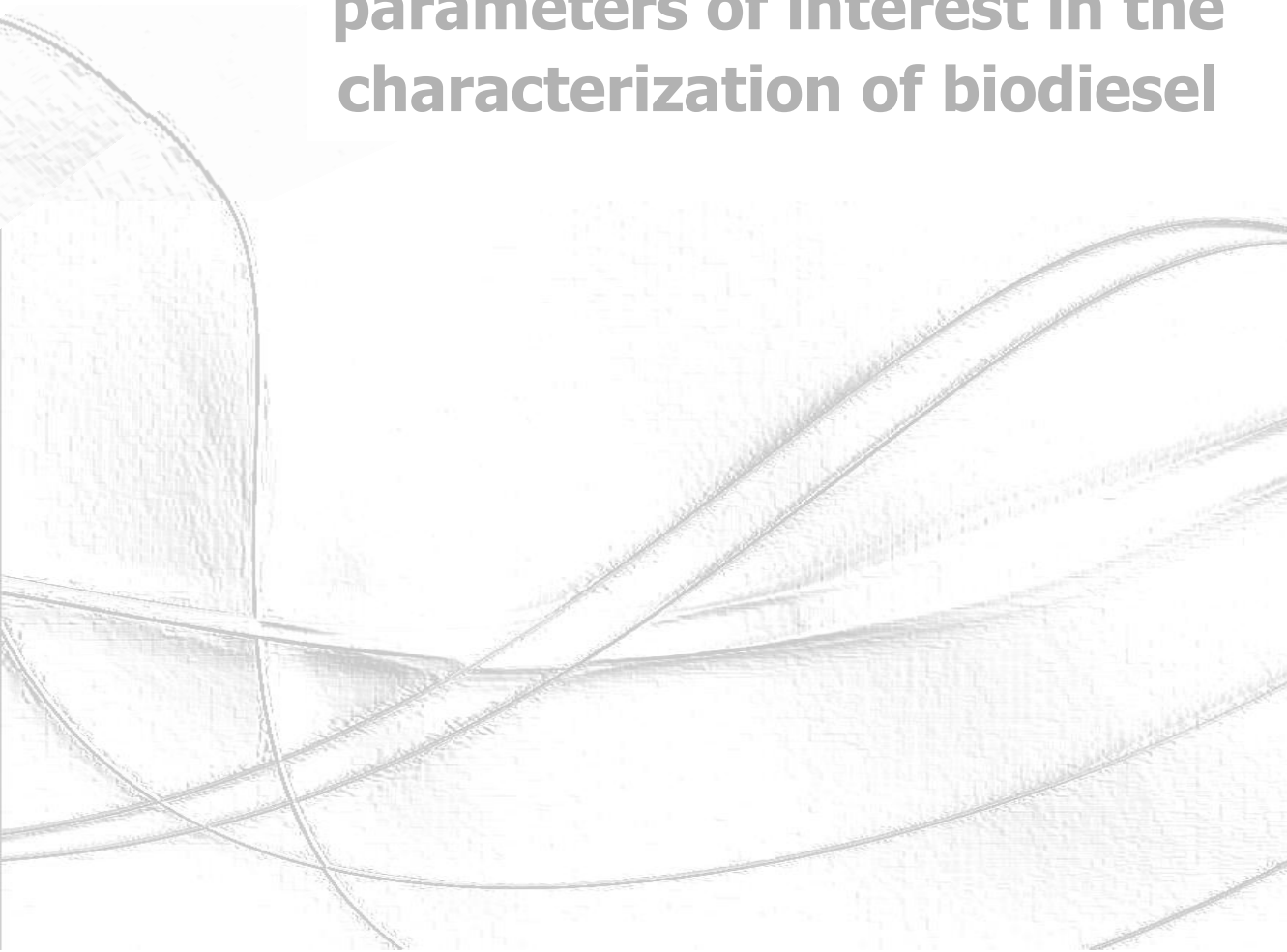
- [36] M. Garrido, M.S. Larrechi, F.X. Rius, J.C. Ronda and V. Cádiz, *J. Polym. Sci.: Part A: Polym. Chem.* **44** (2006) 4846.
- [37] L.A. Mercado, M. Galià, J.A. Reina, M. Garrido, M.S. Larrechi and F.X. Rius, *J. Polym. Sci.: Part A: Polym. Chem.* **44** (2006) 1447.
- [38] N. Spegazzini, I. Risánchez, A. Serra, A. Mantecón and M.S. Larrechi, *Appl. Spectrosc.* **64** (2010) 177.
- [39] N. Spegazzini, I. Ruisánchez, M.S. Larrechi, A. Serra and A. Mantecón, *Appl. Spectrosc.* **64** (2010) 104.
- [40] N. Spegazzini, I. Ruisánchez and M.S. Larechi, *Anal. Chim. Acta* **642** (2009) 155.
- [41] N. Spegazzini, I. Ruisánchez, M.S. Larrechi, V. Cádiz and J. Canadell, *Analyst* **133** (2008) 1028.
- [42] N. Spegazzini, I. Ruisánchez, M.S. Larrechi, A. Serra and A. Mantecón, *J. Appl. Polym. Sci.: Part A: Polym. Chem.* **46** (2008) 3886.
- [43] M. Blanco, M. Castillo and R. Beneyto, *Talanta* **72** (2007) 519.
- [44] M. Blanco, M. Castillo, A. Peinado and R. Beneyto, *Appl. Spectrosc.* **60** (2006) 641.
- [45] N. Boquillon and C. Fringant, *Polymer* **41** (2000) 8603.
- [46] F.T. Wallenberger and N. Weston, *Natural Fibers, Plastics and Composites*, Kluwer Academic Publisher, USA, p. 171, 2004.
- [47] C.S. Wu, Y.L. Liu and Y.S. Chiu, *Polymer* **43** (2002) 1773.
- [48] L. Montero de Espinosa, J.C. Ronda, M. Galià and V. Cádiz, *J. Polym. Sci.: Part A: Polym. Chem.* **48** (2010) 869.



UNIVERSITAT ROVIRA I VIRGLI  
FAST ANALYTICAL METHODOLOGIES BASED ON MOLECULAR SPECTROPHOTOMETRIC TECHNIQUES  
AND MULTIVARIATE DATA ANALYSIS  
Vanessa del Rio Sánchez  
ISBN:978-84-693-9439-7/ DL:T.64-2011

# 4

## **A** nalytical methods based on sequential injection analysis and second-order data treatment for determining parameters of interest in the characterization of biodiesel



UNIVERSITAT ROVIRA I VIRGLI  
FAST ANALYTICAL METHODOLOGIES BASED ON MOLECULAR SPECTROPHOTOMETRIC TECHNIQUES  
AND MULTIVARIATE DATA ANALYSIS  
Vanessa del Rio Sánchez  
ISBN:978-84-693-9439-7/ DL:T.64-2011

## 4.1. INTRODUCTION

This chapter consists of two papers with one main objective: to develop fast analytical methods based on sequential injection analysis (SIA) with UV-visible detection and multivariate curve resolution – alternating least squares (MCR-ALS) for determining parameters of interest in biodiesel. More specifically, the developed methods permit the determination of acidity and sulphate content.

The determination of fuel quality is an issue of great importance to the successful commercialization of biodiesel. The purity and quality of fuel is significantly influenced by numerous factors and low quality of the end product can lead to severe operational problems when using biodiesel, including engine deposits, filter clogging or fuel deterioration. Therefore, standards such as those in Europe (EN 14214; EN 14213 when using biodiesel for heating oil purposes) and the United States (ASTM D6751) regulate the specifications that the pure biodiesel must meet before being used as a pure fuel or being blended with petroleum-based diesel [1,2]. Under these standards, restrictions are placed on the individual parameters.

One of these parameters is the free fatty acid (FFA) content, which depends on the original feedstock and the oil refining steps, because high acid values can cause corrosion and engine deposits. Furthermore, this parameter has also to be determined in the vegetable oils used in the production of biodiesel, because the higher the acidity of the oil, the smaller the reaction yield. FFAs react with basic catalyst forming soaps, which lower the catalytic activity, reduce the reaction yield and emulsify the final product impeding glycerol

separation. Thus, the acid number of fats and oils has to be below a desired value (ranging from less than 0.5% to less than 3%) [3-6].

When the vegetable oils have a high FFA content, acid-catalysed transesterification is suitable [7,8]. Therefore, if sulphuric acid is used as a catalyst, sulphates can be found in the final biodiesel. Excessive sulphates can cause engine deposits and high abrasive wear levels, so the determination of this parameter is also important to achieve a high-quality end product.

The developed method for sulphate determination in biodiesel can also be applied to sulphate determination in aqueous samples, so it was applied to the determination of sulphate in natural and residual waters. The importance of sulphate determination from the standpoint of pollution monitoring is reflected in the maximum legally admissible concentration of  $250 \text{ mg L}^{-1}$  in natural waters [9].

In this thesis, a diode-array spectrophotometer has been used as a detector in a sequential injection analysis (SIA) system. Absorption UV-visible spectroscopy has been used for the analysis of the composition of a sample and for monitoring and controlling processes for over 60 years. This is a very flexible technique that is used in nearly every laboratory and a high number of methods have been developed for determining an elevated number of analytes in diverse application fields [10,11]. Robustness and simplicity are the key parameters for the further broadening of applications and the increase of the number of parameters that can be measured using this technique.

Since its introduction in the nineties [12], sequential injection analysis (SIA) has proved to be a powerful and a versatile instrumental tool, especially for the automation of analytical processes in a great variety of application fields, and

it has spawned extensive solutions to real world problems [13-16]. In SIA, the sample and reagent zones are sequentially aspirated into a channel using a selection valve to subsequently reverse the flow and transport the stacked zones into the detector. During the course of these operations, the zone undergoes some mutual dispersion and the analyte interacts with the reagents, evolving into another species.

It has been pointed out that the penetration zone (related to dispersion) is the key parameter to design a SIA system and some authors have published several articles describing the most important parameters to be optimized [17-20]. Depending on the experimental conditions, the contact between the reagent and the analyte before passing through the detector can be total or partial. If the reagent interacts totally, the analyte will be converted into the reaction product and in the detector only one signal is observed. Nevertheless, if the interaction is partial, as the solution passes through the detector, a diffusive mixture of reagent, analyte and product will be observed [21]. Depending on the kind of interaction and the detector coupled to the system, data of different dimensions can be obtained, as shown in Figure 4.1.

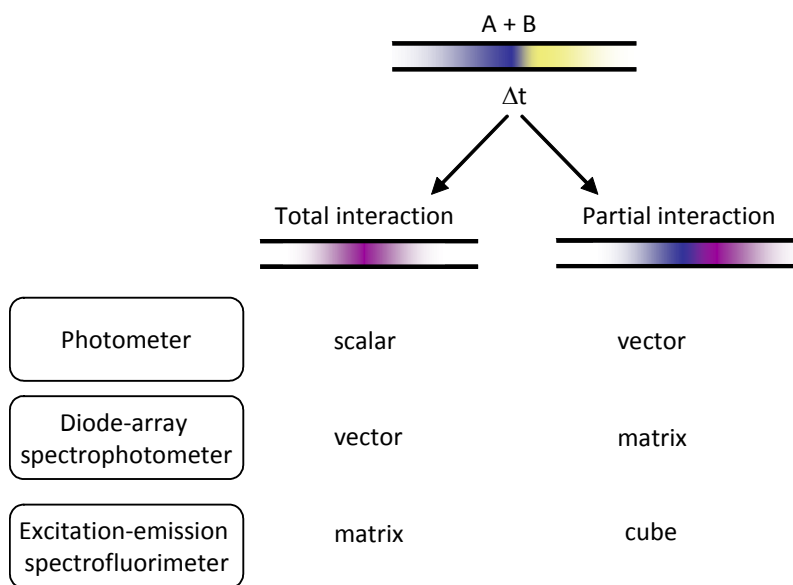


**Figure 4.1.** Different types of data that can be obtained by a SIA and different types of detector. A: analyte; B: reagent.

If a data matrix has been obtained, it is possible to resolve the various species present in a multicomponent sample with multivariate curve resolution – alternating least squares (MCR-ALS) [22,23].

Second-order calibration can reconstruct the response of the analyte in the presence of unknown and uncalibrated interfering species. The pure analyte is often used as a standard, while the interferences are not taken into account in the calibration stage, which is a clear advantage over first-order or multivariate calibration.

To establish a calibration model, a set of calibration standards of known concentrations is used in the linear range. Afterwards, the ALS algorithm is applied to obtain the areas of the concentration profiles of each species of the

system. Then, the area of the species of interest obtained in the resolution process is the signal employed to establish the following univariate linear relation:

$$A_i = b_1 c_i + b_0 \quad (4.1)$$

where  $A_i$  is the area obtained from the resolution process for each calibration standard and  $c_i$  is the corresponding concentration value. The value of the concentration of the analyte in the sample is obtained from its corresponding  $A_i$  value and the calibration parameters.



UNIVERSITAT ROVIRA I VIRGLI  
FAST ANALYTICAL METHODOLOGIES BASED ON MOLECULAR SPECTROPHOTOMETRIC TECHNIQUES  
AND MULTIVARIATE DATA ANALYSIS  
Vanessa del Rio Sánchez  
ISBN:978-84-693-9439-7/ DL:T.64-2011

## 4.2. Paper

Sequential injection titration method using  
second-order signals. Determination of acidity in  
plant oils and biodiesel samples

Vanessa del Río, M. Soledad Larrechi, M. Pilar Callao

*Talanta*, 81 (2010) 1572-1577

UNIVERSITAT ROVIRA I VIRGLI  
FAST ANALYTICAL METHODOLOGIES BASED ON MOLECULAR SPECTROPHOTOMETRIC TECHNIQUES  
AND MULTIVARIATE DATA ANALYSIS  
Vanessa del Rio Sánchez  
ISBN:978-84-693-9439-7/ DL:T.64-2011

**Sequential injection titration method using second-order signals.  
Determination of acidity in plant oils and biodiesel samples**

**Vanessa del Río, M. Soledad Larrechi, M. Pilar Callao**

*Chemometrics, Qualimetrics and Nanosensors Research Group  
Analytical Chemistry and Organic Chemistry Department, Rovira i Virgili  
University  
Marcel·li Domingo s/n, Campus Sescelades, 43007 Tarragona, Spain*

**Abstract**

A new concept of flow titration is proposed and demonstrated for the determination of total acidity in plant oils and biodiesel. We use sequential injection analysis (SIA) with a diode array spectrophotometric detector linked to chemometric tools such as multivariate curve resolution – alternating least squares (MCR-ALS). This system is based on the evolution of the two species of an acid-base indicator, alizarine, when it comes into contact with a sample that contains free fatty acids. The gradual pH change in the reactor coil due to diffusion and reaction phenomena allows the sequentially appearance of both species of the indicator in the detector coil, recording a data matrix for each sample.

The SIA-MCR-ALS method helps to reduce the amounts of sample, the reagents and the time consumed. Each determination consumes 0.413 ml of sample, 0.250 ml of indicator and 3 ml of carrier (ethanol) and generates 3.333 ml of waste. The frequency of the analysis is high (12 samples h<sup>-1</sup> including all

steps, *i.e.*, cleaning, preparing and analysing). The utilized reagents are of common use in the laboratory and it is not necessary to use the reagents of perfect known concentration.

The method was applied to determine of acidity in plant oil and biodiesel samples. Results obtained by the proposed method compare well with those obtained by the official European Community method that is time consuming and uses large amounts of organic solvents.

**Keywords:** Sequential injection analysis; Acidity value; Multivariate curve resolution; Oil samples; Biodiesel samples.

## 1. Introduction

Free fatty acid (FFA) content is one of the most frequently determined quality indices in food quality control [1,2]. It also needs to be determined in biodiesel since it is one of the main factors that affects the transesterification process and if the lipid contains more than 0.5 % FFA, soaps can be formed and the efficiency of the catalyst can be compromised [3].

Official methods for determining FFA content are based on non-aqueous titrimetry [4]. The procedure is time-consuming and involves high volumes of organic reagents and manual operations which are subject to personal error. To overcome these drawbacks an automated procedure is highly desirable.

Flow injection (FI) analytical methods, developed in 1975 by Ruzicka and Hansen [5], and sequential injection analysis developed later by Ruzicka [6], have proven to be extremely versatile for the precise and rapid automated analysis of

samples for a vast number of analytes of interest, both species or chemical parameters [7-11]. These systems are highly versatile because they can be adapted to most analytical instruments [12] and enable data of different dimensions to be obtained, that allows the use of various data treatments to get the required information [13].

Various flow and sequential injection titration procedures have been developed since the late 1970s. Wójtowicz [14] indexes a series of pioneering works in this area in a paper on novel approaches to analysis by flow injection gradient titration. Most total acidity determination is carried out in oil samples [15,16], but it is also of interest in such other matrices and as fruit juices [17-19], vinegar [20-22], soft drinks [22] and metallurgical solutions [23]. Flow-titrations have also been developed to determine such other analytical indexes as the antioxidant potential in wines [24] or basic index in lubricants [25] or concentrated hydrochloric acid [26].

The aim of this study is to develop a new concept of titration using sequential injection analysis (SIA) with a diode array UV-visible detector to obtain second order data that permits to resolve the components of a sample when unknown interferences are present.

The method is based on introducing sequentially into the system a solution of an acid-base indicator, whose basic and acidic species have different spectra in the UV-vis range, and the solution sample. If the absorbance is recorded in a range of wavelengths at different times, a data matrix is obtained when the sample-indicator reaches the detector. The number of rows of this matrix corresponds to the number of spectra and the number of columns corresponds to the number of wavelengths [13]. When the data matrix has been

obtained, multivariate curve resolution – alternating least squares (MCR-ALS) can be used to resolve the species present in a sample to obtain the spectra and the concentration profiles [27,28]. These profiles will correspond to the acidic and basic species of the indicator and to any other species contained in the sample that gives response in the UV-visible zone.

When a sample with free fatty acid is injected into the system, the concentration of the acidic species of indicator increases and the basic species decreases, so it is possible to establish a calibration relating the above mentioned indicator concentration profiles (areas) to the acidity.

Although nowadays there are numerous applications of second-order data to quantitative analysis [29-32] and among them there are those which use SIA to generate second order data [33-35], we have found no references in which this sort of data was used to do an indirect determination of a quality index, as acidity, with a wide application area.

This method has all the advantages of flow systems: high frequency of analysis, automatization, low consumption of reagents and samples, and low production of waste. Moreover, it does not need a reagent of known concentration and the reagents are easy to obtain in any laboratory. It also has the “second-order advantage” [36], that permits to quantify the components of a sample when unknown interferents are present, which is a characteristic of high interest in the analysis of complex samples.

The novelty of this work with regard to other methodologies that uses second-order data is that the employed signal is indirectly related with the analyte of interest, what increases the application possibilities of these techniques.

## 2. Experimental

### 2.1. Procedure

#### 2.1.1. SIA method

The carrier, sample and indicator solution are sequentially aspirated towards the syringe and then pushed towards the detector through the reactor coil. During this operation, the zone undergoes some mutual dispersion. Due to the sample contains free fatty acids, a pH gradient is created between the pH of the acid solution and the basic pH of the indicator. When the solution reaches the detector, the first species of the indicator detected is the basic species and then the acidic species. In one zone both species are present, as well to other UV-vis sensitive species. This process is schematized in the enlargement of the holding and reaction coils in Fig. 1. As response we obtain a data matrix whose columns are the SIA peaks at a specific wavelengths and whose rows are spectra recorded at a specific time (Fig. 2a and 2b).



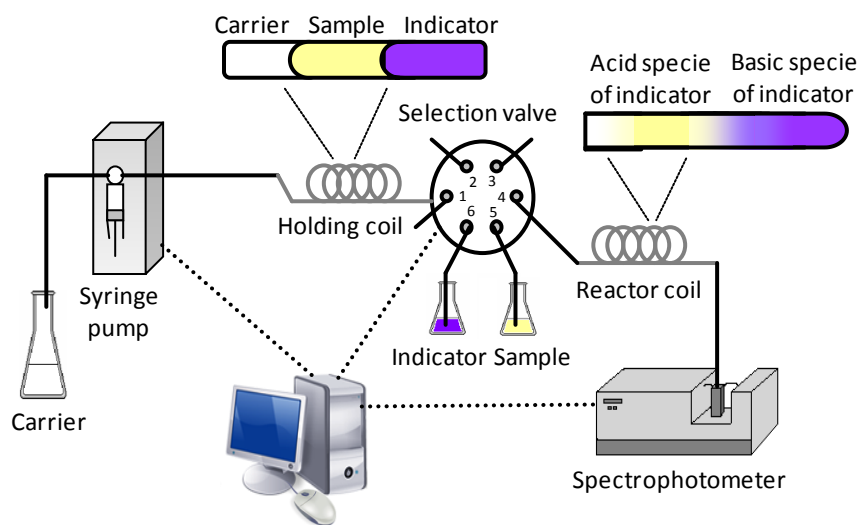


**Figure 1.** Sequential injection analyzer and analytical process in the coils.

### 2.1.2. Data treatment

The aim of the MCR-ALS method [37] is the bilinear decomposition of experimental data set  $\mathbf{D}$  in order to obtain matrices  $\mathbf{C}$  and  $\mathbf{S}^T$ , which have real chemical significance, according to Eq. (1):

$$\mathbf{D} = \mathbf{C}\mathbf{S}^T + \mathbf{E} \quad (1)$$

where the dimensions of the matrices are:  $\mathbf{D}$  ( $n \times m$ ),  $\mathbf{C}$  ( $n \times c$ ),  $\mathbf{S}^T$  ( $c \times m$ ),  $\mathbf{E}$  ( $n \times m$ );  $n$  is the number of spectra or times in which the signal has been obtained,  $m$  is the number of wavelengths in which the signal has been obtained and  $c$  is the number of components considered (chemical species contributing to the signal).  $\mathbf{C}$  is the matrix that describes the concentration profiles of the species in the system and can be used to obtain the areas of each species, which are directly

related to the concentration.  $\mathbf{S}^T$  is the matrix that contains the response profiles of these species (spectra profiles) and  $\mathbf{E}$  is the matrix of the residuals.

The first step in MCR-ALS is to analyse the rank of the data matrix to determine how many species are present in the sample; the second step is to make an initial estimation of the concentration profiles or of the pure spectra. The final step is to perform alternating least squares optimization to calculate new matrices  $\mathbf{C}$  and  $\mathbf{S}^T$  from initial estimates of  $\mathbf{C}$  or  $\mathbf{S}^T$ . In this optimization process, we imposed the constraint of non-negativity for the concentrations ( $\mathbf{C}$ ) and spectral ( $\mathbf{S}^T$ ) profiles and the constraint of unimodality for the concentration profiles ( $\mathbf{C}$ ) [38]. The resolution can be improved by treatment with what are known as augmented matrices [27], appending the spectra of the pure acid and basic species of the indicator.

The right side of Fig. 2 shows the concentration matrix  $\mathbf{C}$  and the spectra matrix  $\mathbf{S}^T$  profiles obtained by MCR-ALS. As an example, in Fig. 2c and d it is shown the results obtained from the resolution of an oleic acid standard matrix. If the analysed sample was complex and there were more absorbent species, the number of components would be superior to two, but it would continue having the same information with regard to the indicator signals (the called second-order advantage).

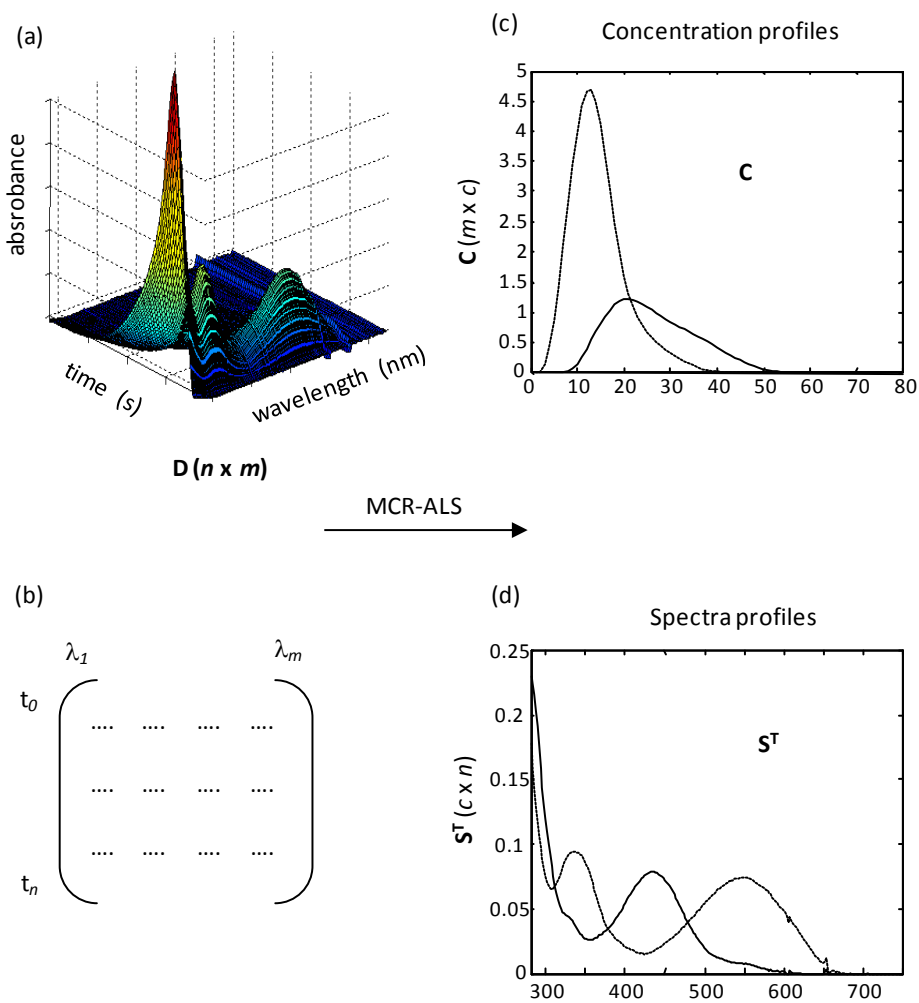


**Figure 2.** (a and b) Data matrix resulting from the analytical process applied to an oleic acid standard, (c) matrix of concentration profiles ( $\mathbf{C}$ ) and (d) spectra profiles ( $\mathbf{S}^T$ ). (---) acid species of the indicator and (—) basic species of the indicator.

To evaluate the quality of model fit we considered the percentage of variance explained by the product  $\mathbf{CS}^T$ , which is given by

$$R^2(\%) = 100 \times \sqrt{\frac{\sum_{i,j} d_{ij}^{*2}}{\sum_{i,j} d_{ij}^2}} \quad (2)$$

Another parameter that we used to determine the quality of the resolution process is the lack of fit, which is expressed as

$$lof(\%) = 100 \times \sqrt{\frac{\sum (d_{ij}^* - d_{ij})^2}{\sum d_{ij}^2}} \quad (3)$$

where  $d_{ij}$  are each of the elements of the experimental matrix  $\mathbf{D}$  and  $d_{ij}^*$  are each of the elements of the reproduced data matrix  $\mathbf{D}$ , obtained by the MCR-ALS decomposition.

The correlation coefficient of the spectra obtained in the resolution step (X) and the pure spectra (Y), calculated from (4), for the two species of the indicator was also used to assess the quality of the MCR-ALS results.

$$r = \sqrt{\frac{ss_{xy}^2}{ss_{xx}ss_{yy}}} \quad (4)$$

where  $ss$  is the sum of squared values of a set of  $n$  points.

### 2.1.3. Calibration model

To establish a calibration model we prepared a series of standard calibrations whose concentrations of free acid are known. The areas of the acidic and basic species of the indicator, obtained in the resolution process (Fig. 2c),

are the analytical signal that we use to establish a univariate calibration versus the concentration of free acid.

The samples were analysed by the same procedure and the concentration of acid in the samples was obtained from its corresponding response value (areas of the species of the indicator) and the calibration parameters.

Subsequently, the acidity value is obtained from expression (5)

$$Acidity = c \cdot \frac{V}{P} \quad (5)$$

where  $c$  is the concentration of free acid obtained by the proposed method,  $P$  is the weight of the oil and  $V$  is the volume to which the sample has been diluted before the analysis by SIA-MCR-ALS.

#### 2.1.4. Official method

The Official European Community method [4] involves the following steps: (a) weighing 2.5-20 g of oil (according to expected acidity); (b) solubilization in 50-150 ml of an 1:1 ethanol-diethylether solvent and (c) titration with a 0.1000 M ethanolic KOH solution using phenolphthalein indicator.

The acidity, expressed as the percentage of oleic acid, is calculated according to the following expression

$$Acidity = \frac{V_{KOH} MN}{10 P_{oil}} \quad (6)$$

where  $V$  is the volume in ml of KOH solution,  $M$  is the molecular weight of oleic acid ( $282 \text{ g mol}^{-1}$ ),  $N$  is the normalized concentration of KOH solution ( $\text{mol l}^{-1}$ ) and  $P$  is the weight in  $g$  of the sample.

## 2.2. Reagents and samples

In all analyses, we used analytical grade chemicals. Oleic acid was purchased from SIGMA-ALDRICH, sodium hydroxide from PROLABO and Alizarine from PANREAC. The carrier stream was absolute ethanol provided by Scharlab S.L. The oil and biodiesel samples were obtained from Bionet [39].

Oleic acid standards and samples were prepared by weighing the required amount of oleic acid (or sample) and dissolving in absolute ethanol. Indicator solutions were prepared by weighing the appropriate amount of alizarine and dissolving in NaOH solution.

The samples and reagent volumes used for the SIA analysis are detailed in Table 1.

**Table 1.** Protocol and selected operating conditions in the SIA system.

SIA method		
Steps	Parameter	Volume (ml)
<i>Preparation cycle</i>		
1	Sample aspiration from reservoir to waste	0.33
2	Indicator aspiration from reservoir to waste	0.33
3	Carrier aspiration from reservoir to syringe	4.670
<i>Analytical cycle</i>		
4	Sample aspiration from reservoir to syringe	0.083
5	Indicator aspiration from reservoir to syringe	0.250
6	Expulsion to detector	2.333
7	Carrier aspiration from reservoir to syringe	2.000
<i>Cleaning cycle</i>		
8	Carrier aspiration from reservoir to detector valve	1.000

Flow rate in step 6: 0.5 ml min<sup>-1</sup>  
Flow rate in the rest of steps: 5 ml min<sup>-1</sup>

### 2.3. Instrumental and software

The sequential injection analyzer (see Fig. 1) comprised a Cavro XL 3000 syringe pump (5 ml) equipped with a six-port multiposition automatic selection valve (Eurosas EPS 1306 BPB) and a HP8452A diode-array spectrophotometer with a Hellma 178.711QS flow-through cell. All tubes connecting the various components of the flow system were made of Omnifit PTFE with an i.d. of 0.8 mm. The lengths of the holding and reaction coils were 2.0 and 0.7 m, respectively. The syringe pump, the automatic valve and the data acquisition provided by the spectrophotometer were controlled by a personal computer via an RS-232 interface, a PCL-711S PC Lab-Card and an HP-IB IEEE488 interface for communications.

The spectra were recorded between 280 and 750 nm in 2 nm steps. As each sample passed through the detector, 80 measurements were taken (one every 0.7 s). The data were acquired and monitored by the spectrophotometer using the HP89531A software. The instrumentation was controlled by customised software.

All calculations for multivariate curve resolution with alternating least squares (MCR-ALS) were performed with MATLAB 6.5 [40]. The software used in this study was written by the Chemometrics Group of Barcelona University and can be downloaded from the Web page [41].

### 3. Results and discussion

To do the calibrate it could have been used as standard any fatty acid since the parameter of interest is an index (acidity) that measures the non specific content in acids presents in the sample. Among different possibilities, the oleic acid was chosen because it is the acid to which one refers in the official method to determine the acidity.

Like in case of the acid, the choice of the alizarine as indicator is not an indispensable requirement to carry out the proposed method. Due to the acid-basic properties of alizarine ( $pK_a$  is 5.7), it is a suitable indicator to the analysis because it does not need a too acid medium in order to evolves from its basic species, as is injected into the system, to the acidic species. Moreover, its spectral characteristics (the acid solution is yellow and the basic solution is violet) make alizarine a suitable indicator. Other indicators can fulfil the exposed conditions.



To establish an initial analytical sequence, we choose the working conditions (flow rate and volume of carrier, indicator and sample) in accordance with operational restrictions (length of tubes, volume of syringe, etc.). In this stage the essential requirements are that both species of indicator are present and the acid area increases when the acid concentration in the sample is higher.

The conditions selected for the SIA method and the analysis protocol are summarized in Table 1. The steps 2 and 3 of preparation cycle are performed at the beginning of a series of measures and after the first analysis only step 1 is repeated to clean the sample tube and to fill it with the following one.

In the application of MCR-ALS it has been proven that the resolution does not suffer significant changes if the data was resolved with two or three components, due to the poor sensitive signal of the oleic acid in the UV-visible zone. The iterative method of optimization was applied working with augmented matrices, adding to the response matrix  $\mathbf{D}$ , the vectors related to the spectra of the two species of the indicator and of the oleic acid. The product of the  $\mathbf{C}$  matrix and  $\mathbf{S}^T$  matrix accounts for 98.5042% of the variance associated with the experimental data and the lack of fit is 1.58%, which in quantitative terms means that it explains practically all the variability of the experimental data. The goodness of the spectra profiles recovered by MCR-ALS for the chemical species was evaluated quantitatively by calculating the similarity coefficients between the recovered spectra and the pure spectra recorded for both species (acid and basic species), respectively. The values were 0.9851 for the acid species and 0.9909 for the basic species, which indicates that the recovered profiles have a high degree of concordance with the original profiles.

In the second step, we optimised the analytical sequence in order to work in the conditions that provide the best parameters (work range, slope and correlation coefficient) of the calibration graph. Two experimental factors were selected as the main variables involved in the response of the SIA-MCR-ALS method: (a) concentration of indicator and (b) concentration of NaOH solution. The concentration of indicator is important because the higher concentration, the greater global response. But it is also necessary to control that it stays within the linearity range, so the response of the matrix obtained can be decompose according to the minimum squares criteria. When the indicator solution, which contains NaOH, comes into contact with the sample, which contains free acids, a gradual pH change takes place in the reactor coil due to the diffusion phenomenon and to the neutralization. Thus, both phenomena will be more or less marked depending on the level of NaOH concentration in the indicator, so it has an influence on the concentration profiles of the two species of indicator.

We evaluated the influence of these factors with a full factorial design  $2^2$ , which has the experimental domain showed in the first two columns of Table 2. The levels of indicator concentration have been selected in order to obtain absorbance values between 0.2 and 1. The levels of NaOH concentration have been selected for the purpose of obtaining both indicator species at the expected free acidity. In each experiment, 12 oleic acid standards solutions were analysed in triplicate in the range between 0.0 and 128 mg l<sup>-1</sup>. The average of the areas found for every experiment is shown in the last columns in table 2. In all cases, and even when the standard of 0 mg l<sup>-1</sup> was aspirated, both species of the indicator were present. This is due to the acid character of the ethanol used as a carrier, which provides enough acidity for there to be a small amount of the acidic species. When the high level of indicator concentration is considered, higher areas are obtained in the total concentration profiles. When the high level

of NaOH concentration is considered, the area of the basic species is larger than the area of the acidic species. There is an interaction between the two factors: the response does not depend exclusively on the indicator concentration, but it is also affected by the relation between the acid and basic area. This might be because the two species have different spectral sensitivities.

**Table 2.** Experimental conditions of the  $2^2$  factorial design and average response.

Experiment number	[alizarina] · 10 <sup>-4</sup> (mol l <sup>-1</sup> )	[NaOH] · 10 <sup>-4</sup> (mol l <sup>-1</sup> )	Acid area	Basic area
1	2.7	2.5	18.4795	22.5421
2	4.0	2.5	182.7724	35.3814
3	2.7	7.5	15.4252	71.7880
4	4.0	7.5	40.5479	126.6145

For the results obtained, which present different sensitivity to the acidic and the basic signal, 4 calibration graphs were constructed for each experiment. The response was considered to be the area of the acidic species, the area of the basic species and the relative area (area of the acidic or basic species relative to the total area of indicator). These last two calibrations have been built to verify if some randomness of the data is corrected and better precisions are obtained.

Applying the ANOVA test to each calibration graph, we observed that in the overall calibration line there is a loss of linearity in the most concentrated standards. Table 3 shows some parameters of the calibration curves obtained from the acidic and the basic species, which passed the ANOVA test for a 0.05% level of significance and the corresponding degrees of freedom. The results obtained for the calibrations curves using relative areas are not shown because the precision of the regression line does not improve, which indicates that the

variability in the total area of the indicator is negligible in comparison to other sources of variability in the measures.

**Table 3.** Some calibration parameters evaluated in the different experimental conditions.

Parameters	Acid calibrate	Basic calibrate
<i>Experiment 1</i>		
Working range (mg l <sup>-1</sup> )	0 – 20.5	0 – 5.13
Slope	8.44	-16.13
Intercept	9.24	33.53
Correlation coefficient	0.9684	0.7675
<i>Experiment 2</i>		
Working range (mg l <sup>-1</sup> )	0 – 12.8	0 – 25.6
Slope	13.16	-10.36
Intercept	170.97	47.18
Correlation coefficient	0.9424	0.9741
<i>Experiment 3</i>		
Working range (mg l <sup>-1</sup> )	0 – 25.6	0 – 25.6
Slope	10.84	-13.75
Intercept	1.55	89.08
Correlation coefficient	0.9924	0.9842
<i>Experiment 4</i>		
Working range (mg l <sup>-1</sup> )	0 – 10.2	0 – 12.8
Slope	22.57	-31.87
Intercept	13.03	164.32
Correlation coefficient	0.9347	0.9876

The table shows that there are any experience that jointly provides the best work range, the best slope and the best correlation coefficient. Considering the benefit of each parameter, we selected experiment 3 because it has the highest work range. This enables samples of different acidities to be used without doing previous dilutions. We used the absolute response of the acidic

species because its correlation coefficient was best, which led to lower uncertainty in the results. Figures of merit for the calibration model selected are shown in Table 4. The limit of detection (LOD) was calculated by taking into account the uncertainty of the regression line [42] with 95% confidence. RRMSC is the relative root mean square error of the calibration values and it was calculated to evaluate the accuracy of the curve calibration.

**Table 4.** Figures of merit for the selected calibration.

Working range (mg l <sup>-1</sup> )	0 – 26.0
Slope	10.8359
Intercept	1.5488
R	0.9924
n	30
lod (mg l <sup>-1</sup> )	1.49
RRMSC	0.3488
Standard error	1.2756
Standard deviation of the slope	0.4754
Standard deviation of the intercept	0.5600
ANOVA test	
F calculated	2.16
F tabulated (0.05, 8, 20)	4.00

Five oil samples and four biodiesel samples were analysed in triplicate under the selected conditions (0.083 ml sample volume aspiration, 0.5 ml min<sup>-1</sup> flow rate, 2.7 x 10<sup>-4</sup> mol l<sup>-1</sup> indicator concentration and 7.5 x 10<sup>-4</sup> mol l<sup>-1</sup> NaOH concentration). After the acid area had been obtained for every sample, the concentration was calculated in mg l<sup>-1</sup> by interpolation in the calibration curve. Subsequently, the acidity was determined by expression 5. In Table 5 it is possible to observe the analysed samples, the experimental conditions for each

sample, the results obtained from SIA-MCR-ALS in  $\text{mg l}^{-1}$  and acidity values and the acidity values obtained from the official method.

**Table 5.** Acidity values in oil and biodiesel samples obtained by the Official method and the SIA-MCR-ALS method.

Samples	Weight (g)	Acidity value (s)		
		SIA method ( $\text{mg l}^{-1}$ )	SIA method	Official method
Refined sunflower oil	0.4150	1.577	0.095 (0.012)	0.080 (0.007)
Refined soybean oil	0.3752	1.681	0.112 (0.012)	0.0827 (0.0009)
Crude soybean oil	0.1773	4.589	0.647 (0.014)	0.697 (0.001)
Refined palm oil	0.2230	2.542	0.285 (0.009)	0.270 (0.004)
Refined waste oil	0.1081	5.06	1.17 (0.02)	1.19 (0.03)
Sunflower biodiesel	0.3680	1.62	0.11 (0.01)	0.11 (0.01)
Soybean biodiesel	0.6330	1.519	0.06 (0.01)	0.06 (0.05)
Palm biodiesel	0.2990	1.722	0.144 (0.031)	0.158 (0.006)
Waste biodiesel	0.3730	1.64	0.11 (0.02)	0.12 (0.2)

(\*) The Volume of each sample was 25 ml.

The accuracy of the SIA-MCR-ALS method was validated by comparing its results with those obtained by the official titration method. We constructed a regression graph where the Y axis represented the results from the SIA method and the X axis represented the results from the official titration method. The regression parameters were 0.9591 for the slope and 0.0096 for the intercept. Using the elliptic joint confidence region (EJCR) test [42], statistical comparison was carried out. The critical value of the Snedecor-Fisher statistic at a 95% confidence level was 4. The F-value of 2.48 (20 and 8 freedom degrees) was obtained. This indicates that the point (1, 0) lies within the EJCR. Therefore, the ellipse includes the theoretically expected value of (1, 0), and the method is reliable.

#### 4. Conclusions

A new concept of flow titration was proposed and demonstrated for the determination of total acidity in plant oils and biodiesel samples. The advantages of using this method are that automatization is easy and the amounts of sample, reagents and waste are reduced. It is also less time-consuming and it is not necessary to use reagents of known concentration.

The use of second-order chemometric techniques make it possible to obtain the concentration profiles without having to do any sample treatment, except dilution process, even if other absorbent species are present in the sample.

The acidity results for various oil and biodiesel samples are statistically comparable to those obtained by the official method.

It should be possible to adapt the proposed system to study other acids or other substances involving reactions that produce or consume acids or bases and other types of samples.

**Acknowledgements.** The authors would like to thank the Spanish Ministry of Science and Innovation (Project CTQ2007-61474/BQU) for economic support, the Rovira i Virgili University, for providing Vanessa del Río with a doctoral fellowship and Bionet Europa S.L. (Spain) for supplying the samples.

## 5. References

- [1] K.L. Gemene and E. Bakker, *Anal. Chem.* **80** (2008) 3743.
- [2] M.R. Mazalli and N. Bragagnolo, *Lipids* **42** (2007) 483.
- [3] Y.C. Sharma, B. Singh and S.N. Upadhyay, *Fuel* **87** (2008) 2355.
- [4] Determination of the free fatty acids in European Commission Regulation (ECC) No. 2568/91. Official Journal of the European Communities, No L 248 (5.9.91) p. 6.
- [5] J. Ruzicka and E.H. Hansen, *Anal. Chim. Acta* **18** (1975) 145.
- [6] J. Ruzicka, *Anal. Chim. Acta* **237** (1990) 329.
- [7] J.F. van Staden and R.I. Stefan, *Talanta* **64** (2004) 1109.
- [8] R. Pérez-Olmos, J.C. Soto, N. Zárate, A.N. Araújo, J.L.F.C. Lima and M.L.M.F.S. Saraiva, *Food Chem.* **90** (2005) 471.
- [9] E.H. Hansen and M. Miró, *Trends Anal. Chem.* **26** (2007) 14.
- [10] A.N. Araújo, J.L.F.C. Lima, A.O.S.S. Rangel and M.A. Segundo, *Talanta* **52** (2000) 59.
- [11] M.A. Segundo, J.L.F.C. Lima and A.O.S.S. Rangel, *Anal. Chim. Acta* **513** (2004) 3.
- [12] V. Gómez and M.P. Callao, *Trends Anal. Chem.* **26** (2007) 714.
- [13] A. Pasamontes and M.P. Callao, *Trends Anal. Chem.* **25** (2006) 77.
- [14] M. Wójtowicz, J. Kozak and P. Koscielniak, *Anal. Chim. Acta* **600** (2007) 78.
- [15] E. Mariotti and M. Mascini, *Food Chem.* **73** (2001) 235.
- [16] B. Saad, C.W. Ling, M.S. Jab, B.P.Lim, A.S.M. Ali, W.T. Wai and M.I. Saleh, *Food Chem.* **102** (2007) 1407.
- [17] J. Jakmune, L.Pathimapornlernt, S.K. Hartwell and K. Grudpan, *Analyst* **130** (2005) 299.
- [18] K. Grudpan, P. Sritharathikhun and J. Jakmune, *Anal. Chim. Acta* **363** (1998) 199.



- [19] J. Jakmunee, T. Rujiralai and K. Grudpan, *Anal. Sci.* **22** (2006) 157.
- [20] J. Moros, F.A. Iñón, S. Garrigues and M. de la Guardia, *Talanta* **74** (2008) 632.
- [21] C.M.N.V. Almeida, R.A.S. Lapa, J.L.F.C. Lima, E.A.G. Zagatto and M.C.U. Araújo, *Anal. Chim. Acta* **407** (2000) 213.
- [22] M. Wójtowicz, J. Kozak, D. Górnacka and P. Koscielniak, *Anal. Sci.* **24** (2008) 1593.
- [23] F. Albertus, A. Cladera and V. Cerdà, *Analyst* **125** (2000) 2364.
- [24] P.C.A.G. Pinto, M. Lúcia, M.F.S. Saraiva, S. Reis and J.L.F.C. Lima, *Anal. Chim. Acta* **531** (2005) 25.
- [25] K. Jyonosono, T. Imato, N. Imazumi, M. Nakanishi and J.I. Yagi, *Anal. Chim. Acta* **438** (2001) 83.
- [26] J.F. van Staden, M.G. Mashamba and R.I. Stefan, *Talanta* **58** (2002) 1089.
- [27] J. Saurina, S. Hernández-Cassou and R. Tauler, *Anal. Chim. Acta* **335** (1996) 41.
- [28] A. Izquierdo-Ridorsa, J. Saurina, S. Hernández-Cassou and R. Tauler, *Chemom. Intell. Lab. Syst.* **38** (1997) 183.
- [29] V. Gómez and M.P. Callao, *Anal. Chim. Acta* **627** (2008) 169.
- [30] G.M. Escandar, A.C. Olivieri, N.M. Faber, H.C. Goicoechea, A.M. de la Peña and R.J. Poppi, *Trends Anal. Chem.* **26** (2007) 752.
- [31] A. de Juan and R. Tauler, *Crit. Rev. Anal. Chem.* **36** (2006) 163.
- [32] R. Bro, *Crit. Rev. Anal. Chem.* **36** (2006) 279.
- [33] V. Gómez and M.P. Callao, *Anal. Bioanal. Chem.* **382** (2005) 328.
- [34] A. Pasamontes and M.P. Callao, *Anal. Sci.* **22** (2006) 131.
- [35] V. Gómez, J. Font and M.P. Callao, *Talanta* **71** (2007) 1393.
- [36] K.S. Booksh and B.R. Kowalski, *Anal. Chem.* **66** (1994) 782A.
- [37] A. de Juan and R. Tauler, *Anal. Chim. Acta* **500** (2003) 195.

[38] R. Tauler, A. Izquierdo-Ridora and E. Casassas, *Chemom. Intell. Lab. System.* **18** (1993) 293.

[39] Bionet Europa S.L., Reus, Tarragona, Spain.

[40] The Mathworks, MATLAB Version 6.5, Natick, MA, 2004.

[41] [http://www.ub.es/gesq/eq1\\_eng.htm](http://www.ub.es/gesq/eq1_eng.htm)

[42] D.L. Massart, B.G.M. Vandeginste, S.N. Deming, Y. Michotte and L. Kaufman, *Handbook of Chemometrics and Qualimetrics*, Part A, Elsevier, Amsterdam, 1997.

UNIVERSITAT ROVIRA I VIRGLI  
FAST ANALYTICAL METHODOLOGIES BASED ON MOLECULAR SPECTROPHOTOMETRIC TECHNIQUES  
AND MULTIVARIATE DATA ANALYSIS  
Vanessa del Rio Sánchez  
ISBN:978-84-693-9439-7/ DL:T.64-2011

## 4.3. Paper

Determination of sulphate in water and biodiesel  
samples by a sequential injection analysis –  
multivariate curve resolution method

Vanessa del Río, M. Soledad Larrechi, M. Pilar Callao

*Analytica Chimica Acta*, 676 (2010) 28-33

UNIVERSITAT ROVIRA I VIRGLI  
FAST ANALYTICAL METHODOLOGIES BASED ON MOLECULAR SPECTROPHOTOMETRIC TECHNIQUES  
AND MULTIVARIATE DATA ANALYSIS  
Vanessa del Rio Sánchez  
ISBN:978-84-693-9439-7/ DL:T.64-2011

## Determination of sulphate in water and biodiesel samples by a sequential injection analysis-multivariate curve resolution method

Vanessa del Río, M. Soledad Larrechi, M. Pilar Callao

*Chemometrics, Qualimetrics and Nanosensors Research Group  
Analytical Chemistry and Organic Chemistry Department, Rovira i Virgili  
University*

*Marcel·li Domingo s/n, Campus Sescelades, 43007 Tarragona, Spain.*

### Abstract

A spectrophotometric sequential injection analysis (SIA-DAD) method linked to multivariate curve resolution – alternating least squares (MCR-ALS) has been developed for sulphate determination. This method involves the reaction, inside the tubes of the SIA system, of sulphate with barium-dimethylsulfonazo (III) complex, Ba-DMSA (III), displacing  $\text{Ba}^{2+}$  from the complex and forming DMSA (III). When the reaction products reach the detector a data matrix is obtained, which allows a second-order calibration to be developed. The experimental conditions (concentration and sample and reagent volumes) to obtain the highest sensitivity have been chosen applying a  $2^{4-1}$  fractional factorial design.

The proposed sequential flow procedure permits up to  $15 \text{ mg SO}_4^{2-} \text{ L}^{-1}$  to be determined with a limit of detection of  $1.42 \text{ mg L}^{-1}$  and it is able to monitor sulphate in samples at a frequency of 15 samples per hour.

The method was applied to determine sulphate in natural and residual waters and in biodiesel. The reliability of the method was established for water samples by parallel determination using a standard turbidimetric method for sulphate in natural and residual water samples with results within statistical variation. For biodiesel samples, the method was validated comparing the concentration of some spiked samples with the expected concentration using a test-*t*.

**Keywords:** Sulphate determination; Sequential injection analysis; Multivariate curve resolution; Water analysis; Biodiesel analysis.

## 1. Introduction

Sulphate concentration is a parameter of high analytical interest in an extensive variety of application fields. Sulphate is the predominant sulphur species available to plants, so its determination in soil solutions and plants is of relevance [1]. Sulphuric acid is widely used in numerous industries, as in biodiesel production from the esterification of vegetable oils by an acid catalysis [2]. Thus, sulphates can be found in the biodiesel obtained, which affects the quality of the final product. The extensive industrial use of sulphates causes them to be widely distributed in the environment and, therefore, it is necessary to determine their presence in order to monitor water quality.

In this work, a sequential injection analysis system with diode array detection was developed for the determination of sulphates in natural and residual waters and biodiesel.

In water analysis, the turbidimetrically official method is a well known procedure for the determination of sulphates [3]. In biodiesel samples, the standard method determines sulphated ashes from petroleum products [4] and is based on burning the sample until a carbonaceous residue is obtained. In bioethanol samples, which have a low level limit of sulphate specified ( $< 4 \text{ mg Kg}^{-1}$ ) [5], ion chromatography [6] and potentiometry [7] are the standard methods used for sulphate determination. These procedures are time-consuming. Hence, the development of a rapid methodology for determining sulphates is of great interest.

Several alternatives have been reported for the determination of sulphate ion; for example, ion-selective electrode [8-10], ion chromatography [11-14] and capillary electrophoresis [15-17]. However, these processes are slow and require large volumes of reagents. In an attempt to overcome these drawbacks, some researchers have developed spectrophotometric turbidimetric flow-injection procedures for the determination of sulphates in environmental samples. The spectrophotometric methods include the colorimetric reaction with  $\text{Fe}^{3+}$  to form the cationic complex  $[\text{Fe}(\text{SO}_4)]^+$  [18-20], with barium-dimethylsulfonazo (III) [1,21,22] or with barium-chloroanilate [23]. The turbidimetric methods use the precipitation reaction of barium [24-26] or lead [27,28] ion with sulphate in the sample to form barium sulphate or lead sulphate suspension.

The developed method is based on the reaction between barium-dimethylsulfonazo (III) (Ba-DMSA (III)) and sulphate ions, as referenced in previous works [1,21,22]. The proposed methodology consists of generating a system that evolves gradually in the reactor coil from Ba-DMSA (III) to DMSA (III), which have different spectra in the UV-vis range. Recording the absorbances in a



range of wavelengths at different times allows a data matrix for each sample to be obtained, which, when treated by means of the MCR-ALS algorithm, leads to the spectral and concentration profiles of both species of the reagents. Both concentration profiles are related to the sulphate concentration: the more sulphate concentration, the higher DMSA (III) area and the lower Ba-DMSA (III) area.

The methodology presented is experimentally simple and, furthermore, as all flow systems, it has the following advantages: high frequency of analysis, low consumption of reagents and samples and low waste generation. Obtaining and treating second-order data provides information about the presence of interferences in the sample and the analyte of interest can be quantified even when these are present.

Nowadays, although the use of second-order data treatment is not generalized, it is gaining widespread acceptance and it has been used in a number of real and complex systems to solve various analytical problems [29-31]. If the applications of second-order data treatment are restricted to flow systems, methods have been described for the determination of a wide range of analytes in an extensive variety of matrices: acidity in plant oils and biodiesel samples [32], chromium [33] and dyes [34] in tanning waste waters, amoxicillin and clavulanic acid in pharmaceuticals [35], phenolic compounds in disinfection products [36], dyes [37] and antimicrobials [38] in juices, sulfonamides in milk [39], hydroquinone in cosmetics [40] and mixtures of amino acids [41] and nucleic acid components in complex mixtures [42], among others.

To the best of our knowledge, no studies have yet been reported to determine sulphate by SIA and MCR-ALS, which is an adequate methodology for aqueous and organic samples.

## 2. Experimental

### 2.1. Reagents and samples

All the reagents used were of an analytical reagent grade from SIGMA-ALDRICH. Water purified with a Milli-Q water system from MILLIPORE, USA, was used throughout the experiments.

A standard sulphate stock solution ( $1000 \text{ mg L}^{-1}$ ), obtained by dissolution of previously dried  $\text{K}_2\text{SO}_4$ , was used to prepare working standards.

A solution of  $8.7 \times 10^{-5} \text{ mol L}^{-1}$  Ba-DMSA (III) reagent was prepared by dissolving the corresponding weight of Na-DMSA (III) in a solution of  $3.48 \times 10^{-4} \text{ mol L}^{-1}$   $\text{BaCl}_2$ ,  $5 \times 10^{-4} \text{ mol L}^{-1}$   $\text{KNO}_3$  and 1% in acetic acid. The chromogenic reagent was stored in amber flask.

The carrier stream was Ultrapure Milli-Q water.

Thirteen samples of water (seven of natural water and six of residual water) from different sources were provided by EMATSA [EMATSA, Empresa Municipal Mixta de Aguas de Tarragona S.A., Tarragona, Spain]. To carry out the SIA analysis, the water samples were prepared by dilution of the appropriate aliquots. Residual water samples were first filtered through an Ahlstrom Filter Paper Circle PK100.

Four biodiesel samples (palm biodiesel, sunflower biodiesel, soybean biodiesel and waste biodiesel) were provided by BIONET [Bionet Europa S.L., Reus, Tarragona, Spain]. To carry out the SIA analysis, the samples were first filtered through an Ahlstrom Filter Paper Circle PK100 and then prepared by weighing the required amount of biodiesel and dissolving in ethanol:water (25:75).

## 2.2. SIA manifold and measurement conditions

A schematic diagram of the flow manifold is depicted in Fig. 1. The sequential injection analyser comprised a Cavro XL 3000 stepper motor driven syringe pump of 5 mL equipped with a six-port multi-position automatic selection valve (Eurosas EPS 1306 BPB) and a Hewlett-Packard 8452A spectrophotometer with a Hellma 178.713-QS flow-through cell, which has a pathlength of 10 mm and its inner volume is 8  $\mu$ l. All tubes to connect the various components of the flow system were made of Omnifit PTFE with 0.8 mm (i.d.). The lengths of the holding and reaction coils were 2.0 and 7.0 m, respectively. The syringe pump, the automatic valve and the data acquisition provided by the spectrophotometer were controlled by a personal computer (PC) via an RS-232 interface, a PCL-711S PC- Lab-Card and an HP-IB IEEE488 interface for communications, respectively.

Spectra were recorded between 250 and 725 nm in 2 nm steps. As each sample passed through the detector, 80 measurements were taken (one every 0.7 s).

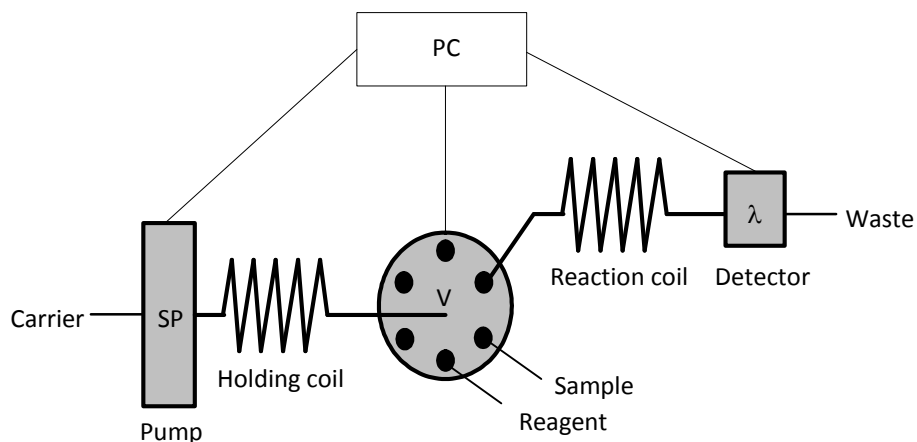


**Figure 1.** Schematic diagram of the sequential injection analyser. SP: syringe pump; HC: holding coil; V: selection valve; RC: reaction coil; λ: spectrophotometer; PC: personal computer; C: carrier; R: reagent; S: sample; W: waste.

### 2.3. Turbidimetric analyzer

A Seal Analytical (AQ2+) turbidimeter was used. This instrument was operated according to the manufacturer's instructions: *Sulphate in drinking and surface waters and domestic and industrial wastes* (UKAS-515-A rev.1 method), based on HMSO method [3].

### 2.4. Procedure

#### 2.4.1. SIA method basis

The proposed method involves the reaction of sulphate ions with a barium-dimethylsulfonazo (III) complex, Ba-DMSA (III), displacing  $\text{Ba}^{2+}$  from the complex and forming DMSA (III), as is shown in Figure 2. The proposed method

involves the formation of the slightly soluble barium sulphate, but turbidity was not observed in any case. It should be pointed out that, although in some experiences the  $\text{BaSO}_4$  ionic product would lightly overcome the  $\text{BaSO}_4$  solubility product, a dilution process takes place in the coils due to the interdiffusion between the species.

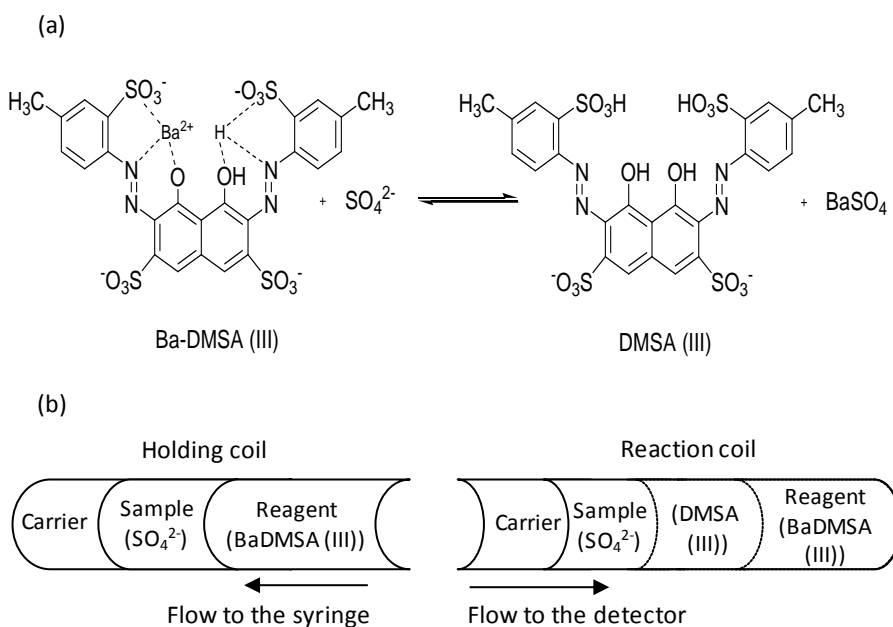


**Figure 2.** (a) Reaction between sulphate ions with barium-dymethylsulfonazo (III) complex; (b) Schematic diagram of the process for mixing sample, reagent and carrier in the channel of the SIA system.

The sequence of the analysis was as follows: (1) carrier aspiration to holding coil (4750  $\mu\text{l}$ ); (2) sample aspiration to holding coil (83  $\mu\text{l}$ ); (3) reagent aspiration to holding coil (166  $\mu\text{l}$ ); (4) flush out to reactor coil and detector; and (5) recording of the spectrum. The flow rate was 1  $\text{mL min}^{-1}$  for all steps.

Samples, with no previous treatment except dilution when it was necessary, were aspirated into the system and injected in triplicate.

At the bottom of Figure 2 the process that takes place in step 4 is schematized, in which the reagent mixed with the sample via an interdiffusion process. When the solution reached the detector, the first species detected was the chromogenic reagent Ba-DMSA (III), followed by a mixture of Ba-DMSA (III) and DMSA (III) species and finally DMSA (III). By measuring the absorbance at different times and different wavelengths, a data matrix  $\mathbf{D}$  ( $n \times m$ ) was obtained, where  $n$  represents the times and  $m$  the wavelengths at which the signal is recorded.

#### 2.4.2. Data treatment

The aim of second-order data treatment such as MCR-ALS [43] is to decompose the raw matrix  $\mathbf{D}$  ( $n \times m$ ) into the product of two matrices according to Eq. (1)

$$\mathbf{D} = \mathbf{C}\mathbf{S}^T + \mathbf{E} \quad (1)$$

where matrix  $\mathbf{C}$  ( $n \times c$ ) has column vectors corresponding to the profiles of concentration of the  $c$  pure components that are presented in matrix  $\mathbf{D}$ . The row vectors of matrix  $\mathbf{S}^T$  ( $c \times m$ ) correspond to the spectra of the  $c$  pure components, and  $\mathbf{E}$  ( $n \times m$ ) is the matrix of the residuals.

Specifically, MCR-ALS is an iterative method that, at each cycle, calculates new matrices  $\mathbf{C}$  and  $\mathbf{S}^T$ . During these iterative calculations, a series of constraints with the purpose of giving solutions with physical meaning and of

limiting their possible number are applied [44,45]. Iterations continue until an optimal solution is obtained that fulfils the constraints postulated and the established convergence criteria. Constraints applied in this work were non-negativity for the concentration (**C**) and spectra profiles (**S<sup>T</sup>**) and unimodality for the concentration profiles (**C**). We also used the augmented matrices strategy [46] to improve the resolution, appending the spectra of the pure Ba-DMSA (III) and DMSA (III) species of the reagent.

At the end of the optimization process, the performance of the model was evaluated from the following parameters [43]: the lack of fit (*lof*) of the model, the percentage of explained variance by the product **CS<sup>T</sup>** and the correlation coefficient of the spectra obtained in the resolution step and the pure spectra of the two species of the reagent: Ba-DMSA (III) and DMSA (III).

To establish a calibration model, the Ba-DMSA (III) area of the concentration profiles obtained in the resolution process was used as an analytical signal versus the concentration of sulphate ion in each standard, following the model:

$$A_i = b_1 c_i + b_0 \quad (2)$$

where  $A_i$  is the area and  $c_i$  is the concentration for each  $i$  standard. The regression lines obtained were validated using the ANOVA test [47]. In the prediction step, we use the expression 2 and the experimental area obtained from the considered sample.

The samples were analysed by the same procedure and the value of the concentration of  $\text{SO}_4^{2-}$  in each sample was obtained from its corresponding

response value (area of the Ba-DMSA (III) species) and the calibration parameters.

#### *2.4.3. Reference analysis*

In order to assess the quality of the results obtained in water analysis by the proposed method, they were compared with those obtained by a method based on the standard method produced by the Standing Committee of Analysis [2]. In this method, sulphate is determined turbidimetrically by precipitation with  $\text{BaCl}_2$  (under controlled acidic and stirring conditions) to form  $\text{BaSO}_4$  crystals of uniform size. Turbidity was measured at 505 nm and the  $\text{SO}_4^{2-}$  concentration was determined by comparison with a standard curve (0 – 40 mg  $\text{SO}_4^{2-}$  L<sup>-1</sup>).

In biodiesel analysis, the validation of the results was carried out from the obtained sulphate recovery in the samples, which had been spiked with different quantities of sulphate.

#### **2.5. Software**

HP89531A software was used to record and store the spectra. Customised software was used to control the SIA.

All calculations relating to MCR-ALS were performed with laboratory-written software under MATLAB 6.5 [48]. This software is available from the authors [49].



### 3. Results and discussion

A first study to determine the optimum experimental conditions in order to obtain the best regression line, which relates the area of one of the species to the sulphate concentration, was carried out. In this step, we considered the following factors: the concentration of DMSA (III), the concentration of  $\text{KNO}_3$ , the volume of the sample and the volume of the reagent. The flow rate was set at  $1 \text{ mL min}^{-1}$  and the relationship between the concentrations of DMSA (III) and  $\text{Ba}^{2+}$  was maintained constant. To determine the effects of the above parameters, we developed a fractional factorial design of  $2^{4-1}$  experiments. The considered response was the slope of the regression between the concentration profiles and the sulphate concentration. The experimental domain was chosen bearing in mind the values established in the previous references on which the detection system is based [1,21,22]. The experiments were conducted with standards of  $\text{SO}_4^{2-}$ , which were analysed in triplicate in the range between 0 and  $15 \text{ mg L}^{-1}$ . In the first columns of Table 1 the conditions of the experiments are described.

**Table 1.** Experimental domain of the fractional factorial design applied.

Experiment number	Factor				Response
	[DMSA] <sup>a</sup>	[KNO <sub>3</sub> ] <sup>b</sup>	Vs <sup>c</sup>	Vr <sup>d</sup>	Slope
1	43.5	0	83	166	-3.71
2	87	0	83	83	-4.25
3	43.5	0.5	83	83	-1.99
4	87	0.5	83	166	-7.50
5	43.5	0	166	166	-3.64
6	87	0	166	83	-4.32
7	43.5	0.5	166	83	-1.58
8	87	0.5	166	166	-8.11

<sup>a</sup> DMSA (III) concentration in  $\mu\text{mol L}^{-1}$

<sup>b</sup> KNO<sub>3</sub> concentration in  $\text{mmol L}^{-1}$

<sup>c</sup> Sample volume in  $\mu\text{L}$

<sup>d</sup> Reagent volume in  $\mu\text{L}$

Data matrices were analysed using MCR-ALS. For all concentrations of  $\text{SO}_4^{2-}$ , both species of the reagent were observed and, as expected, as the sulphate concentration increased, the Ba-DMSA (III) area decreased and the DMSA (III) area increased. The quality of the MCR-ALS resolution was assessed by the lack of fit and the explained variance, ranging from 0.503 to 2.341 and from 99.75% to 99.93%, respectively. The goodness of the spectra profiles was determined, in quantitative terms, using the correlation coefficient ( $r$ ) between the recovered spectra and the experimental spectra. The  $r$  values calculated were superior to 0.9900 for both species in all the experiments, indicating that the recovered profiles have a high degree of concordance with the originals.

Figure 3 shows the results obtained from the resolution process of a data matrix corresponding to a standard of  $10 \text{ mg L}^{-1} \text{SO}_4^{2-}$  analysed in the conditions

of experience 4. In Fig. 3a it is possible to observe that approximately during the first 20 seconds no signal appeared; in the following 14 seconds only the Ba-DMSA (III) signal was present; after 32-80 seconds both signals (Ba-DMSA (III) and DMSA (III)) coexisted and finally, only the DMSA (III) signal was detected.

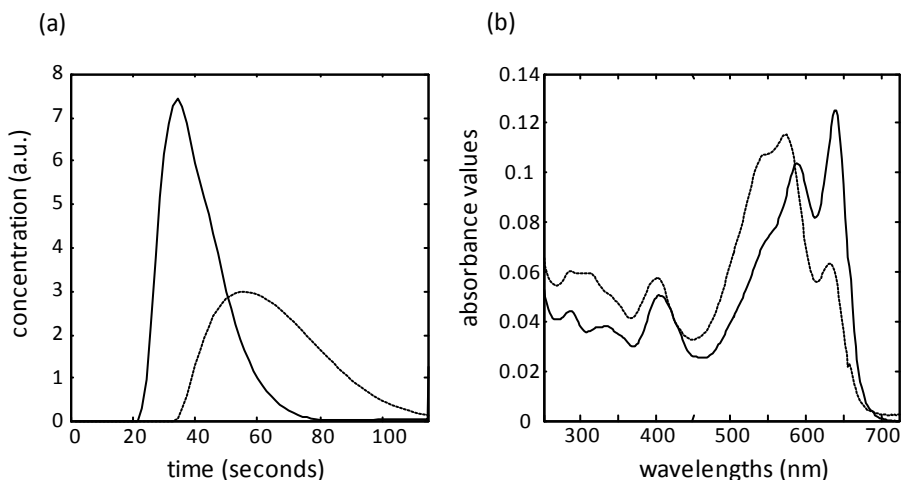


**Figure 3.** Concentration profiles (a) and spectra profiles (b) after applying MCR-ALS. Continue line corresponds to Ba-DMSA (III) complex and dotted line corresponds to DMSA (III). In 3a, *a.u.* means arbitrary units.

For each experience, 2 calibration graphs were constructed, considering as a response the Ba-DMSA (III) or the DMSA (III) area, with comparable results. So the Ba-DMSA (III) area was considered as a response. The results can be seen in the last column of Table 1. Each regression line passed the ANOVA test for a 95% of confidence and the corresponding degrees of freedom.

In Table 2, the significance of the estimated effects in the slope (evaluated in absolute value) was demonstrated. We considered that three- and four- factor interactions were neither likely nor important. We concluded that

the sample volume effect was not noteworthy, both considering it as principal effect and its interactions with the other factors. On the other hand, the response was affected by the reagent concentration and the reagent volume and, in low measure, by the  $\text{KNO}_3$  concentration. These factors affected the response in the same way, i.e. the results were better for the high level of the factors.

**Table 2.** The effect of factors on the response. A: DMSA (III) concentration; B:  $\text{KNO}_3$  concentration; C: sample volume; D: reagent volume; AB, AC; AD, BC, BD, CD: interaction between factors.

Factor	Effect Value
A + BD	3.32
B + AD	0.82
C	0.048
D + AB	2.71
BC	0.05
AC	0.29
CD	0.22

The statistical data and figures of merit of the regression line corresponding to experience 4, which was the one chosen to analyse the samples, are shown in Table 3. The detection limit was estimated according to the uncertainty of the calibration model with 95% of confidence [47].

**Table 3.** Figures of merit for the calibration curve.

Working range (mg L <sup>-1</sup> )	0 – 15
Slope	-7.5
Intercept	194.7
R	0.9902
n	24
Iod (mg L <sup>-1</sup> ) <sup>a</sup>	1.42
RRMSC <sup>b</sup>	0.32
Standard error	5.51
Standard deviation of the slope	0.2
Standard deviation of the intercept	1.9
ANOVA test	
F calculated	2.49
F tabulated (0.05, 6, 16)	3.41

<sup>a</sup>Detection limit

<sup>b</sup>Relative root mean squared error

Study of the effect of the presence of potential interfering chemical species for sulphate determination by SIA procedure were performed for Ca<sup>2+</sup>, Mg<sup>2+</sup> and CO<sub>3</sub><sup>2-</sup>. The results obtained when different amounts of the considered interference were added to three different standards of SO<sub>4</sub><sup>2-</sup> are shown in Table 4. The sulphate concentrations found which are statistically different from the real concentration of sulphate are marked in bold letter. Non-significant interference levels were obtained for Ca<sup>2+</sup>, even though the Ca<sup>2+</sup> content was between 3-20 times the SO<sub>4</sub><sup>2-</sup> content. Magnesium ion interfered when the sulphate concentration was lowest and the magnesium concentration was between 10-20 times more, and carbonate ion interfered when its concentration was 10 times the sulphate concentration.

**Table 4.** Effect of some interfering species on the flow determination of sulphate for sulphate solutions of 5, 10 and 15 mg L<sup>-1</sup> containing interferents at 25, 50, 75 or 100 mg L<sup>-1</sup>.

Sulphate added (mg L <sup>-1</sup> )	Sulphate found (mg L <sup>-1</sup> )								
	Ca <sup>2+</sup> added (mg L <sup>-1</sup> )			Mg <sup>2+</sup> added (mg L <sup>-1</sup> )			CO <sub>3</sub> <sup>2-</sup> added (mg L <sup>-1</sup> )		
	50	75	100	25	50	100	25	50	100
5.07	5.18	5.21	4.99	5.02	<b>3.16</b>	<b>3.58</b>	5.52	<b>7.74</b>	<b>7.67</b>
10.12	10.80	10.99	10.37	10.20	10.02	10.50	10.47	9.98	<b>12.17</b>
15.10	14.93	15.21	15.09	15.52	15.01	15.04	15.35	15.01	14.96

The presence of carbonate and magnesium causes higher and lower sulphate concentrations than the real sulphate concentration, respectively. Focusing on the scheme depicted in Figure 2, both interferences can be explained due to the affinity of the carbonate to the barium, which competes with the sulphate, displacing the reaction equilibrium to the right, or due to the competition of the magnesium with the barium in the formation of the complex or in its union with the sulphate.

In any case, it should be noted that the concentrations of evaluated potential interferences were higher than those expected in natural water samples and these interferences should only be considered in those waste waters that, because of their origin, make one suspect that there may be a high content of magnesium and/or carbonate. It is not expected that these interferences would be present in biodiesel samples.

The feasibility of the proposed method was ascertained by analysing a set of water and biodiesel samples.

Water samples were already analysed by the official method, which is employed for routine analysis at EMATSA, and the results are presented in Table 5. The average values and the standard deviation in the analysis are of three replicates from thirteen different samples of sulphate. The sulphate concentrations of these samples were out of the linear working range of the sequential injection analysis methodology. Therefore, sample dilution was needed.

The accuracy of the flow methodology was assessed through the elliptic joint confidence region (EJCR) test [47]. The critical value of the Snedecor-Fisher statistic at a 95% confidence level was 3.98 and F-value was 3.37. This indicates that the point (1,0) lies within the EJCR, so the ellipse includes the theoretically expected value of (1,0). Therefore, it can be concluded that there is no statistically significant difference between the two methods for the determination of sulphate in water samples at the 95% confidence level and the method is reliable.

**Table 5.** Results obtained by SIA procedure and reference method for sulphate determination in natural and residual water samples.

Samples	Kind of sample	Source	Dilution factor	Sulphate	Sulphate in sample	
				(mg L <sup>-1</sup> )	(mg L <sup>-1</sup> )	
				SIA method	SIA method	Official method
		Wastewater pipeline				
1	Residual water	(urban and industrial waters)	250	5.43	1357	1360
2	Clean water	Golf well	12.5	9.02	112.0	111
3	Clean water	Well water	12.5	8.26	103.2	104
4	Residual water	Paper industry spill	62.5	8.75	547	552
5	Clean water	Golf well	12.5	8.68	108.6	108
6	Residual water	Naval industry spill	25	7.19	180	182
7	Clean water	Golf well	25	4.59	115	115
8	Clean water	Unknown	12.5	7.93	99.2	98
9	Residual water	Unknown	50	5.56	277	278
10	Residual water	Unknown	50	8.03	402	404
11	Residual water	Unknown	50	9.16	458	456
12	Clean water	Golf well	25	5.23	130	132
13	Clean water	Unknown	25	4.96	124	125



The validation of the proposed methodology for the biodiesel samples was carried out analyzing the real samples and the samples generated by the addition of known sulphate concentration (2 and 4 mg L<sup>-1</sup>) and evaluating the recovery. The recovery results are shown in Table 6. A test-*t* [47] of comparison between the ideal 100% value and the experimentally found value was applied and no significant differences between both values were found.

**Table 6.** Results obtained by SIA procedure for sulphate determination in biodiesel.

Sample	Sulphate concentration (s) (mg L <sup>-1</sup> )		Recovery (%)
	Added	Found	
Soybean biodiesel	0.00	6.55 (0.06)	—
	2.00	8.52 (0.09)	98.5
	4.00	11.43 (0.15)	122
Sunflower biodiesel	0.00	6.73 (0.35)	—
	2.00	8.44 (0.49)	85.5
	4.00	11.64 (0.33)	123.5
Palm biodiesel	0.00	6.51 (0.26)	—
	2.00	8.52 (0.36)	100.5
	4.00	11.24 (0.09)	118.25
Waste biodiesel	0.00	6.63 (0.65)	—
	2.00	8.88 (0.23)	112.5
	4.00	10.96 (0.16)	108.25

#### 4. Conclusions

A sequential injection system was developed for the determination of sulphates by using spectrophotometric detection and multivariate curve resolution-alternating least squares. The results for natural and residual water

samples are comparable to those obtained by the reference method. For spiked biodiesel samples we have obtained recovery statistically comparable to 100%.

The proposed flow methodology can be applied in aqueous and organic samples and allows in-line preparation of the samples, with the corresponding increase in sampling rate and simplicity analysis. The use of second-order chemometric techniques avoids the need for sample pre-treatment and separation of interferences, which provides suitable conditions to determine sulphate in complex samples.

In conclusion, the proposed method can be applied to water and biodiesel analysis as an inexpensive and rapid technique that yields results with good precision and accuracy. Alternatively, the reagent consumption and waste generation is minimal, only 0.166 ml and 3.16 ml per sample, respectively, which meets the requirement of the modern tendency towards Clean Chemistry.

**Acknowledgements.** The authors would like to thank the Spanish Ministry of Science and Innovation (Project CTQ2007-61474/BQU) for economic support, the Universitat Rovira i Virgili, for providing Vanessa del Río with a doctoral fellowship and EMATSA (Spain) and BIONET Europa S.L. (Spain) for supplying the samples.

## 5. References

- [1] S.R.P. Meneses, N. Maniasso and E.A.G. Zagatto, *Talanta* **65** (2005) 1313.
- [2] Y.C. Sharma, B. Singh and S.N. Upadhyay, *Fuel* **87** (2008) 2355.

- [3] Methods for the Examination of Water and Associated Materials. Sulphate in Waters, Effluents and Solids. Standing Committee of Analysis, HMSO, London, 1979.
- [4] ASTM D482, Standard Test Method for Ash from Petroleum Products.
- [5] ASTM D4806, Standard Specification for Denatured Fuel Ethanol for Blending with Gasolines for Use as Automotive Spark-Ignition Engine Fuel.
- [6] ASTM D7319, Standard Test Method for Determination of Total and Potential Sulfate and Inorganic Chloride in Fuel Ethanol by Direct Injection Suppressed Ion Chromatography.
- [7] ASTM D7318, Standard Test Method for Total Inorganic Sulfate in Ethanol by Potentiometric Titration.
- [8] M. Morigi, E. Scavetta, M. Berrettoni, M. Giorgetti and D. Tonelli, *Anal. Chim. Acta* **439** (2001) 265.
- [9] V.V. Egorov, V.A. Nazarov, E.B. Okaev and T.E. Pavlova, *J. Anal. Chem.* **61** (2006) 382.
- [10] S.V. Lomako, R.I. Astapovich, O.V. Nozdrin-Plotnitskaya, T.E. Pavlova, Shi Lei, V.A. Nazarov, E.B. Okaev, E.M. Rakhman'ko and V.V. Egorov, *Anal. Chim. Acta* **562** (2006) 216.
- [11] J.A. Morales, L.S. de Graterol and J. Mesa, *J. Chromatogr. A* **884** (2000) 185.
- [12] S. D. Kumar, B. Maiti and P. K. Mathur, *Talanta* **53** (2001) 701.
- [13] M. Biesaga, N. Schmidt and A. Seubert, *J. Chromatogr. A* **1026** (2004) 195.
- [14] Q. Xu, C. Xu, Y.P. Wang, W. Zhang, L.T. Jin, K. Tanaka, H. Haraguchi and A. Itoh, *Analyst* **125** (2000) 1799.
- [15] L. Arce, A. Ríos and M. Valcárcel, *J. Chromatogr. A* **791** (1997) 279.
- [16] S. Kulka, G. Quintas and B. Lendl, *Analyst* **131** (2006) 729.
- [17] D. Yiwei, *Water Res.* **32** (1998) 2249.
- [18] A. Kojlo, J. Michalowski and M. Trojanowicz, *Anal. Chim. Acta* **228** (1990) 287.

- [19] A. Rius, M.P. Callao and F.X. Rius, *Analyst* **122** (1997) 737.
- [20] R.A.S. Lapa, J.L.F.C. Lima and I.V.O.S. Pintos, *J. Braz. Chem. Soc.* **11** (2000) 170.
- [21] R. Burakham, K. Higuchi, M. Oshima, K. Grudpan and S. Motomizu, *Talanta* **64** (2004) 1147.
- [22] F.S. de Oliveira and M. Korn, *Talanta* **68** (2006) 992.
- [23] K. Ueno, F. Sagara, K. Higashi, K. Yakata, I. Yoshida and D. Ishii, *Anal. Chim. Acta* **261** (1992) 241.
- [24] J.F. Van Staden and R.E. Taljaard, *Anal. Chim. Acta* **331** (1996) 271.
- [25] W.R. Melchert and F.R.P. Rocha, *Anal. Chim. Acta* **616** (2008) 56.
- [26] J.A. Vieira, I.M. Raimundo Jr. and B.F. Reis, *Anal. Chim. Acta* **438** (2001) 75.
- [27] R.E. Santelli, P.R.S. Lopes, R.C.L. Santelli and A.L.R. Wagener, *Anal. Chim. Acta* **300** (1995) 149.
- [28] S.M.B. Brienza, R.P. Sartini, J.A. Gomes Neto and E.A.G. Zagatto, *Anal. Chim. Acta* **300** (1995) 269.
- [29] V. Gómez and M.P. Callao, *Anal. Chim. Acta* **627** (2008) 169.
- [30] G.M. Escandar, N.M. Faber, H.C. Goicoechea, A. Muñoz de la Peña, A.C. Olivieri and R.J. Poppi, *Trends Anal. Chem.* **26** (2007) 752.
- [31] M.M. Galera, M.D.G. García and H.C. Goicoechea, *Trends Anal. Chem.* **26** (2007) 1032.
- [32] V. del Río, M.S. Larrechi and M.P. Callao, *Talanta* **81** (2010) 1572.
- [33] V. Gómez, A. Pasamontes and M.P. Callao, *Microchem. J.* **83** (2006) 98.
- [34] V. Gómez, J. Font and M.P. Callao, *Talanta* **71** (2007) 1393.
- [35] A. Pasamontes and M.P. Callao, *Anal. Sci.* **22** (2006) 131.
- [36] V. Gómez, M. Miró, M.P. Callao and V. Cerdà, *Anal. Chem.* **79** (2007) 7767.
- [37] N.R. Marsili, A. Lista, B.S. Fernández Band, H. Goicoechea and A.C. Olivieri, *Analyst* **130** (2005) 1291.

- [38] N.R. Marsili, A. Lista, B.S. Fernández Band, H. Goicoechea and A.C. Olivieri, *J. Agric. Food Chem.* **52** (2004) 2479.
- [39] R. Díez, L.A. Sarabia, M.S. Sánchez and M.C. Ortiz, *Chem. Intell. Lab. Syst.* **92** (2008) 71.
- [40] L.E. Rueda, L.A. Sarabia, A. Herrero and M.C. Ortiz, *Anal. Chim. Acta* **479** (2003) 173.
- [41] J. Saurina, S. Hernández-Cassou and R. Tauler, *Anal. Chim. Acta* **335** (1996) 41.
- [42] J. Saurina, S. Hernández-Cassou, A. Izquierdo-Ridora and R. Tauler, *Chemom. Intell. Lab. Syst.* **50** (2000) 263.
- [43] R. Tauler, *Chemom. Intell. Lab. Syst.* **30** (1995) 133.
- [44] R. Tauler, A. Smilde and B.R. Kowalski, *J. Chemom.* **9** (1995) 31.
- [45] R. Tauler, *J. Chemom.* **16** (2002) 117.
- [46] J. Saurina, S. Hernández-Cassou and R. Tauler, *Anal. Chim. Acta* **335** (1996) 41.
- [47] D.L. Massart, B.G.M. Vandeginste, S.N. Deming, Y. Michotte and L. Haufman, *Handbook of Chemometrics and Qualimetrics*, Part A, Elsevier, Amsterdam, 1997.
- [48] The Mathworks, MATLAB Version 6.5, Natick, MA, 2004.
- [49] [http://www.ub.es/gesq/eq1\\_eng.htm](http://www.ub.es/gesq/eq1_eng.htm)

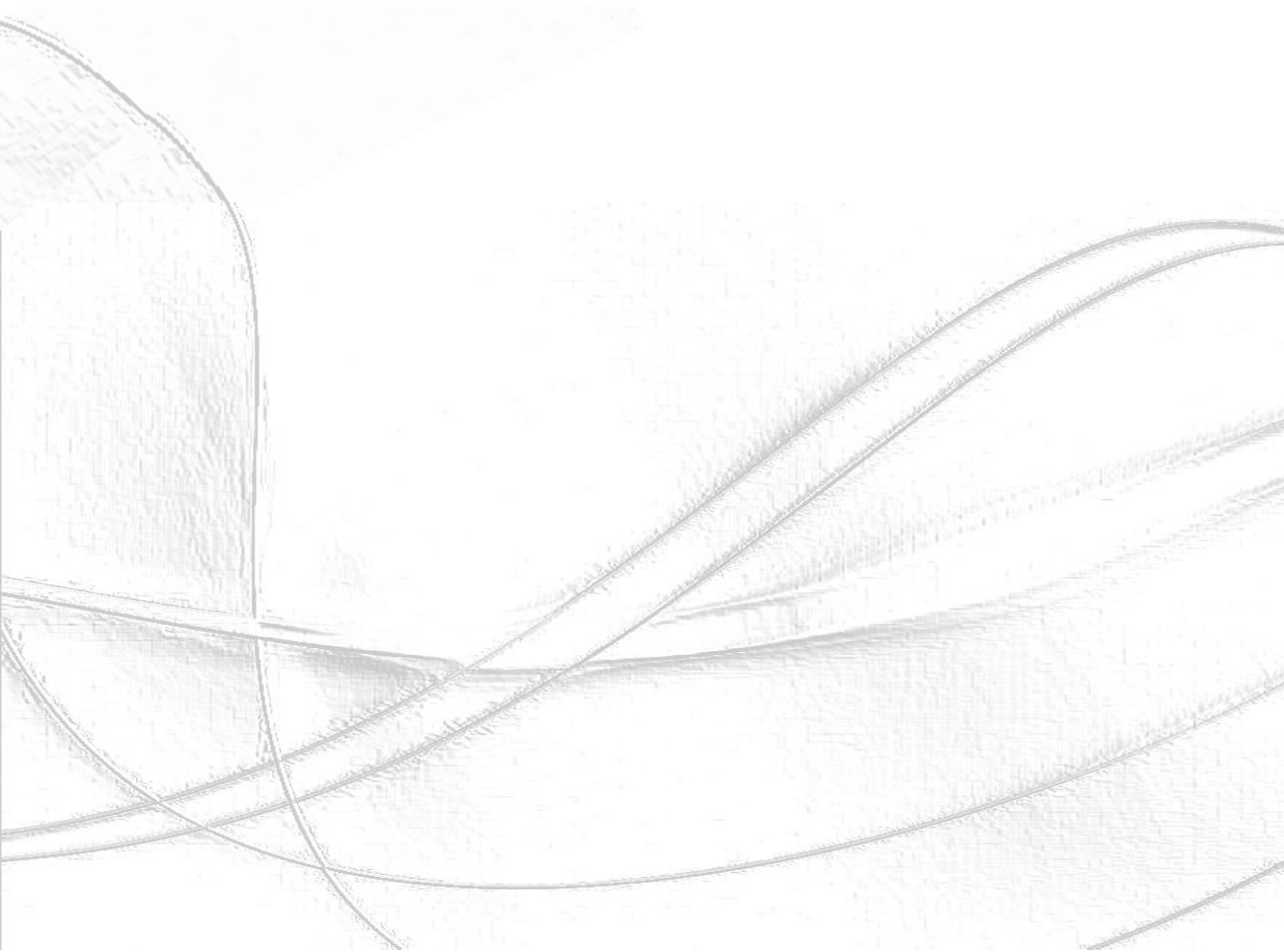
#### 4.4. REFERENCES

- [1] G. Knothe, J. Krahl and J.V. Gerpen, *The Biodiesel Handbook*, AOCS Press, Champaign, 2005.
- [2] A. Bemirbas, *Biodiesel. A Realistic Fuel Alternative for Diesel Engines*, Springer, London, 2008.
- [3] Y.C. Sharma, B. Singh and S.N. Upadhyay, *Fuel* **87** (2008) 2355.
- [4] Y.C. Sharma and B. Singh, *Renew. Sust. Energ. Rev.* **13** (2009) 1646.
- [5] F. Ma and M.A. Hanna, *Bioresour. Technol.* **70** (1999) 1.
- [6] A.K. Tiwari, A. Kumar and H. Reama, *Biomass Bioenerg.* **31** (2007) 569.
- [7] H. Fukuda, A. Kondo and H. Noda, *J. Biosci. Bioeng.* **92** (2001) 405.
- [8] E. Lotero, Y. Liu, D.E. López, K. Suwannakarn, D.A. Bruce and J.G. Goodwin Jr., *Ind. Eng. Chem. Res.* **44** (2005) 5353.
- [9] R.D. 1183/90, 14 September 1990. *Drinkable waters for human consumption. Supply and quality*. Technical-Sanitary regulation (BOE, 20 September 1990).
- [10] C. Bosch Ojeda and F. Sánchez Rojas, *Anal. Chim. Acta* **635** (2009) 22.
- [11] C. Bosch Ojeda and F. Sánchez Rojas, *Appl. Spectrosc. Rev.* **44** (2009) 245.
- [12] J. Ruzicka and G.D. Marshall, *Anal. Chim. Acta* **237** (1990) 329.
- [13] V. Cerdà, A. Cerdà, A. Cladera, M.T. Oms, F. Mas, E. Gómez, F. Bauzá, M. Miró, R. Forteza and J.M. Estela, *Trends Anal. Chem.* **20** (2001) 407.
- [14] K. Mervartová, M. Polášek and J.M. Calatayud, *J. Pharm. Biomed. Anal.* **45** (2007) 367.
- [15] R.B.R. Mesquita and A.O.S.S. Rancel, *Anal. Chim. Acta* **648** (2009) 7.
- [16] R. Pérez-Olmos, J.C. Soto, N. Zárate, A.N. Araújo, J.L.F.C. Lima and M.L.M.F.S. Saraiva, *Food Chem.* **90** (2005) 471.
- [17] V. Gómez, A. Pasamontes and P. Callao, *Microchem. J.* **83** (2006) 98.
- [18] A.M. Idris, F.N. Assubaie and S.M. Sultan, *Microchem. J.* **83** (2006) 7.
- [19] A. Pasamontes and M.P. Callao, *Talanta* **68** (2006), 1617.

- [20] A.C.V. dos Santos and J.C. Masini, *Talanta* **77** (2009) 1081.
- [21] A. Pasamontes and M.P. Callao, *Trends Anal. Chem.* **25** (2006) 77.
- [22] A. Izquierdo-Ridorsa, J. Saurina, S. Hernández-Cassou and R. Tauler, *Chemom. Intell. Lab. Syst.* **38** (1999) 183.
- [23] J. Saurina, S. Hernández-Cassou and R. Tauler, *Anal. Chim. Acta* **335** (1996) 41.

# 5

## General conclusions





UNIVERSITAT ROVIRA I VIRGLI  
FAST ANALYTICAL METHODOLOGIES BASED ON MOLECULAR SPECTROPHOTOMETRIC TECHNIQUES  
AND MULTIVARIATE DATA ANALYSIS  
Vanessa del Rio Sánchez  
ISBN:978-84-693-9439-7/ DL:T.64-2011

This chapter summarizes the general conclusions of the work presented in this thesis. Specific conclusions have been drawn at the end of each paper.

The obtained results have demonstrated that molecular spectrophotometric techniques, as infrared and UV-visible spectroscopy, combined with second-order data analysis methods are very valuable tools to develop fast analytical methodologies.

More specifically, the combination of infrared spectroscopy with chemometric analysis of the data has allowed to:

- Detect the number of steps involved in the model reactions studied.
- Identify the sequential order of the reactions that take part in the systems.
- Evaluate quantitatively the concentration of each of the chemical species involved throughout the reactions.
- Postulate different kinds of mechanism depending on the working temperature.

For the particular application field of this thesis, the above mentioned states constitute powerful information to evaluate the possibilities that vegetable oils offer as precursors of pre-polymers.

Likewise, with regard to the combination of sequential injection analysis with UV-visible detection and second-order data treatment, it can also be concluded that:

- Traditional determinations based on UV-visible spectroscopy can be adapted to automated systems, which will increase the frequency of the analysis and minimize the amount of sample, reagent and waste, in accordance with the requirements of Green Chemistry.
- The use of second-order chemometric methods is an appropriate solution to minimize the interference problems present in real samples.
- Methods have been developed that enable up to aqueous and organic samples to be determined, what has considerable potential in conventional analysis.



# Appendix



UNIVERSITAT ROVIRA I VIRGLI  
FAST ANALYTICAL METHODOLOGIES BASED ON MOLECULAR SPECTROPHOTOMETRIC TECHNIQUES  
AND MULTIVARIATE DATA ANALYSIS  
Vanessa del Rio Sánchez  
ISBN:978-84-693-9439-7/ DL:T.64-2011

List of papers by the author presented in this Thesis.

Vanessa del Río, M. Pilar Callao, M. Soledad Larrechi, Lucas Montero de Espinosa, J. Carles Ronda and Virginia Cádiz. *Chemometric resolution of NIR spectra data of a model aza-Michael reaction with a combination of local rank exploratory analysis and multivariate curve resolution-alternating least squares (MCR-ALS) method*. *Analytica Chimica Acta*, 642 (2009) 148-154.

Vanessa del Río, M. Soledad Larrechi and M. Pilar Callao. *Sequential injection titration method using second order signals: Determination of acidity in plant oils and biodiesel samples*. *Talanta*, 81 (2010) 1572-1577.

Vanessa del Río, M. Soledad Larrechi and M. Pilar Callao. *Determination of sulphate in water and biodiesel samples by a sequential injection analysis – multivariate curve resolution method*. *Analytica Chimica Acta*, 676 (2010) 28-33.

Vanessa del Río, Nicolás Spegazzini, M. Pilar Callao and M. Soledad Larrechi. *Spectroscopic and quantitative chemometric analysis of the epoxidized oil/amine system*. *Journal of Near Infrared Spectroscopy*, 18 (2010) 281-290.

Vanessa del Río, M. Pilar Callao and M. Soledad Larrechi. *Quantitative analysis of the influence of the temperature on a model curing reaction of epoxy resins from vegetable oils using FTIR spectroscopy and MCR-ALS*. Submitted.

Contributions to international meetings.

Vanessa del Río, M. Soledad Larrechi and M. Pilar Callao.

*Sequential injection with second-order data treatment for the determination of fatty acids in vegetable oils.*

VI Colloquium Chemometricum Mediterraneum

Saint Maximim La Sainte-Baume (France, 2007)

Poster communication

Vanessa del Río, M. Pilar Callao, M. Soledad Larrechi, Lucas Montero de Espinosa, J. Carles Ronda and Virginia Cádiz.

*Study of a model reaction for obtaining thermosets from vegetable oils using NIR spectroscopy and Multivariate Curve Resolution – Alternating Least Squares.*

11<sup>th</sup> Conference on Chemometrics in Analytical Chemistry

Montpellier (France, 2008)

Poster communication

Vanessa del Río, M. Pilar Callao, M. Soledad Larrechi, Lucas Montero de Espinosa, J. Carles Ronda and Virginia Cádiz.

*Chemometric resolution of NIR spectra data of a model aza-Michael reaction with a combination of local rank exploratory analysis and multivariate curve resolution-alternating least squares (MCR-ALS) method.*

III Workshop de Qimiometría

Burgos (Spain, 2008)

Poster and Flash communication

Vanessa del Río, M. Pilar Callao and M. Soledad Larrechi.

*Exploratory and quantitative analysis of a model curing reaction of epoxy resins from renewable resources by chemometric analysis of NIR data.*

XV Reunión de la Sociedad Española de Química Analítica

San Sebastián (Spain, 2009)

Poster communication

Vanessa del Río, M. Soledad Larrechi and M. Pilar Callao.

*Sequential injection analysis for the determination of sulphate in water using second-order data.*

VII Colloquium Chemometricum Mediterraneum

Granada (Spain, 2010)

Poster communication



UNIVERSITAT ROVIRA I VIRGLI  
FAST ANALYTICAL METHODOLOGIES BASED ON MOLECULAR SPECTROPHOTOMETRIC TECHNIQUES  
AND MULTIVARIATE DATA ANALYSIS  
Vanessa del Rio Sánchez  
ISBN:978-84-693-9439-7/ DL:T.64-2011

UNIVERSITAT ROVIRA I VIRGILI  
FAST ANALYTICAL METHODOLOGIES BASED ON MOLECULAR SPECTROPHOTOMETRIC TECHNIQUES  
AND MULTIVARIATE DATA ANALYSIS  
Vanessa del Rio Sánchez  
ISBN:978-84-693-9439-7/ DL:T.64-2011

*Lo que con mucho trabajo se adquiere, más se ama.*

*Aristóteles*